The Activation of the Adenovirus type 2 protease and Nuclear Localisation studies on the protease and pVI protein

By

Kirsi Susanna Honkavuori

Biomolecular Sciences Building, The School of Biology,
University of St Andrews

A thesis presented for the degree of Doctor of Philosophy at the University of St Andrews, September 2004

Contents ***page***

Declaration

I, Kirsi Susanna Honkavuori hereby certify that this thesis, which is approximately 35,000 words in length, has been written by me, that it is a record of my work carried out by me and that it has not been submitted in any previous application for higher degree.

Date 28/3/2005 Signature of candidate

I was admitted as a research student in September 2000 and as a candidate for the degree of Doctor of Philosophy in September 2000: the higher study for which this is a record was carried in the University of St. Andrews between 2000 and 2003.

Date 28/3 2005 Signature of candidate

I hereby certify that the candidate has fulfilled the conditions of the Resolution and Regulations appropriate for the Degree of Doctor of Philosophy in the University of St. Andrews and that the candidate is qualified to submit this thesis in application for that degree.

Date 28/3/05 Signature of supervisor

In submitting this thesis to the University of St. Andrews I understand that I am giving permission for it to be made available for use in accordance with the regulations of the University Library for the time being in force, subject to any copyright vested in the work not being affected thereby. I also understand that the title and abstract will be published, and that a copy of the work may be made and supplied to any *bona fide* library or research worker.

Date 28/3 2005 Signature of candidate

Kiitoksena rakkaalle perheelleni

Velulle, Jatalle, Heidille & Paulille

Acknowledgements

Most importantly, I would like to thank my supervisor Dr Graham Kemp for giving me guidance and support throughout the project.

I would also like to thank the brilliant academic staff and all the people in the BMS building, past and present, for advice and friendship.

Abbreviations

A	Absorbance
Amp	Ampicillin
APS	Ammonium persulphate
AVP	Adenovirus protease, adenain
β-MeSH	β-mercaptoethanol
CE	Capillary electrophoresis
ddH_2O	Distilled water
DAPI	4',6-Diamidino-2-phenylindole
D-MEM	Dulbecco's modified Eagle's medium
DMSO	Dimethyl sulphoxide
DNA	Deoxyribonucleic acid
dsDNA	Double-stranded DNA
ECL	Enhanced chemiluminesence
E.coli	*Escherichia coli*
FCS	Foetal calf serum
FITC	Fluorescein isothiocyanate
HEPES	4-(2-hydroxyethyl)-1-piperazine ethanesulphonic acid
HPLC	High-performance liquid chromatography
h	Hour(s)
hpi	Hour(s) post-infection
hpt	Hour(s) post-transfection
Ig	Immunoglobulin
IPTG	Isopropyl- β-D-thiogalactopyranoside
ITC	Isometric Titration Calorimetry
LB	Luria-Bertani medium
min	Minute(s)
MW	Molecular weight
NLS	Nuclear localisation signal
PAGE	Polyacrylamide gel electrophoresis
PCR	Polymerase Chain Reaction
PBS	Phosphate buffered saline
PEG	Polyethylene glycol
pH	Pondus hydrogenii ($-\log_{10}[H^+]$)
PVDF	Polyvinylidene difluoride
RNA	ribonucleic acid
rpm	revolutions per minute
SBTI	Soya bean trypsin inhibitor
SDS	Sodium dodecyl sulphate
sec	second (s)
ssDNA	single-stranded DNA
ssRNA	single-stranded RNA
SV40	Simian virus 40
TEMED	N,N,N', N'-Tetramethylethylenediamine
TFA	Trifluoroacetic acid
Tris	2-amino-2-(hydroxymethyl)propane-1,3-diol
TTBS	Tris buffered saline with Tween 20
uv	ultra violet
v/v	volume per volume ratio
wt	wild-type
w/v	weight per volume ratio

1 & 3 letter codes for amino acids			*Genetic code*
A	Ala	Alanine	GCU, GCC, GCA, GCG
C	Cys	Cysteine	UGU, UGC
D	Asp	Aspartic acid	GAU, GAC
E	Glu	Glutamic acid	GAA, GAG
F	Phe	Phenylalanine	UUU, UUC
G	Gly	Glycine	GGU, GGC, GGA, GGG
H	His	Histidine	CAU, CAC
I	Ile	Isoleucine	AUU, AUC, AUA
K	Lys	Lysine	AAA, AAG
L	Leu	Leucine	UUA, UUG
M	Met	Methionine	AUG*
N	Asn	Asparagine	AAU, AAC
P	Pro	Proline	CCU, CCC, CCA, CCG
Q	Gln	Glutamine	CAA, CAG
R	Arg	Arginine	CGU, CGC, CGA, CGG
S	Ser	Serine	AGU, AGC, UCU, UCC, UCA, UCG
T	Thr	Threonine	ACU, ACC, ACA, ACG
V	Val	Valine	GUU, GUC, GUA, GUG
W	Trp	Tryptophan	UGG
Y	Tyr	Tyrosine	UAU, UAC

Stop codons: UAA, UAG, UGA

****Start codon: Met***

List of Figures & Tables

Abstract

A crucial component of an Adenovirus virion is the 23 kD cysteine endoprotease (AVP), which requires activation by an 11 amino acid residue, substrate-derived, cofactor peptide (pVIct) residing at the C-terminus of the adenovirus pVI protein. This unique activation and binding mediated by the GVQSLKRRRCF-peptide was subject to further analysis in this thesis.

The importance of the C-terminal residues along the peptide, especially the KRRR-motif, in the activation and binding of the protease was examined. Binding and activation experiments conducted with synthesised peptides containing single Alanine-substitutions indicated that the most important residue, in addition to the previously described Cysteine'10, was the 11^{th} residue Phenylalanine. The positively charged tetrapeptide on the pVIct was found not to be crucial for binding or for activation, however, its potential role as a nuclear localisation signal (NLS), as suggested by Pollard (2001), was confirmed.

Different fluorescent protein fusions were constructed in order to study the NLS function of the activating peptide *in vivo*. Whilst no evidence was found that the protease is nuclear translocated by the action of the activating peptide, the experiments illustrated how the activating peptide sequence could be employed as a signal for providing nuclear access for other proteins. Furthermore, mutational analysis on the pVI protein demonstrated that this motif is required for the successful nuclear accumulation of the pVI protein itself.

In this thesis, the application of native gel electrophoresis for the determination of binding dissociation constants is described. In addition, the double fluorescent constructs produced, containing different length sequences from the pVI gene, were shown to be successful *in vitro* and *in vivo* indicators for the protease activity.

The results presented herein demonstrate additional characteristics and roles for the peptide and their relevance in the course of adenoviral infection is discussed.

1. Introduction to Adenoviruses

1.1 Introduction to Adenoviridae

Year 2003 welcomed the 50th anniversary of research into Adenoviruses. Since its first isolation in 1953, the virus, its lifecycle, the complexity of its structure and virion components have been studied in detail. This has not only benefited adenovirologists but also contributed to the discovery and understanding of several fundamental themes in molecular biology such as viral and cellular gene expression, DNA replication and mRNA splicing. Currently, adenovirus-vectors are assessed for their utility in gene delivery for therapeutic purposes, illustrating how adenovirus as an archetype, after decades of devoted research, still offers interesting areas for further analysis.

1.1.1 Clinical importance of Adenoviruses

These transmissible agents, responsible for cytopathic changes in children's adenoidal tissue, were discovered coincidentally following attempts to establish cell-lines for the growth of polioviruses (Rowe *et al.*, 1953). The following year, the viruses were isolated from military recruits suffering from acute respiratory illness (Hilleman & Werner, 1954). According to their tissue source or clinical manifestation, the viruses were referred to by different names, such as adenoid degeneration agents (ADs), until 1956 when they were subsequently renamed as adenoviruses according to the tissue of the prototype virus isolation (Shenk, 1996 and references therein).

Different human adenovirus serotypes, spread by nosocomial and by faecal-oral routes, are etiological agents of acute upper respiratory tract (URT) infections, epidemic conjunctivitis and gastroenteritis (review: Shenk, 1996, Erdman *et al.*, 2002). While adenovirus infections are very common and often asymptomatic, they are endemic and a cause for concern in infants and amongst those with an underlying immunologic compromise. Adenoviruses (Ads) can persist as latent infections in peripheral blood lymphocytes, tonsils, or in the upper airways where they can become reactivated due to immunosuppression, such as in AIDS patients (De Jong *et al.*, 1999, Hayashi, 2002). Recent studies have highlighted that bronchiolitis caused by adenoviruses in children could predispose them to the development of asthma and chronic obstructive pulmonary disease (COPD) (Hogg, 1999, Hayashi 2002). They have also been recognised as an important pathogen in children who have received bone marrow transplants, where

disseminated adenovirus infections result in fatality rates up to 60% (review: Walls *et al.*, 2003).

Furthermore, the cessation in the production of live enteric-coated vaccines for Ad4 and Ad7 has resulted in re-emerging respiratory disease epidemics amongst military recruits in the United States, which were previously prevented through immunization (Erdman *et al.*, 2002, Ryan *et al.*, 2002). Despite their clinical importance, there are only a few, non-specific antiviral chemotherapeutics available for treating severe Ad infections, such as ribavirin and cidofovir, but even these exhibit limited efficacy and can have severe side-effects (Gavin & Katz, 2002, Walls *et al.*, 2003). While the ability to diagnose adenovirus infections has improved through developments in techniques such as Polymerase Chain Reaction (Chakrabarti *et al.*, 2002), the failure to treat disseminated infections still remains.

1.1.2 Classification

Until relatively recently the family of *Adenoviridae,* containing over 100 serotypes, comprised of only two genera, *Aviadenoviridae* and *Mastadenoviridae*, infecting birds and mammals, respectively (review: Shenk, 1996). Adenoviruses belonging to the above two genera are distinguished by the presence of a genus-specific antigen, characteristic to the mammalian serotypes. The isolation and identification of adenoviruses from a range of exotic hosts, however, led to the introduction of two new genera, *Siadenoviridae* and *Atadenoviridae* (review: Davison *et al.*, 2003).

Mastadenoviridae consist of serotypes infecting human, simian, bovine, equine, porcine, ovine, canine and opossum hosts. The human serotypes within this genus are arranged into six subgroups (A-F) based on their red-cell haemagglutination abilities, guanine-cytosine content and the percent homology of their genomes, as well as according to their oncogenic potential in rodents (Shenk, 1996). The latter has only been demonstrated in subgroup A of human adenoviruses (types 12, 18, 31) (Trentin *et al.*, 1962) and to date, there has been no evidence for their ability to initiate tumours in humans. The classification scheme of the human adenovirus serotypes, including clinical manifestations, is summarised in Table 1. The recently identified human serotypes 50 and 51, isolated from HIV-infected individuals (De Jong *et al.*, 1999), are included.

Aviadenoviridae genus consists currently of only a few isolates, fowl adenovirus type 1 or chick embryo lethal orphan (CELO) virus, fowl types 4, 9 and 10 (Davison *et al.*, 2003). Egg Drop Syndrome (EDS) virus, with its compact genome and ovine-bovine-related nucleotide sequence (Harrach *et al.*, 1997), differs from the other avian adenoviruses and has therefore been assigned to the *Atadenoviridae* genus. *Atadenoviridae* genus was named according to the high A + T content in the genomes of the representative viruses (Benkő *et al.*, 2002, review: Davison *et al.*, 2003) and contains adenoviruses infecting a range of hosts, from reptilian to marsupial. Adenovirus isolated from corn snake (*Elaphe guttata*) is an example of a recent species included in this genus (Farkas *et al.*, 2002).

There are currently only two members in the fourth, *Siadenoviridae* genus: an isolate from leopard frog *Rana pipiens* (Clark *et al.*, 1973, Davison *et al.*, 2000) and turkey adenovirus 3, THEV (Davison *et al.*, 2003). Following the isolation of a fish (white sturgeon) adenovirus, it is likely that a fifth genus will be introduced (Kovács *et al.*, 2003). And as illustrated by the wide range of isolates within the *Atadenoviridae*, host origin forms only one of the several criteria used for the genus taxon. A recent review into the evolutionary differences between the four current genera highlighted that additional niche-specific genes are contained near the termini of the genomes (Davison *et al.*, 2003).

1.2 Adenovirus virion

Adenovirus particles are non-enveloped, approximately 60-90 nm in size and display icosahedral morphology (Horne *et al.*, 1959, Shenk, 1996). Approximately 13% of a single Ad2 particle, with a molecular mass of 150 x 10^6 daltons, is made up by the 35, 937 bp double-stranded DNA genome (Green & Piña, 1963, van Oostrum & Burnett, 1985, Stewart *et al.*, 1991). The remainder of the virion consists of protein: a third of which is contained in the core while the majority forms the capsid or 'coat' of the virion (Hosokawa & Sung, 1976). The structural polypeptides of the adenovirus virion have been named II to IX according to their molecular weight following separation by sodium dodecyl sulfate (SDS)-polyacrylamide gel electrophoresis (Maizel *et al.*, 1968). The role and spatial organisation of each structural protein in the virion will now be discussed in more detail (see Figure 1).

1.2.1 Capsid-associated proteins

Hexon

The major structural protein accounting for over 60% of the total protein mass of the virion is the hexon, protein II (Athappilly *et al.*, 1994). The 240 copies of the 967 amino acid (Ad2) hexon (Akusjärvi *et al.*, 1984) are located on the rounded icosahedral outer capsid, composed of altogether 252 morphological units or capsomers (Horne *et al.*, 1959, Stewart *et al.*, 1991), and in association with protein IX, penton base (III) and protein IIIa. The majority of hexon trimers are associated as groups of nine (GON) forming the 20 facets of the virion. The remainder are referred to as peripentonal hexons, functioning as linkers between the pentons and hexon facets (see Figure 1).

The 109 kD hexon (Akusjärvi *et al.,* 1984) requires an association with another adenoviral protein, the 100 kD protein, for its homotrimerisation and assembly (Oosterom-Dragon & Ginsberg, 1981). Following successful structural modification of the hexon, it relies on the precursor polypeptide VI (pVI) for its nuclear accumulation (Kauffman & Ginsberg, 1976, Wodrich *et al.*, 2003).

The crystallographic structure of the adenovirus type 2 hexon reveals that it consists of two morphologically distinct parts: the N-terminal pseudo-hexagonal base inside the capsid portion and the triangular shape of the extended top structure (Roberts *et al.*, 1986, Athappilly *et al.*, 1994). Amongst the predominant β-barrel structure of hexons, it is the loops of the hexon-trimers, which are exposed on the surface of the virion (Toogood *et al.*, 1989). These loops exhibit variability between adenovirus serotypes and possess type-specific epitopes, which function as a criterion in the subdivision of adenoviruses (Russell *et al.*, 1981, Toogood *et al.*, 1992). Recently, the solved structure of the Ad5 hexon has been shown to represent an improved structure-model, compared to the earlier Ad2 hexon, and subsequently refines the epitope positions on the hexon (Rux & Burnett, 2000).

Penton

Penton base

The penton consists of the pentameric penton base (protein III) and fiber (protein IV), both of which are involved in the association with cellular receptors and proteins. At each of the 12 vertices of the virion, five copies of the 63 kD (571 aa) protein III

Table 1. Classification of human adenoviruses. Table adapted and updated from that by Shenk (1996).

Figure 1. Schematic diagram of the mature adenovirus type 2 particle. Figure is based upon current view on the disposition of proteins (updated from that by Brown *et al.*, 1975, Stewart *et al.*, 1991).

Table 1. Classification of human adenoviruses

Subgroup	Hamagglutination groups	Serotypes	Oncogenic potential	Percentage of G-C in DNA	Infections caused
A	little or no agglutination	12, 18, 31	High	48-49	respiratory, urinary, gastrointestinal
B	complete agglutination of monkey erythrocytes	3, 7, 11, 14, 16, 21, 34, 35, 50	Moderate	50-52	respiratory, gastrointestinal, ocular, urinary
C	partial agglutination of rat erythrocytes	1, 2, 5, 6	Low-none	57-59	respiratory, urinary, gastrointestinal
D	complete agglutination of rat erythrocytes	8-10, 13, 15, 17, 19, 20, 22-30, 32, 33, 36-39, 42-49, 51	Low-none	57-61	ocular, gastrointestinal
E	little or no agglutination	4	Low-none	57-59	ocular, respiratory
F	little or no agglutination	40, 41	Unknown	52	gastrointestinal

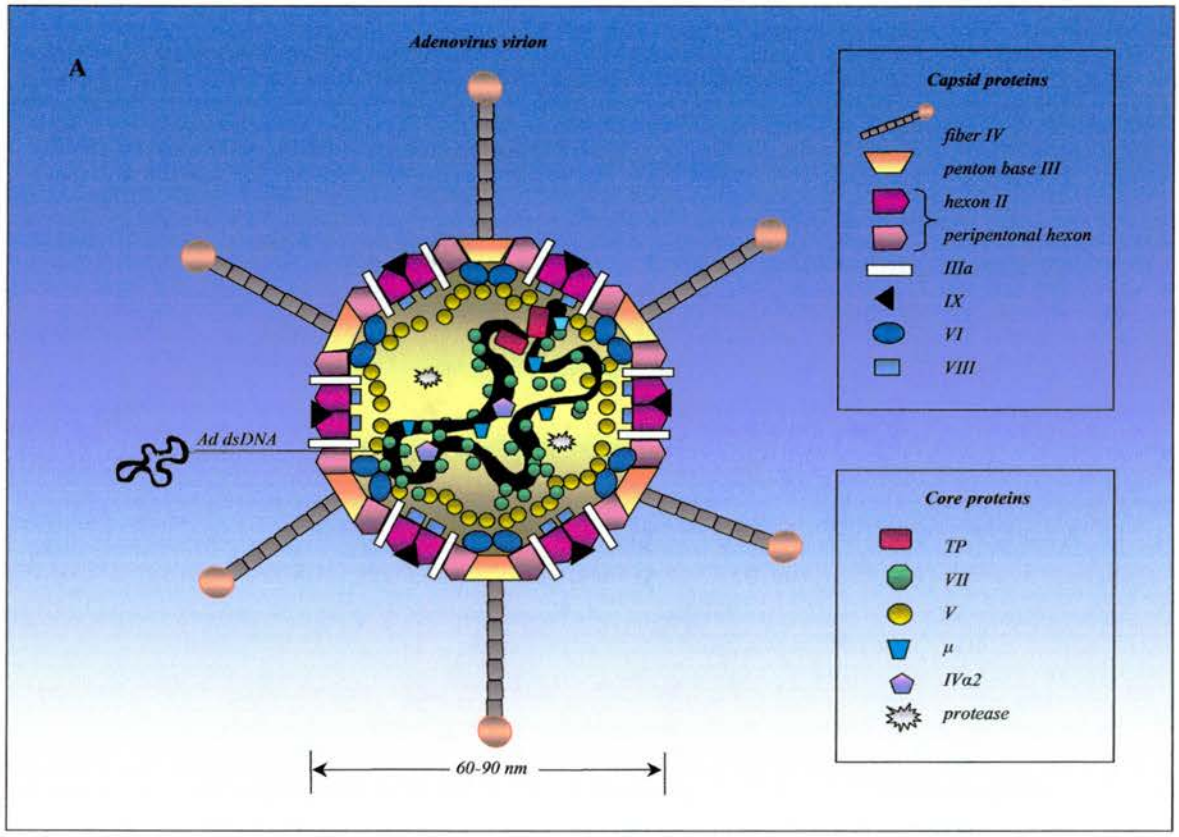

(Boudin *et al.,* 1979, Aleström *et al.,* 1984) are found interacting non-covalently with the peripentonal hexons (Stewart *et al.*, 1991). The penton base contains an RGD-motif (Arg-Gly-Asp), which interacts with cellular adhesion molecules during the internalisation of the virion (Wickham *et al.*, 1993). The RGD-motif also confers toxin-like, cell-rounding and -detaching activity, which may aid in lysing of the endosomes during the entry of the virion into the cytoplasm (Boudin *et al.*, 1979, Bai *et al.*, 1993), (see section 1.3.1).

Fiber

A homotrimer of the protein IV (fiber) forms the elongated, protruding structure of the penton complex (van Oostrum & Burnett, 1985). The amino-terminal tail region of the 62 kD (582 aa) fiber has noncovalent interactions with the penton base (Devaux *et al.*, 1987) while the approximately 180 residues of the carboxy-terminus form the 'knob' of the shaft, interacting with the cellular receptors on host cells (Louis *et al.*, 1994). Between different adenovirus serotypes, the length of the fiber varies according to the number of a 15 amino acid repeat in the polypeptide (shaft region) (Green *et al.*, 1983). Adenovirus serotype 40 exhibits two fibers of different lengths on its virion, which is most likely an adaptation for enhancing attachment to several cellular receptors (Russell & Kemp, 1995 and references therein).

Protein IIIa

The approximate 74 copies of protein IIIa per virion are located at the vertex regions (van Oostrum & Burnett, 1985), next to the peripentonal and GON hexons. IIIa proteins are most likely to function as linkers strengthening the capsid structure, however, they are also thought to extend to the side of the viral core and to interact with proteins V and VII (Everitt *et al.*, 1975, Boudin *et al.*, 1980). In addition to possessing a protease cleavage site (Webster *et al.*, 1989a) and being subject to phosphorylation (Tsuzuki & Luftig, 1983), the disassociation of this ~ 65 kD protein (585 aa) is presumed important at the uncoating stage of the virion during entry into a host cell (Greber *et al.*, 1996).

Protein VI

The mature protein VI, a 22 kD minor capsid protein, is found inside the capsid in association with viral DNA and core protein V as a dimer, linking the external capsid and the internal DNA-protein core together (Everitt *et al.*, 1975, Chatterjee *et al.,* 1985). In addition to its DNA binding ability (Russell & Precious, 1982), protein VI demonstrates hexon-binding affinity, specific to two sites, between amino acids 48-74 and 233-239 of the protein VI (Matthews & Russell, 1995). The precursor of protein VI, a 27 kD (250 aa) pVI is cleaved by the adenovirus protease at two sites: 33-34 and at 238-239 (Akusjärvi & Persson, 1981, Anderson, 1990). The C-terminal cleavage site of pVI is preferentially cleaved (Diouri *et al.*, 1996), leading to the formation of an intermediate form of protein VI, iVI (Matthews & Russell, 1994). Mature VI has also been proposed to be subject to cleavage at a degenerate site during the uncoating (endosome-cycle); its proteolysis together with that of some of the hexon particles would result in the entry of the virion into the cytoplasm (see section 1.3.1).

Protein VIII

Protein VIII is of relatively small size, 15 kD, and its exact function as a monomer in the virion is not yet understood. Approximately 211 copies of the protein (van Oostrum & Burnett, 1985) are found in association with hexons at the inner face of the capsid (Everitt *et al.*, 1975) and studies with mutant adenoviruses suggest that this protein may play a role in the stabilisation of the virion (Liu *et al.*, 1985). Webster *et al.* (1989a) reported that there are three potential viral protease cleavage sites on the 25 kD precursor (pVIII), however, the order of cleavages in its maturation has not yet been characterised.

Protein IX

The 14 kD, 139 aa, protein IX (Aleström *et al.*, 1980) is not only of similar size to protein VIII, but is also thought to contribute to the stabilisation of the capsid structure, as revealed by experiments with thermolabile virions lacking the protein (Colby & Shenk, 1981). One virion contains approximately 247 copies of protein IX (van Oostrum & Burnett, 1985) found on the outside of the capsid in association with GON hexons. Together with protein IVα2, protein IX is a structural component of the virion,

which is not transcribed from the Major Late Promoter but as an intermediate gene prior to the onset of late transcription (Crossland & Raskas, 1983). Recent studies also suggest additional roles for protein IX as a transcriptional activator and as a component reorganizing nuclear structures for the benefit of viral infection (review: Parks, 2005).

1.2.2 Core proteins

Similarly to the adenovirus capsid, the protein components of the core are structurally organised, as indicated by Brown *et al.* (1975). The spatial organisation of the core polypeptides is depicted in Figure 1 according to generally accepted views.

Terminal protein, TP

Each 5'-end of the dsDNA adenoviral genome contained in the core is attached to the terminal protein, TP, via 5'phosphodiester bonds (King & van der Vliet, 1994 and references therein). The terminal protein is synthesised as an 80 kD precursor, pTP, processed by the protease via an intermediate iTP into its mature 55 kD form (Challberg & Kelly, 1981, Tremblay *et al.*, 1983, Webster *et al.*, 1994). The importance of the pTP as a component of the adenovirus DNA replication machinery is discussed in further detail in section 1.3.4.

Protein V

Protein V is a minor core protein (Brown *et al.*, 1975) and the only core protein not processed by the viral protease into its mature form. Approximately 160 copies of the 41.6 kD protein are found (per virion) in association with the penton and protein VI (Chatterjee *et al.*, 1985, van Oostrum & Burnett, 1985). This protein most likely functions as a link between the capsid and core structures by 'coating' the protein VII-DNA complex (Everitt *et al.*, 1975), as supported by its non-specific DNA-binding ability (Russell & Precious, 1982). Recent studies on protein V have identified several nuclear and nucleolar targeting sequences (Matthews & Russell, 1998, Matthews, 2001), which are evident in the lysine and arginine rich N and C-termini, respectively.

Protein VII

With over 800 copies per virion (van Oostrum & Burnett, 1985), protein VII is the major component of the core and like protein V, is highly basic in nature. The mature 19 kD VII is derived from the 22 kD precursor pVII via cleavage by the viral protease (Anderson, 1990, Houde & Weber, 1990). In the core, this arginine/alanine-rich polypeptide is closely associated with viral DNA (Russell & Precious, 1982), and perhaps evenly distributed around the DNA molecule (Everitt *et al.*, 1975). It is thought that protein VII could be a histone-like protein of the virus (Russell & Kemp, 1995). The identified nuclear and nucleolar targeting signals in protein VII are most likely to be involved in the delivery of the Ad genome to the nucleus following capsid dissociation (Lee *et al.*, 2003). Furthermore, the aforementioned authors made an interesting observation that pVII co-localises with chromosomes.

Protein μ

Approximately 125 μ proteins are found in the core of a single adenovirus particle (van Oostrum & Burnett, 1985). The adenovirus protease matures the 11 kD (79 amino acid) precursor μ into a 3 kD fragment (Weber, 1995 and references therein). As with the other core components, μ is a highly basic protein and found in association with protein V and VII and with viral DNA (Hosokawa & Sung, 1976, Chatterjee *et al.*, 1985). Recent subcellular localisation experiments have shown that the pμ is a nucleolar protein with its target signal contained within the 19 aa μ sequence (Lee *et al.*, 2004).

Protein IVα2

Protein IVα2 is transcribed from the intermediate gene transcript (delayed early) and its expression is required for the activation of Major Late Promoter (Crossland & Raskas, 1983, Lutz & Kedinger, 1996). This ~54 kD protein is a minor component of the virion (Weber *et al.*, 1983), present in mature as well as assembly intermediates of the adenovirus particles (Winter & D'Halluin, 1991). IVα2 has an affinity for viral DNA (Russell & Precious, 1982) and its localisation in the nucleolus, in addition to being found in the nucleoplasm, has been suggested to indicate an additional role in virus infection, which is yet to be revealed (Lutz & Kedinger, 1996).

Protease

A crucial component of the infectious adenovirus virion is the 23 kD protease, which is responsible for the maturation of structural pre-proteins. The discovery of a temperature sensitive Ad mutant *ts*1 in 1976 (Weber) suggested the existence of an adenoviral endoprotease; the virion particles formed at a nonpermissive temperature of 39°C contained unprocessed structural proteins and were non-infectious following their failure to uncoat. The *ts*1 mutant was subsequently mapped to the L3 late region and identified as a single C/T transition at position 137 resulting in a Proline to Leucine change in the gene encoding the protease (Yeh-Kai *et al.*, 1983). Subsequently, the recombinantly expressed, 204-amino-acid Ad2 protease was shown to possess *in vitro* activity (Anderson, 1990, Houde & Weber, 1990). The role of the protease in adenovirus lifecycle is discussed in more detail in section 1.4.

1.3 Productive Adenovirus infection

1.3.1 Attachment, penetration and uncoating of the virion

The entry of adenovirus into a host cell, for successful replication, is a process requiring a stepwise dismantling of the virion structure (Figure 2A). First, the binding between the globular fiber 'knob' and a cellular receptor assures the adsorption of the virion to a host cell surface (Louis *et al,* 1994). The primary receptor for Ad2 and Ad5 is a 46 kD transmembrane protein from an immunoglobulin gene family, which is also referred to as a coxsackie-adenovirus receptor (CAR), following the reported binding by both coxsackie B viruses and subgroup C adenoviruses (Bergelson *et al.*, 1997, Tomko *et al.*, 1997, Tomko *et al.*, 2000). It has also been proposed that, in the absence of CAR receptors, subgroup C adenoviruses are capable of using major histocompatibility complex class I (MHC-I) $\alpha 2$ subunit as an alternative cellular receptor (Hong *et al.*, 1997), although this has been since disproved by McDonald *et al.* (1999). Furthermore, since Ad37 from subgroup D and Ad11 from subgroup B have been reported to bind α(2-3)-linked sialic acid saccharides on glycoproteins (Arnberg *et al.*, 2000) and membrane cofactor CD46 (Segerman *et al.*, 2003), respectively, adenovirus serotypes are likely to employ different receptors according to their cellular tropism and pathogenicity.

Following the attachment, endocytosis of the virus particle via clathrin-coated vesicles ensues (Greber *et al.*, 1993). The penton base with its RGD-motif interacts with secondary receptors, cellular integrins $\alpha v\beta 3$ and $\alpha v\beta 5$, promoting the internalisation of the virion (Bai *et al.*, 1993, Wickham *et al.*, 1993). According to Wang *et al.* (1998), successful internalisation of the Ad virion also requires dynamin, a 100 kD cytosolic protein involved in the regulation of clathrin-coated pit pathway.

The receptor-mediated endocytosis is followed by a subsequent disintegration of structural components of the virion (Greber *et al.*, 1993). During this uncoating process, fibers are the first structural proteins to dissociate followed by some of the penton base complexes and stabilising components, proteins IIIa, VIII and IX. An acidification of the

endosome has been proposed to cause a change in the structure of the penton base thereby triggering the release of the partly-uncoated virion into the cytosol (review: Greber, 1998). As the virion penetrates into the cytosol, the reduced environment of the host cell is believed to re-activate the viral protease resulting in the degradation of VI (Cotten & Weber, 1995, Greber, 1998). Cleavage of VI at an additional, degenerate consensus site (possibly at position, $LASG^{54}$-ISGV) is thought to weaken the capsid structure and to unfasten the DNA from the capsid wall, in preparation for its release at the nuclear pore (review: Greber, 1998, Ruzindana-Umunyana *et al.*, 2002).

Following the detachment of several structural components, the capsid finally disassembles at the nuclear pore complex (NPC) where the transport of the viral DNA to the nucleus takes place (Greber *et al.*, 1997, Trotman *et al.*, 2001). Docking of the capsid to the NPC, and more specifically interacting with the CAN/Nup214 NPC-filament protein has been shown to be necessary for Ad DNA import (Saphire *et al.*, 2000, Trotman *et al.*, 2001). Furthermore, the hexons on the capsid at the NPC are thought to interact with nuclear histone H1, which in turn interacts with H1 import-factors importin7 and importinβ (Trotman *et al.*, 2001). While this results in the nuclear import of hexons, the viral DNA could be nuclear transported via an association with the basic core proteins V, VII and μ, which carry reported nuclear or nucleolar localisation signals (Matthews & Russell, 1998, Lee *et al.*, 2003, Lee *et al.*, 2004). Recently, a cellular transport protein p32, which interacts with core protein V, has been proposed as the candidate shuttling component responsible for the nuclear transport of

Figure 2 (A). The entry and uncoating process of the adenovirus type 2 virion. Figure is based upon the current view on the order of events and components involved (adapted from that by Greber *et al.*, 1993, Greber, 1998, Trotman *et al.*, 2001).

Figure 2 (B) & (C). Adenovirus gene expression and its genome organisation.
(B) The division of gene expression into early, E and late, L phases.
(C) The schematic representation of adenovirus type 2 genome indicates the localisation of early and late transcripts as well as individual genes encoded. The arrowheads show the direction of transcription and the dashed line indicates that each region encodes several spliced mRNAs. (Figure adapted from that in Dimmock & Primrose, 1994).

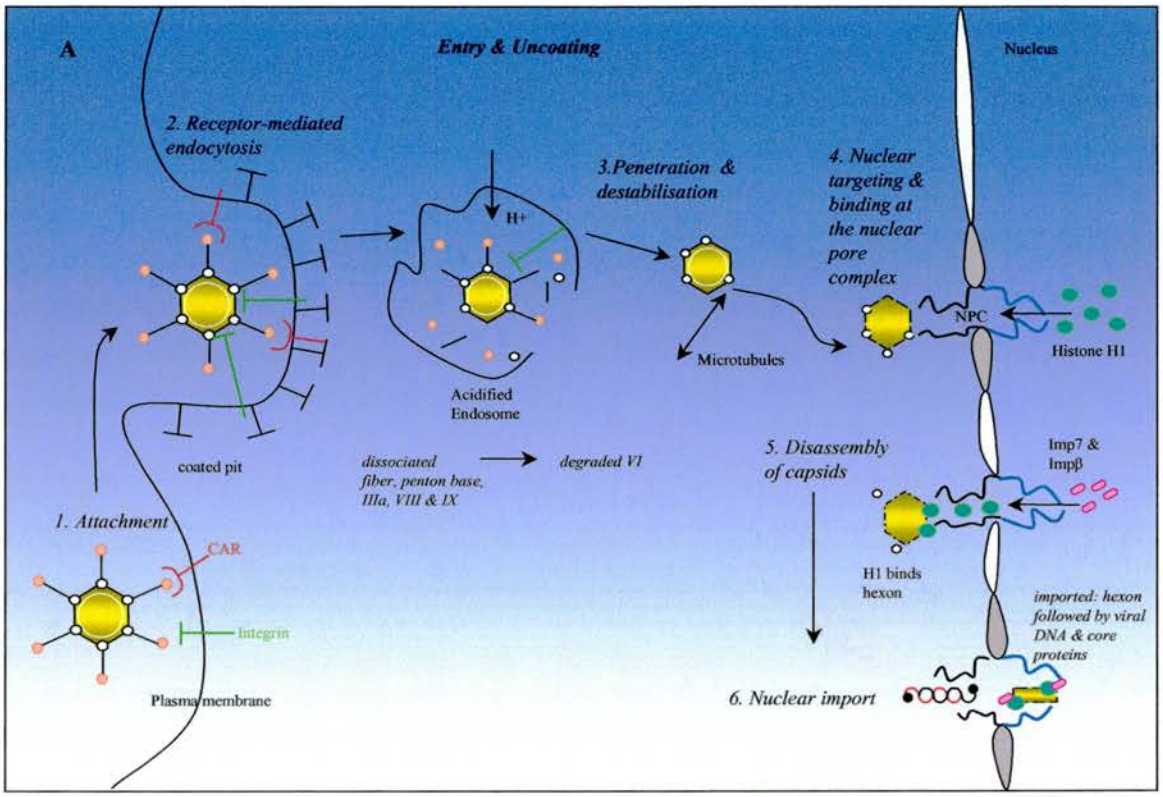
A
Entry & Uncoating
Nucleus
2. Receptor-mediated endocytosis
3.Penetration & destabilisation
4. Nuclear targeting & binding at the nuclear pore complex
H+
Acidified Endosome
Microtubules
NPC
Histone H1
coated pit
dissociated fiber, penton base, IIIa, VIII & IX
degraded VI
5. Disassembly of capsids
Impβ
1. Attachment
CAR
Integrin
Plasma membrane
H1 binds hexon
imported: hexon followed by viral DNA & core proteins
6. Nuclear import

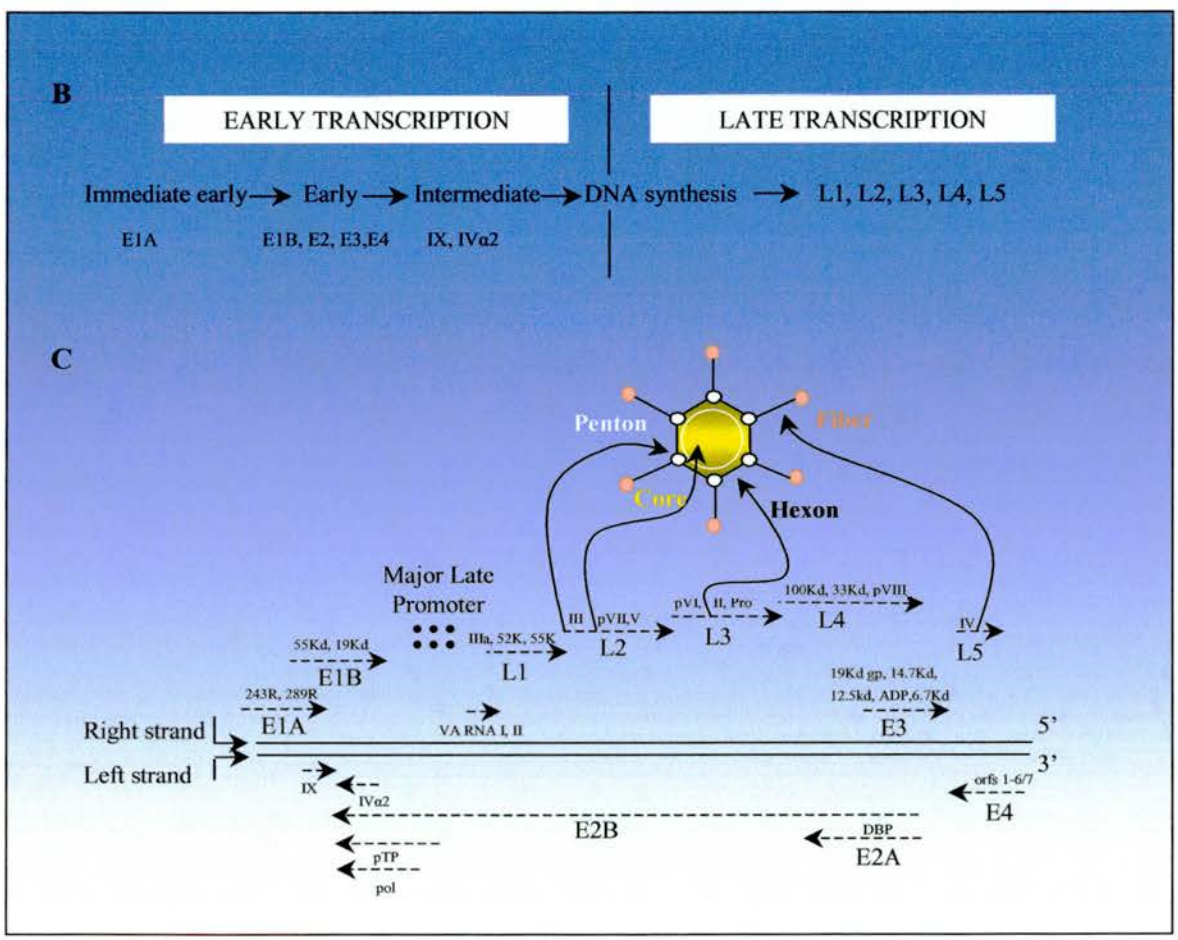
B
EARLY TRANSCRIPTION
LATE TRANSCRIPTION
Immediate early → Early → Intermediate → DNA synthesis → L1, L2, L3, L4, L5
E1A
E1B, E2, E3,E4
IX, IVa2
C
Penton
Fiber
Core
Hexon
Major Late Promoter
55Kd, 19Kd
E1B
IIIa, 52K, 55K
L1
III
pVII,V
L2
pVI, II, Pro
L3
100Kd, 33Kd, pVIII
L4
IV
L5
243R, 289R
E1A
VA RNA I, II
19Kd gp, 14.7Kd, 12.5kd, ADP,6.7Kd
E3
Right strand
Left strand
5'
3'
IX
IVa2
E2B
orfs 1-6/7
E4
DBP
E2A
pTP
pol

viral DNA (Matthews & Russell, 1998). For a successful intracellular passage from the cytoplasm to the nucleus, the Ad5 virion is also reported to interact with microtubule cytoskeleton and dynein (Leopold *et al.*, 2000).

Once in the nuclei, the Ad chromatin-like genome binds to the cell nuclear matrix (NM), a process mediated by the covalently attached viral TP (as well as pTP later on during replication) (Fredman & Engler, 1993), which complexes with a cellular, multifunctional pyrimidine synthesis enzyme, CAD (*c*arbamyl phosphate synthetase, *a*spartate transcarbamylase, and *d*ihydroorotase) (Angeletti & Engler, 1998). As proposed by the authors, this interaction between the components may serve to chain the viral genome in the vicinity of cellular factors necessary for replication. Furthermore, Ad infection proceeds as transcription and replication complexes form at discrete foci on the NM (Puvion-Dutilleul *et al.*, 1992).

1.3.2 Transcription of Adenoviruses

Adenovirus gene expression, similar to that of *Papovaviridae*, a family of circular dsDNA viruses including simian virus type 40 (SV40), can be divided into two main phases: early and late phase that is pre-and post-DNA synthesis, respectively (review: Dimmock & Primrose, 1994). More specifically, there are in fact four temporal sub-phases (see Figure 2B & 2C). Early transcription takes place from five early regions, on both DNA strands, resulting in the synthesis of several mRNAs, which are further subject to splicing events. After the expression of immediate early transcription unit, E1A, the delayed early genes of E1B, E2, E3 and E4 are transcribed. Following the onset of virus DNA replication, around 6-8 h after initial infection (Crossland & Raskas, 1983), the transcription of intermediate genes IVa2 and IX ensues. Subsequently, the expression of late genes from the Major Late Promoter (MLP) follows, encoded on the right side of the Ad genome. The order of events in adenovirus gene expression will now be discussed in more detail.

1.3.3 Early gene expression

Virus-encoded *trans*-acting regulatory factors control the transcription of the Ad genome and are crucial for successful Adenovirus replication. The immediate early,

E1A proteins are necessary for the transcriptional activation of early genes, which are required for replication (E2 gene products) and for the conversion of the host cell into a productive environment for the viral infectious cycle. The role of the E1A 289R $^{(13S)}$ and E1A 243R $^{(12S)}$ proteins is to directly or indirectly affect cellular proteins involved in cell cycle and to interfere with cell regulation mediated by NF-κB and p53, a nuclear transactivator and a tumour suppressor, respectively (review: White, 2001).

The functional domains of the E1A proteins, especially the constant regions CR 1-3, represent sites through which the proteins interact with several important cellular regulators, some of which are shown in Figure 3A (note: only E1A 289R contains CR3). By interacting with a signal transducer and activator of transcription, STAT-1, via its N-terminus, E1A protein aims to suppress the host immune response (Look *et al.,* 1998). Binding to the cell growth regulator Rb (retinoblastoma protein), and to the transcriptional co-activator p300, on the other hand, results in the cell cycle deregulation and entry into S-phase, which enables viral DNA synthesis (review: White, 2001). Via its CR2, the E1A binds to the UBC9 protein, involved in the small ubiquitin-like modifier (SUMO) pathway, possibly in order to interfere with the required p53 modification (Hateboer *et al.*, 1996, Rodriguez *et al.*, 1999). The CR3 region of the E1A 289R is responsible for transactivating the expression of early units E2, E3, E4 and that of some cellular genes, as exemplified by the reported interaction with a multiprotein complex Sur-2 (Boyer *et al.*, 1999).

However, due to the fact that the cell-cycle deregulation activities of E1A are pro-apoptotic, there is a requirement for the expression of early E1B 55K and 19K proteins. The latter, a homologue of the cell survival gene Bcl-2, counteracts the induction of apoptosis caused by E1A by binding to pro-apoptotic Bax and Bak proteins, which cause caspase activation and mitochondrial death signalling (review: White, 2001). The E1B 55K protein often works in cooperation with two proteins encoded on the E4 cassette, orf3 and orf6, which regulate the complex splicing of Major Late transcripts (review: Leppard, 1997). An example of this is the interaction between E4 orf6, 34 kD protein and E1B 55K protein and their binding to the cellular tumour suppressor protein p53 to deter its stimulation of apoptosis (Grand *et al.,* 1999, Querido *et al.*, 1997). The role of E1B 55K and orf6 proteins as regulators, which together alter the mRNA transport to favour that of late viral message, is further discussed in section 1.3.5.

From the remaining E4 genes, the orf6/7 gene product has been shown to function as a downregulator of E1A activity as well as a transactivator stabilizing the binding of a cellular transcription factor E2F at the E2 early promoter (review: Leppard, 1997). The E4 orf1 protein from adenovirus serotype 9, on the other hand, contributes together with E1A and E1B to mammary tumorigenesis in rats (Javier, 1994). While the full-transformation and tumour formation of primary rodent epithelial cells, characterised in subgroup A adenoviruses, is dependent upon the cooperation between the E1A and E1B oncogenes (review: Lucher, 1995, White, 2001), it seems that Ad serotype 9 represents an exception requiring an additional, E4 component (review: Leppard, 1997).

The role of the E3 gene products, whose transcription is induced by the 289R E1A protein, is to prevent host cell's antiviral defences through different strategies (review: Russell, 2000). The E3 19 kD glycoprotein, for instance, prevents the infected cell from being identified and destroyed by the cytotoxic T lymphocytes (CTL). It binds to the major histocompatibility complex (MHC) class I antigens therefore preventing their transport and display on the cell surface leading to CTL-response (review: Philipson, 1995, review: Ploegh, 1998). Conversely, the E3 11.6 kD protein, also known as the adenovirus death protein (ADP), enhances cytolysis and promotes the release of progeny virions from infected cells (Tollefson *et al.*, 1996).

The E2 early gene products, E2A and E2B, encode for the essential viral replication components, i.e. DNA binding protein (DBP) and pTP, and polymerase, respectively (review: Lucher, 1995). E1A products stimulate their transcription and as the E2 gene products accumulate, the initiation of replication can begin.

1.3.4 DNA replication

The linear adenovirus double-stranded DNA is replicated by a strand-displacement mechanism initiated at the terminal replication origins (*ori*) by protein priming (for review: Hay & Russell, 1989, Hay 1996). The origin of DNA replication is within the inverted terminal repeats (ITRs), which constitute around a 100 bp region depending on the adenovirus serotype (Flint *et al.,* 1976). Within the *ori*, there is a core and an auxiliary region containing *cis*-acting DNA sequences recognised by the different components of the replication machinery (Figure 3B). The core region is the minimal

Figure 3 (A). Schematic diagram of $E1A^{13S}$ and $E1A^{12S}$ proteins and their binding regions, CR1-CR3. Some proteins with which E1A proteins are known to interact are illustrated: see text for further description. (Diagram adapted from that by Russell, 2000).

Figure 3 (B). Initiation of replication of Ad2 DNA synthesis at the origin. The order of events and proteins participating in the initiation are illustrated. Adenovirus terminal and pre-terminal proteins are abbreviated to TP and pTP, respectively, Ad DNA polymerase to DNA pol, DNA binding protein to DBP and nuclear factors I & III to NFI and NFIII. (Figure adapted from that by Hay, 1996).

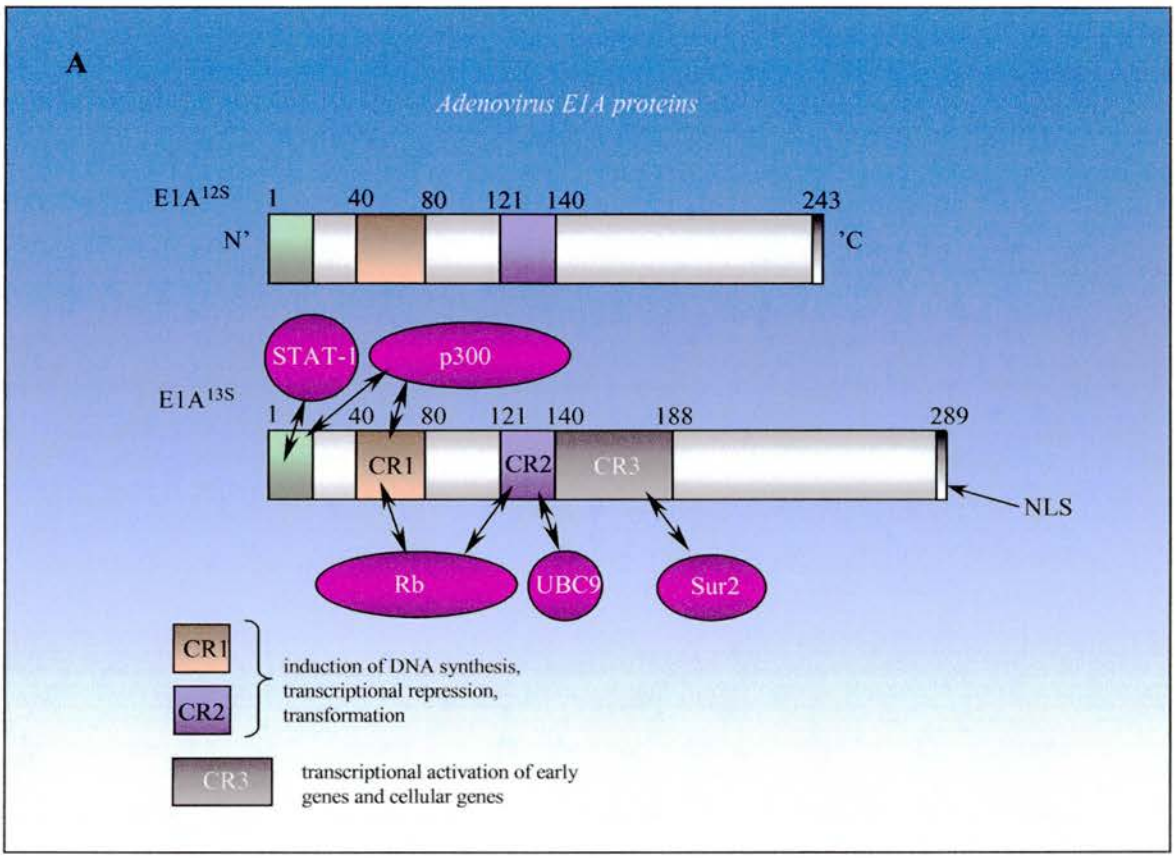
A
Adenovirus E1A proteins
E1A12S
1
40
80
121
140
243
N'
'C
STAT-1
p300
E1A13S
1
40
80
121
140
188
289
CR1
CR2
CR3
NLS
Rb
UBC9
Sur2
CR1
CR2
induction of DNA synthesis, transcriptional repression, transformation
CR3
transcriptional activation of early genes and cellular genes

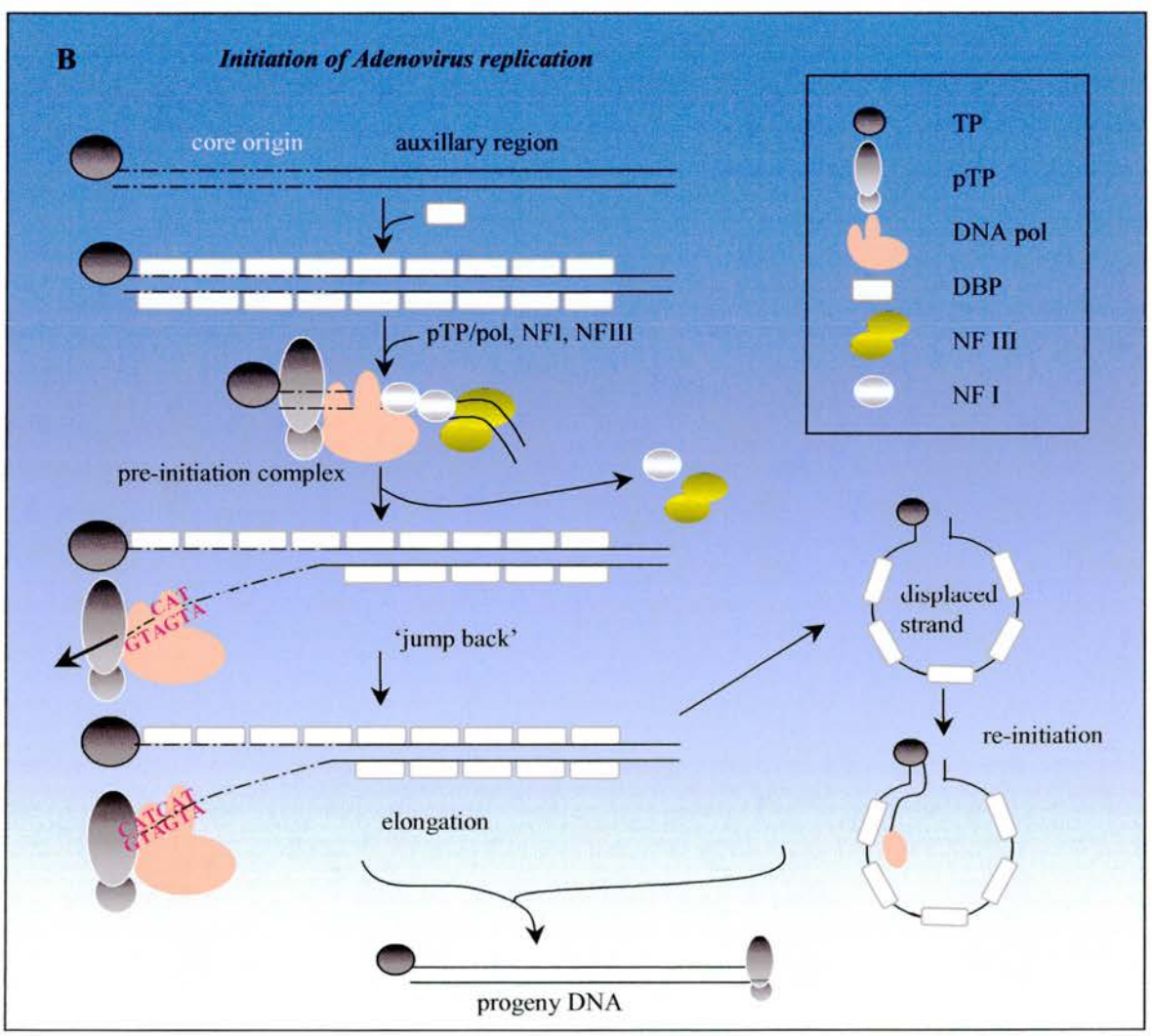
B
Initiation of Adenovirus replication
core origin
auxillary region
pTP/pol, NFI, NFIII
pre-initiation complex
CAT
GTAGTA
'jump back'
CATCAT
GTAGTA
elongation
progeny DNA
displaced strand
re-initiation
TP
pTP
DNA pol
DBP
NF III
NF I

replication origin, consisting of 18 bp in Ad2, followed by the auxiliary region, which has further stimulatory effects on DNA replication. The requirement of the auxiliary region (19-50 bp) seems to be, however, serotype-specific following the discovery that Ad4 compared to Ad2, requires only the core of the origin and no cellular factors for the initiation of its replication (Hay, 1985).

The procedure of DNA replication is initiated by the covalent attachment of deoxycytidine monophosphate (dCMP) to the serine residue 580 of the pre-terminal protein (pTP) by viral DNA polymerase (Ad pol) (review: Hay, 1996). The 3'hydroxyl group of pTP–dCMP is then used as a primer for the synthesis of a new strand of DNA by Ad pol. Other cellular and viral factors are, however, required for, or function to, stimulate the replication. The proposed order of initiation of replication begins with the association of the 72 kD DNA-binding protein with viral dsDNA containing 5'end TP, which in turn enhances the binding of a 47 kD cellular protein, nuclear factor NFI (Nagata *et al.*, 1982), for its recognition site at auxiliary region of *ori* (Stuiver & van der Vliet, 1990). Subsequently, NFI interacts with Ad pol and the tightly bound heterodimer of pTP/Ad pol associates at the core of *ori* at bp 9-18 (Chen *et al.*, 1990). Further interaction of pTP/Ad pol with the conserved DNA-binding domain POU of the nuclear factor III (also known as NFIII or Oct-1) stimulates the formation of the pre-initiation complex at *ori* (Coenjaerts *et al.,* 1994). Following this, the distally positioned NFIII (at bp 39-48) and the NFI (at bp 23-38) dissociate and the origin is unwound for the template of DNA synthesis, possibly catalysed by the bound DBP (review: Hay, 1996). The pTP/Ad pol complex then becomes specifically positioned for initiation; the acceptor serine of pTP is opposite the GTA sequence at positions 4-6 of the template (genome). The resulting pTP-CAT intermediate then 'jumps backwards' to positions 1-3 of the genome for the synthesis of the first CAT sequence (King & van der Vliet, 1994). While using one strand of parent DNA as a template, elongation proceeds with the pTP-dCMP-Ad pol initiation complex and with the help of DBP (Stuiver and van der Vliet, 1990 and references therein) and nuclear factor NFII, a cellular topoisomerase I (review: Lucher, 1995, Hay, 1996). The non-template strand of parent DNA subsequently dissociates forming 'pan-handle' structures as the ITRs of the ssDNA anneal. These circular structures can function as templates for re-initiation (Hay *et al.*, 1984) leading to the synthesis of more progeny DNA, as illustrated in Figure 3B.

1.3.5 Late gene expression

Following the onset of viral DNA replication, the IVα2 and IX intermediate gene products (Crossland & Raskas, 1983), which function as transcriptional, late-phase dependent, activators of the Major Late Promoter (MLP), are transcribed (Lutz & Kedinger, 1996, Lutz *et al.*, 1997). The five late transcripts L1-L5 synthesised under the control of MLP (note however that L1 52K and 55K are also expressed during the early phase of infection) are expressed only from replicated and not from parental genome, DNA template. This is likely to be guaranteed by a change in DNA structure or its associated components during replication, which serves as a *cis*-acting requirement for early-to-late switch in transcription (Thomas & Mathews, 1980). Following the transcription of the late transcripts by cellular polymerase II, a complex series of splicing events, within each late transcript family, generates the distinct mRNAs encoding viral structural components (review: Lucher, 1995).

Viruses have developed different strategies to assure the synthesis of viral polypeptides over those of the host cell. Influenza virus polymerase physically alters the cellular mRNAs by removing their 5-end cap structure for the synthesis of its own polyadenylated mRNAs (review: Whittaker *et al.*, 1996). Unlike vaccinia virus, which mediates the degradation of host cell mRNA (Rice & Roberts, 1983), adenovirus infected and uninfected cells contain similar amounts of cellular mRNA. However, at late phase of Ad infection, 90-95% of the mRNA reaching the cytoplasm is adenoviral (review: Philipson, 1995). Adenoviruses accomplish this by enhancing the rate of cytoplasmic export of the viral mRNAs by the action of a complex consisting of two early proteins, E1B 55K and E4 orf6 (review: Leppard, 1997). This complex also blocks the transport of newly synthesised cellular mRNAs. However, since some cellular mRNA are known to escape the transport block (such as that for hsp 70 gene family and β-tubulin) (Moore *et al.,* 1987), the translational control mediated by viral proteins on the polyribosomes functions as the second checkpoint assuring the preferential synthesis of viral proteins.

Once in the cytoplasm, viral mRNA is preferentially translated over cellular mRNA by the actions of at least three factors encoded in the adenovirus genome. Virus-associated RNAs, VA RNA_I (major species) and VA RNA_{II} (minor species) are viral genes whose synthesis is induced by E1A (review: Philipson, 1995). They are

transcribed by cellular RNA polymerase III in large amounts late in infection and contribute to the viral translational control by combating the inhibitory consequences induced by the virus infection. In response to adenovirus infection, the cellular protein kinase, DAI, capable of inhibiting translation through phosphorylation of the α-subunit of the translation initiation factor eIF-2α, becomes activated by dsRNA. VA RNA_I counteracts DAI by physically binding to it (review: Mathews & Shenk, 1991).

The 200-nucleotide-long tripartite leader sequence, formed by the splicing of three small exons in the 5'noncoding region of all viral mRNAs from the MLP, is also a component of the translational control. The adenoviral tripartite leader sequence confers translation independent from the initiation factor eIF-4F complex (Dolph *et al.*, 1990), which consists of RNA helicase, cap-binding protein (CBP or eIF-4E) and p220 protein parts. While eIF-4F is required for cap-dependent, cellular mRNA translation, adenoviruses further eliminate competition by causing underphosphorylation of CBP thereby inactivating the complex (Huang & Schneider, 1991). Recent experiments have shown that the adenovirus L4 100 kD protein contributes to this by blocking the binding of a Mnk1 kinase component required for the phosphorylation of the cap-binding protein (Cuesta *et al.*, 2004).

1.3.6 Nuclear translocation

Influenza virus, an enveloped single-stranded RNA virus, faces nuclear trafficking problems due to the spatial separation between genome replication and virion maturation taking place in the nucleus and plasma membrane, respectively. A series of nuclear import and export steps of the viral ribonucleoproteins (vRNPs), during influenza virus infection, rely on the cellular transport machinery. These steps are regulated by cellular and viral factors and the virus matrix protein M1 is considered the major regulator of the bidirectional traffic; the dissociation or association of M1 determines the import or export of the vRNPs from the nucleus, respectively (review: Whittaker *et al.*, 1996).

Likewise, adenovirus must orchestrate the transport of its synthesised late structural polypeptides from the cytoplasm to the nucleus where the virion assembly and maturation takes place (see Figure 4 for the overall outlook on adenovirus lifecycle). How does adenovirus accomplish this?

The nucleus of the eukaryotic cell, enclosed from the cytoplasm by the nuclear envelope (NE), is an important organelle containing genes that control the cell's function. It is therefore not surprising that the uptake of proteins by the nucleus is a selective process. The nuclear pore complex (NPC), composed of approximately 30 proteins or nucleoporins, spans through both the inner and outer nuclear membrane. NPC functions as a channel allowing free diffusion of small molecules while also taking part in the receptor-mediated nucleo-cytoplasmic transport of proteins. The latter, a type of active, energy-demanding transport of proteins, is mediated by the nuclear localisation signal(s) (NLS) within the transported polypeptides (review: Garcia-Bustos *et al.,* 1991). While NLS on proteins interact with cytoplasmic import receptors, such as the importin-β, the receptors via their binding domains mediate interactions with phenylalanine-glycine (FG) repeat-domains found on many NPC nucleoporins (review: Fahrenkrog *et al.*, 2004). A single NPC can reportedly support 1000 translocation events per second (Fahrenkrog *et al.*, 2004 and references therein) and, on the basis of the structure of the central pore, NPC is able to confer translocation of molecules with a diameter up to ~40 nm (Panté & Kann, 2002).

Identified NLS governing the posttranslational transport from the cytoplasm contain some unifying protein primary structure motifs. NLS are often short sequences (5-10 aas) rich in positively charged amino acids, lysines and arginines, located anywhere along the protein sequence (review: Garcia-Bustos *et al.*, 1991). In comparison to NLS, nuclear export signals (NES) are typically leucine-rich stretches of amino acids promoting the exit from the nucleus via NPC. The human immunodeficiency virus type 1 (HIV-1) Rev protein is an example of a nuclear-cytoplasmic shuttling protein containing both NLS and NES sequences required for its role in transporting viral transcripts (Meyer & Malim, 1994). The presence of multiple NLS or NES may enable proteins to interact with several transport receptors simultaneously, and thereby accelerating the translocation process (Fahrenkrog *et al.*, 2004).

In addition to nuclear signals of mammalian and yeast origin, several NLS for viral proteins have been characterised (review: Garcia-Bustos *et al.*, 1991). The simian virus 40 (SV40) T antigen contains one of the best-defined NLS, a sequence of Pro-Lys-Lys-Lys-Arg-Lys-Val between residues 425-431 (Kalderon *et al.*, 1984). The herpes simplex virus type 1 (HSV-1) protease (Pra) has also been shown to contain a NLS

(Gly-Lys-Arg-Arg-Tyr) along the UL26 gene, in the middle of the ICP35 polypeptide. The two domains of the HSV-1 protease co-operate for nuclear translocation; the proteolytic N-terminal domain (No) requires an association with the C-terminal (Na) domain in order to successfully accumulate into the nucleus (Gao *et al.*, 1994).

Adenovirus components and viral DNA have been shown to gain access through NPC (Greber *et al.*, 1997) and several adenovirus proteins such as the pre-terminal protein (Zhao & Padmanabhan, 1988), DNA-binding protein (Morin *et al.*, 1989), E1A protein (Lyons *et al.*, 1987), fiber (Hong & Engler, 1991) and core proteins V and VII (Matthews & Russell, 1998, Lee *et al.*, 2003) have NLS included in their sequences. Following the observation that the pTP locates not just itself to the nucleus but is also capable of directing Ad DNA polymerase to the nuclear matrix (Zhao & Padmanabhan, 1988), it is likely that those late adenoviral proteins carrying NLS form complexes with those lacking signals and therefore function as essential transporters.

1.3.7 Assembly and maturation

After their translation, the majority of late viral polypeptides are efficiently transported to the nucleus, within 6 min following their release from polyribosomes (Velicer & Ginsberg, 1970). The first assembly-related events do, however, begin already in the cytoplasm. The hexon trimers are formed within 3-4 min after their synthesis (Horwitz *et al.*, 1969) following a 1:1 complex with L4 100 kD protein (Oosterum-Dragon & Ginsberg, 1981), after which they accumulate in the nucleus with the help of another structural component, the precursor of protein VI (Kauffman & Ginsberg, 1976, Wodrich *et al.,* 2003). Additionally, the formation of capsomers from the penton base and the trimerisation of fibers have been proposed to occur prior to their nuclear translocation (Horwitz *et al.*, 1969, review: D'Halluin, 1995). Once in the nucleus, the assembly of virions proceeds at distinct nuclear sites from those used in viral DNA replication (Puvion-Dutilleul *et al.*, 1992).

Although the exact order of addition of some of the viral structural proteins has not been established, mutational and isolation studies indicate that the assembly of the adenovirus virions proceeds via intermediates (review: Greber, 1998). First, empty capsids consisting of hexons, pentons, and other structural and scaffolding proteins, are formed. This is followed by the accumulation of light intermediate particles. These

Figure 4. Synopsis of the adenovirus lytic cycle and the major events within.

[1] The virus attaches to the host-cell CAR receptors via its fiber. [2] The particle is endocytosed while the viral penton base interacts with cellular integrins. Inside the clathrin-coated vesicle, degradation of some viral sructural proteins begins, which continues until the virion enters the cytoplasm. [3] The partly-uncoated virion finally disassembles at the nuclear pore, followed by the release of the viral DNA genome and transport of it, possibly mediated by the core proteins, to the nucleus. [4] The E1A immediate early gene is the first to be transcribed by the cellular RNA polymerase II, and subject to alternative splicing. [5]. The $E1A^{12S}$ and $E1A^{13S}$ proteins are translated by the cellular machinery, and transported to the nucleus [6] where they regulate viral and host-cell gene expression. [7] The $E1A^{13S}$ stimulates the transcription of viral early genes (E1B-E4) mediated by the cellular RNA polymerase II. [8] Following their transcription, the early mRNAs are translated on the ribosomes [9]. E2 proteins, which are necessary components of the viral DNA replication (Polymerase, DNA Binding Protein and pre-Terminal Protein), accumulate in the nucleus [10] and co-operate with host-cell proteins for efficient viral DNA synthesis [11]. The progeny DNA formed may serve as templates for further rounds of replication [12-13]. The onset of viral replication and the appearance of intermediate genes IX and IVα2 triggers the transcription of late genes from the Major Late Promoter [14]. The late mRNAs encoding the structural components of the virion are preferably exported to the cytoplasm by the action of two early proteins, E1B 55 kD and E4 Orf6 [15]. The translation of the late mRNAs requires the VA RNA_I (transcribed by RNA polymerase III since the beginning of the infection), which helps to avoid cellular defense mechanism as well as a late protein, L4 100 kD [16]. The hexon trimers and the penton base pentamers are already formed in the cytoplasm with the help of L4 100 kD protein, and then transported to the nucleus for assembly, along with other structural proteins [17]. The assembly of the virions via intermediates ensues in the nucleus, requiring scaffolding proteins and the packaging signal on the replicated DNA molecules. [18] The immature particles are rendered infectious as the viral endoprotease performes proteolysis of the viral pre-proteins. [19] The newly-synthesised virions are released from the lysed host cell following the disruption of the cytokeratin network by the viral protease and by the action of the E3 viral death protein. (Figure adapted from that by Flint *et al.*, 2000).

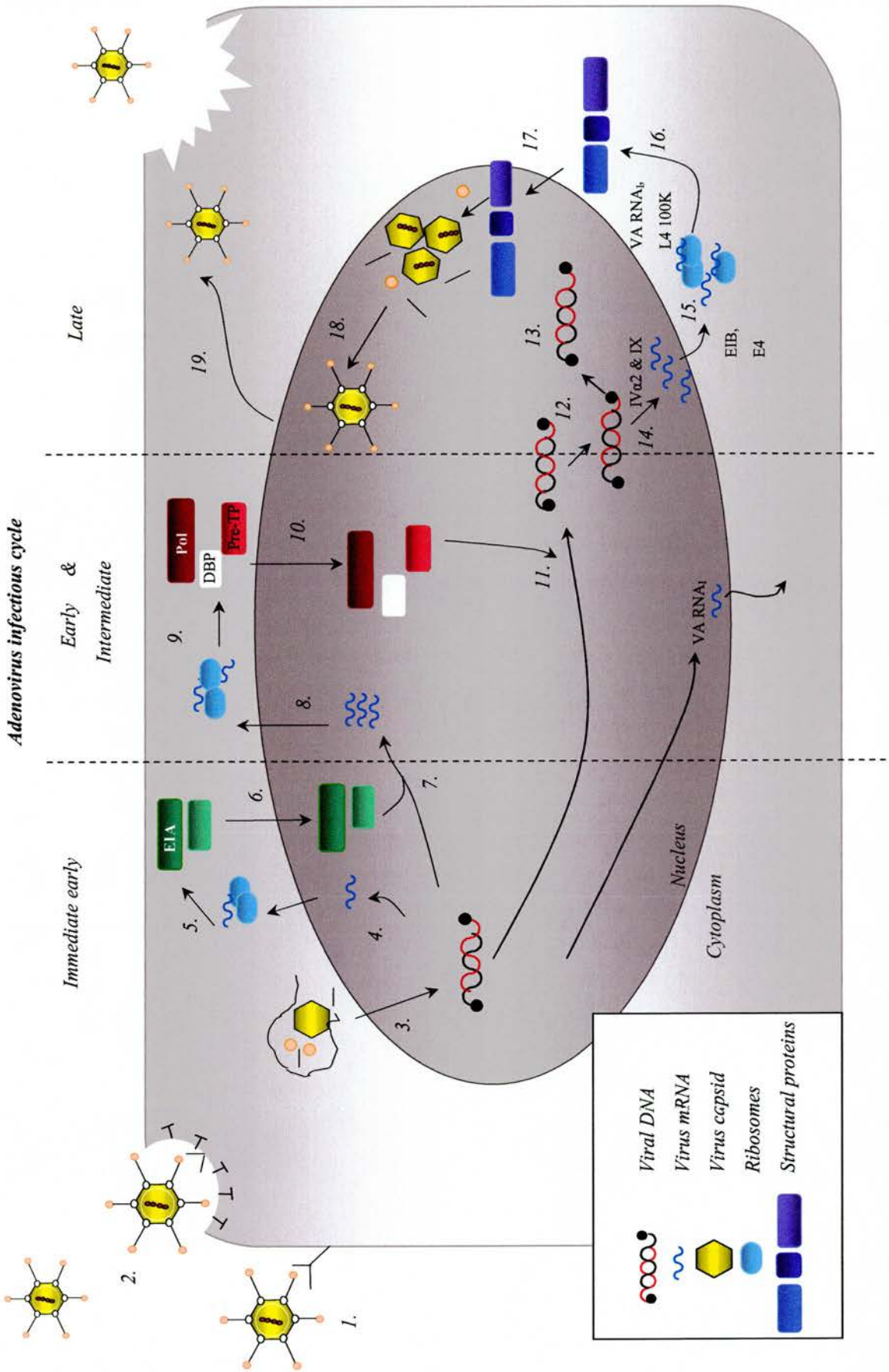
Adenovirus infectious cycle
Immediate early
Early & Intermediate
Late
Nucleus
Cytoplasm
EIA
Pol
DBP
Pre-TP
VA RNA$_I$
VA RNA$_{II}$
L4 100K
IVa2 & IX
EIB, E4
1.
2.
3.
4.
5.
6.
7.
8.
9.
10.
11.
12.
13.
14.
15.
16.
17.
18.
19.
Viral DNA
Virus mRNA
Virus capsid
Ribosomes
Structural proteins

particles contain, in addition to hexon, penton base and fiber, precursors of protein IIIa, VI and VIII as well as some scaffolding proteins not found in mature particles (33K, 39K and 50K). The light intermediates also contain a fragment of DNA, a *cis*-acting sequence rich in A-T repeats derived from upstream of the E1A promoter, which is required for packaging of the progeny genomes (Hearing *et al.*, 1987).

The next stage in adenovirus assembly is the formation of heavy intermediates from the light ones by the encapsidation of viral DNA linked to pTP, a process aided by the scaffolding proteins from the L1 region (52K, 55K and IIIa) (review: D'Halluin, 1995). At this stage, the scaffolding proteins 33K, 39K and 50K are released.

The subsequent assembly intermediates are the young virions containing core proteins, V VII and μ, together with other unprocessed precursor polypeptides. Finally, the L3 region 23 kD protease becomes activated inside the virus particle performing the crucial maturations of pre-proteins. This event renders a young virion into a mature infectious one. Also, at the very late stages, protein IX associates with the capsid while the 100 kD protein involved in scaffolding is lost (review: D'Halluin, 1995).

Unlike certain non-lytic enveloped viruses, such as retroviruses capable of budding from the host cell membranes, non-enveloped viruses such as adenoviruses and polioviruses need to promote lysis of the host cell for efficient release of the synthesised progeny virions (Dimmock & Primrose, 1994). Adenoviruses encode components, which promote successful host cell lysis late in the infection. One of the components is the adenovirus death protein (ADP), an 11.6 kD gene product from the delayed early transcription unit E3 (discussed earlier in 1.1.3). The virus-encoded protease also promotes the escape from the host cell by cleaving the cytoplasmic intermediate filament network (Chen *et al.*, 1993).

1.4 Adenovirus protease

Since the main objectives of work described in this thesis involve the 23 kD protease, its nature, function and regulation is now discussed in further detail.

1.4.1 Role of adenovirus protease in lytic infection

In a single Ad2 particle approximately 10±5 protease molecules (Anderson, 1990), basic in nature, are associated mainly with viral core structures and reportedly bind

DNA non-specifically (Everitt & Ingelman, 1984, Webster *et al.*, 1993). The Ad2 protease (AVP) performs proteolysis of at least six viral precursor proteins pVI, pVII, pVIII, pIIIa, pTP and pμ during virion assembly (Anderson *et al.*, 1973, Bhatti & Weber, 1979, Boudin *et al.*, 1980, review: Weber, 1995). In addition, the protease is known to be active during at least two other stages of the infection; during uncoating and entry into the host cell (Cotten & Weber, 1995, Greber *et al.*, 1996), and during the last stages of the infection by cleaving proteins of the cytoskeleton (cytokeratin 18), thereby promoting the release of the newly-synthesized virions from the host cell (Chen *et al.*, 1993).

An additional role for the adenovirus protease as a deubiquitinating enzyme during viral infection was recently discovered (Balakirev *et al.*, 2002). Given that the ubiquitin-dependent proteolysis is a major histocompatibility complex (MHC) class I antigen presentation- and antiviral defense-pathway, it would seem an apparent target for inhibition by viruses (review: Ploegh, 1998). A similarity between adenovirus protease and influenza B virus NS1 protein is that they both seem to target ISG15 (Balakirev *et al.*, 2002, Yuan & Krug, 2001), an ubiquitin-like protein induced by α/β-interferons. This could be a viral strategy for disarming at least a part of the host antiviral response.

1.4.2 Adenovirus protease cleavage specificity

On the basis of cleavages of the viral pre-proteins as well as of synthetic peptides, two types of consensus cleavage sites for AVP have been proposed: [1](M, L, I) XGG-G or [2](M, L, I) XGX-G (Webster *et al.*, 1989a, Anderson, 1990). Thus, the specificity of this enzyme is determined by P_4, P_2, P_1 and P_1' sites, whereas P_3 could be any amino acid with its side chain pointing away from the enzyme, as suggested by Webster *et al.* (1989a) and Ding *et al.* (1996). In 2002, Ruzindana-Umuyana *et al.* concluded that P_3 and P_1 were variable but never contained C, P, D, H, W, Y and C, P, G, M amino acids in type[1] consensus site, respectively or residues C, D, L, W and C, P, D, Q, H, Y, W in consensus cleavage site type[2], respectively. In fact, the GX-G type[2] consensus cleavage site is hydrolysed more efficiently than the type[1], GG-X site (Diouri *et al.*, 1996). The biological role for this type of preferential cleavage efficacy is well illustrated by the maturation of pVI by the protease at the GX-G site, resulting in the release of the

cofactor peptide (discussed in section 1.4.5), followed by the cleavage at the N-terminal GG-X site.

1.4.3 Adenovirus protease and the new clan of cysteine proteases

Processing of pre-proteins was first considered a trait associated with positive strand RNA viruses and retroviruses. However, following the discovery of AVP, it became apparent that DNA viruses could also encode for proteases (review: Kräusslich & Wimmer, 1988). Whether required to separate structural from non-structural proteins or to cleave host-cell proteins to advance the infection, different types of viruses possess representatives for the four main classes of proteases: retroviruses, such as HIV-1 code, for an aspartic protease (Anderson, 1999), picornaviruses for the 3C cysteine protease (review: Ryan & Flint, 1997), alphavirus for a serine protease in its capsid protein (review: ten Dam *et al.*, 1999) while hepatitis C virus codes for the NS2-3 metalloprotease (Grakoui *et al.*, 1993). A protease is assigned to a particular group on the basis of its active site nucleophiles, inhibitor profile and by comparison of its sequence and structure with those of established proteases (Rawlings & Barrett, 1994).

Initially, adenovirus protease was considered a chymotrypsin-like serine protease (Bhatti & Weber, 1979, Houde & Weber, 1990). Sequence analysis, site-directed mutagenesis and a peptide-based enzyme assay, however, demonstrated that it belonged to the cysteine class of proteases (Webster *et al.*, 1989a, Tihanyi *et al.*, 1993). An additional difficulty in the classification of AVP was its inhibitor profile, which diverges from those of classical serine or cysteine classes, and displays similarity with the rhinovirus 3C proteases from the picornavirus family (Tremblay *et al.*, 1983, Orr *et al.*, 1989, Webster & Kemp, 1993).

While attempting to establish the catalytic triad of the protease, sequence alignments of adenovirus serotypes revealed that only two of the eight cysteine residues present are truly conserved, Cysteine^{104} and Cysteine^{122} (Grierson *et al.*, 1994). Since substitutions at either one of these residues reduced protease activity by more than 95% (Grierson *et al.*, 1994), it appeared that both cysteine residues played an important role. Tryptophan fluorescence experiments further substantiated that Cys^{104} was involved in activation while Cys^{122} participated in catalysis (Jones *et al.*, 1996). The published crystal

structure of the protease (together with its cofactor, discussed later) confirmed this: His^{54}, Glu^{71} and Cys^{122} triplet form the catalytic triad (Ding *et al.*, 1996).

When published, the structure of AVP was found to deviate substantially from other cysteinyl proteases in the Protein Data Bank (Ding *et al.*, 1996). Despite its unique, overall protein fold, the spatial disposition of the AVP's active site amino acids appeared to be identical to that of the conventional cysteine protease papain. In addition, the Gln^{115} residue of AVP and the Gln^{19} of papain, believed to be involved in the formation of the oxyanion hole, have equivalent spatial positions in the active site. Therefore, AVP is believed to employ a catalytic mechanism similar to papain (review: Mangel *et al.*, 1997).

The Ad2 protease was in fact assigned to a new fifth and evolutionarily-distinct cysteinyl protease clan, CE, to which other proteases such as the Ulp-1 endopeptidase from *Saccharomyces cerevisiae* (SUMO-1 specific protease) and the African Swine Fever Virus protease have since been included (Rawlings & Barrett, 2000, Andrés *et al.*, 2001, Barrett & Rawlings, 2001). The characteristics shared by these proteases include N-terminal extensions (possibly involved in substrate specificity), the consensus cleavage site of GG-X, similarity in inhibitor profile, minor sequence similarity and clear structural homology between the members (López-Otin *et al.*, 1989, Li & Hochstrasser, 1999, Mossessova & Lima, 2000). Notably, the catalytic triad and their sequential order in the polypeptide are conserved. Unlike in the more conventional cysteine protease papain, the catalytic histidine precedes the cysteine in the primary protein motif of these proteases (Ding *et al.*, 1996). Interestingly, the crystal structure of the Ulp-1 endopeptidase includes its substrate Smt3 in the active site (Mossessova & Lima, 2000), which can modelled into the active site 'cleft' of the adenovirus protease.

1.4.4 Viral proteases and regulation of their activity

While the virus may benefit from encoding for its own protease, as opposed to relying on a non-specific cellular one, the dilemma with the regulation of the protease activity still exists. Since proteolysis is an irreversible process mediated by enzymes incapable of repairing errors, premature-activation of a protease would be detrimental for the success of the infection (review: Kräusslich & Wimmer, 1988). Consequently, viruses

have developed elaborate mechanisms in order to control the temporal and spatial activity of their proteases.

Human cytomegalovirus (hCMV), a β-herpesvirus, encodes for a 28 kD serine protease required for viral capsid formation and for viral replication (review: Holwerda *et al.*, 1997). The activity of hCMV protease molecule is dependent upon dimerization and the increased concentration of the protein components during capsid assembly may function as a temporal trigger leading to the formation of the active dimeric protease from the inactive monomers (Darke *et al.*, 1996). An interesting characteristic concerning the hCMV protease dimer–structure is that each subunit has a separate active site, which form away from the interface of the subunits (Chen *et al.*, 1996). Furthermore, an intramolecular disulphide bond formation near the active site, between Cys'138 and Cys'161, was shown to inhibit the activity of the hCMV protease *in vitro*, probably by obstructing the access of the substrate to the active site (Baum *et al.*, 1996). Hence, it is possible that once the protease is autoproteolytically cleaved from its precursor, oxidised and reduced surroundings and the non-active site cysteines may control the activity of the hCMV protease for the benefit of the infection.

There are some similarities between the hCMV protease and that of the human immunodeficiency virus type 1 (HIV-1), which cleaves itself from the Gag-Pol polyprotein and further processes precursor proteins into their mature form. The HIV-1 protease also relies on the concentration-dependent dimerization for its activation and the regulation of the protease activity has equally been proposed to occur by the modification of its conserved, non-catalytic cysteine residues (Davis *et al.*, 1996). However, unlike the hCMV dimer, the 22 kD HIV-1 dimer subunits interact to form one active site with Asp-residues contributed by each subunit (Anderson, 1999). Furthermore, it seems that additional cofactors are involved in the activation of HIV-1 protease. One of its substrates, the HIV-1 reverse transcriptase (RT), can increase the activity of the protease and given that its stimulatory role seems to be cleavage-site-dependent, RT may play a part in the regulation of the order of cleavages performed by the protease during the infection (Goobar-Larsson *et al.*, 1995). Moreover, mutational studies with defective retroviruses revealed that budding at the plasma membrane is of importance for the HIV-1 protease since a factor restricted to this membrane, whether of

viral or cellular origin, is required for initiating its activity during virus maturation (Welker *et al.*, 1997).

The cowpea mosaic virus (CPMV) protease demonstrates that another viral polypeptide can also function as a regulator-stimulator for a viral protease. CPMV is a single-stranded bipartite RNA plant virus and its B-RNA-encoded 24 kD protease performs the required proteolysis in the B and M polyproteins (Vos *et al.*, 1988). The 32 kD protein cofactor of the CPMV protease, located at the amino terminus of the B-polypeptide, seems to have a bi-directional regulatory role. While 32 kD stimulates the *trans* cleavage of M-polyprotein encoding capsid proteins at a Gln-Met site, it decreases the B-polyprotein processing by remaining associated with the larger polyprotein (170 kD) after its cleavage (Peters *et al.*, 1992). Therefore, though the exact mechanism is not known, it seems that the presence of the 32 kD protein is important possibly for inducing a certain optimal conformation or folding.

Similarly, this type of structural-stimulus in activity-regulation has been described for the human rhinovirus-14 (HRV14) 3C protease. The low *in vitro* activity of the HRV14 3C protease encouraged the search for potential cofactors and it was discovered that anions were capable of stimulating 3C activity by inducing a conformational change in the protein structure (Wang & Johnson, 2001). Since HRV14 3C has also been reported to complex with negatively charged viral RNA in infected cells (Leong *et al.*, 1993), viral RNA could be the anion-like molecule responsible for regulating 3C's enzymatic activity *in vivo* (Wang & Johnson, 2001).

1.4.5 Regulation and activation of AVP

Despite reports that other viral components were not required for enzyme activity (Houde & Weber, 1990), the fact that the recombinantly expressed and purified AVP had very little activity, which could be stimulated by the addition of disrupted *ts1* virions (Mangel *et al.*, 1993, Webster *et al.*, 1993), suggested otherwise. The proposed autocatalytic processing and maturation of the 23 kD AVP into a 19 kD active form (Chatterjee & Flint, 1987) were found to be inconsistent and therefore not responsible for AVP activation (Anderson, 1990, Webster & Kemp, 1993). A novel activation stimulus for the adenovirus protease was discovered, to which a counterpart was later detected in hepatitis C virus (HCV).

Two groups simultaneously discovered that AVP had a substrate-mediated activation mechanism based on the recruitment of a short peptide (Mangel *et al.*, 1993, Webster *et al.*, 1993). AVP requires the 11-amino acid peptide GVQSLKRRRCF, derived from the C-terminus of the precursor of protein VI following cleavage at site 238-239, as a cofactor for maximal activity (Figure 5C) (Mangel *et al.*, 1993; Webster *et al.*, 1993). In addition, adenovirus DNA has been reported as a second cofactor for the Ad2 protease (Mangel *et al.*, 1993, review: Mangel *et al.*, 1997). The importance of viral DNA or a polymer with high negative-charge density on AVP activity has been disputed (Webster *et al.*, 1994, Diouri *et al.*, 1995). However, data suggests that DNase treatment abolishes AVP activity, which can be restored upon the addition of Ad DNA (Mangel *et al.*, 1993).

In the case of HCV, its polyprotein is processed by the action of cellular and virally encoded proteases. Host cell signalases on the endoplasmic reticulum (ER) are responsible for liberating the amino-terminal structural envelope proteins (E1-E2), whereas the non-structural (NS) proteins located further downstream of the polyprotein are cleaved by the action of two HCV-encoded proteases (Hahm *et al.*, 1995 and references therein). The NS2-3 metalloprotease cleaves the NS2-NS3 junction while the NS3 serine protease performs the cleavages at NS3/4A, NS4A/NS4B, NS4B/5A and NS5A/5B junctions (Grakoui *et al.*, 1993, Hong *et al.*, 1996). NS3 is in fact a bifunctional, 631-residue enzyme possessing both protease and helicase activities (Yao *et al.*, 1997, Howe *et al.*, 1999). Although NS3 is enzymatically active on its own, it requires NS4A, a 54-residue amphipathic peptide cofactor, for the cleavage at the NS4B/NS5A site (Bartenschlager *et al.*, 1994, Failla *et al.*, 1994). While the central portion of NS4A is required for the activation of the protease, its hydrophobic N-terminus is responsible for co-localising the NS3-4A complex at host cell membranes where, together with NS4B, NS5A and NS5B (RNA polymerase), it forms a larger replication complex (Yao *et al.*, 1999).

The proposed activation mechanism of AVP by the peptide is not completely akin to that of the HCV NS3-NS4A association. Whereas NS4A interacts with the extended N-terminal region of the protease as well as with the core of the enzyme (Yao *et al.*, 1999), the 11-mer peptide binds some distance from the active-site residues of AVP (Ding *et al.*, 1996). The crystal structure of the Ad2 protease-peptide heterodimer revealed that

the activating peptide forms a 1:1 complex with the protease, possibly altering the conformation of the active site by tying two non-continuous protease domains together (Ding *et al.*, 1996). Through the formation of a disulphide bond, between cysteine residue 10 of the peptide and 104 of the protease, hydrogen bonds and side-chain interactions, the peptide forms the sixth β-sheet antiparallel to the middle, fifth β-sheet of the protease (Figure 5A & B). Within the overall ovoid shape of the complex, the N-terminal GVQ residues of pVIct are in a pocket formed by the 7th β-sheet loop, while the SLKRRRCF-stretch of pVIct extends to the 3rd helix of the protease.

1.4.6 Order of AVP activation during infection?

Despite the discovery of the activating peptide, there was still a conundrum concerning the specific timing and control over the protease activity during adenovirus lytic cycle. Late in the infection, cytokeratin 18 is cleaved by the protease at two cleavage sequences resulting in the disruption of the cytokeratin network, completed by approximately 36 hours into the infection (Chen *et al.*, 1993). Simultaneously, however, the maturation of viral pre-proteins inside the young virions by the protease takes place in the nucleus, an event stimulated by an association with the peptide and possibly with viral DNA. Hence, not only does the protease need to be activated at the correct time during the infectious cycle to avoid premature lysis, but also there needs to be yet another stimulus responsible for activating the protease in the cytoplasm.

Earlier reports with baculovirus-expressed pTP and Ad2 protease, which resulted in some cleavage of pTP to iTP (Webster *et al.*, 1994), suggested that a cellular component could substitute for the 11-mer peptide. Brown *et al.* (2002) discovered that cellular actin could stimulate the *in vitro* activity of the protease, resulting in the cleavage of cytokeratin and actin itself. Given that the carboxy-terminus of actin, SGPSIVHRKCF, displays sequence homology with the activating peptide, the actin molecule is believed to interact similarly to that of the peptide, forming a 1:1 complex with the protease (Brown & Mangel, 2004). Actin, as a cellular substrate cofactor, therefore completes the puzzle. While the protease molecules in the cytoplasm become activated via an association with actin and disrupt the cytokeratin network, the protease molecules in the nucleus would have performed the maturation events preparing the particles, now infectious, ready for their release.

Figure 5 (A), (B) & (C).

(A). The crystal structure of adenovirus protease together with its cofactor peptide (solved by Ding *et al.*, 1996). The active site residues of the enzyme are highlighted (shown in ball and stick or CPK mode) and coloured. The cofactor peptide, pVIct binds distinct from the active site (shown in white) and the N-and C-terminus have been labelled.

(B). The structure of the activating peptide. The individual residues of the peptide are labelled and shown in CPK mode. The orientation of the peptide is the same as shown in Figure (A). The structures shown were compiled using molecular visualisation and analysis program VMD, version 1.8.1 and the protein sequence for the complex was derived from Protein Data Bank, ID: 1AVP.

(C). Schematic diagram showing the cleavage of Ad2 protein VI into its mature form by the protease. pVI is first cleaved at the C-terminus (between residues 238-239) resulting in the release of the activating peptide (intermediate VI or iVI), followed by the N-terminal cleavage into VI (between residues 33-34). The two karyophilic stretches studied in this thesis, KRRR and KRPRP, have been coloured in blue (discussed in further detail in section 4).


A
C-term
N-term
N-term
C-term
pVIct
His'54
Glu'71
Cys'122

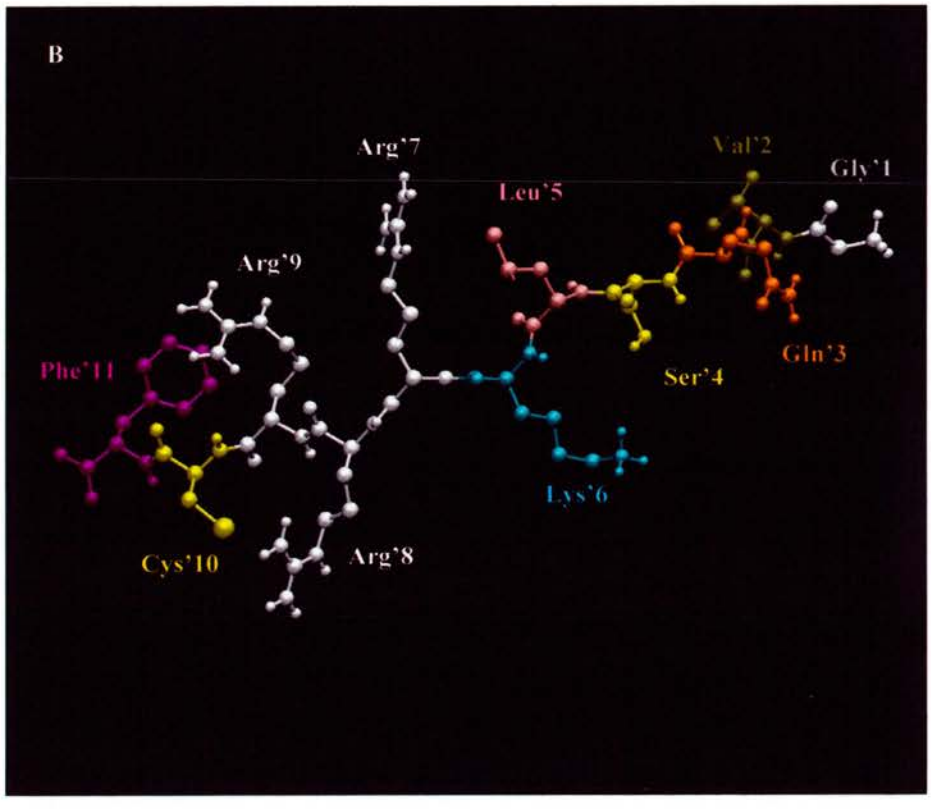
B
Arg'7
Val'2
Gly'1
Leu'5
Arg'9
Gln'3
Phe'11
Ser'4
Lys'6
Cys'10
Arg'8

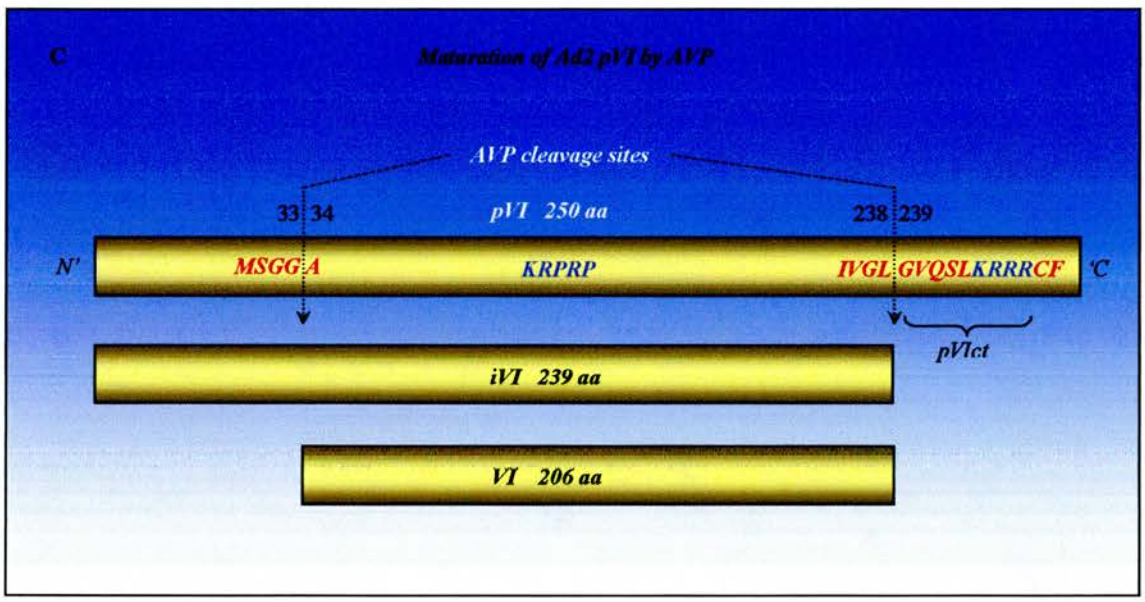
C
Maturation of Ad2 pVI by AVP
AVP cleavage sites
33 34
pVI 250 aa
238 239
N'
MSGGA
KRPRP
IVGLGVQSLKRRRCF
'C
pVIct
iVI 239 aa
VI 206 aa

Finally, there is a third activation time point for the protease, which should be considered. The protease has been reported to cleave the mature VI at a degenerate site, enhancing the entry into the cytoplasm during the uncoating-stage (discussed earlier in section 1.4.1). It is the reducing environment inside the host cell, which is believed to re-activate this cysteine protease (Greber *et al.*, 1996, review: Greber, 1998). According to the theory of Greber (1998), the oxidising extracellular environment inactivates the protease due to the formation of intrachain disulfides after the virus particles are released from the lysed host cell. When the virus enters a new host cell, the reducing milieu within the endocytic vacuole or cytosol causes disulphide bond reduction and re-activates the protease. Greber *et al.* (1996) also concluded that the RGD-dependent interaction of the penton base with integrin receptors, during entry into the cytosol, functions as a signal together with the reducing environment, which is required for protease re-activation.

In conclusion, the adenovirus protease represents an example of a viral protease whose activity, and regulation thereof, exhibit a high degree of adaptation and dependency of several viral and cellular factors, likely to be discovered in other viral systems. The objective of the work described in this thesis was to expand on the characterization of the activating peptide and its role in the regulation of the protease. To this end, the role of individual residues along the peptide for the *in vitro* protease activity was examined and putative, additional *in vivo* functions for the peptide during adenovirus infection were explored. Previous experiments by Pollard (2001) have shown that the KRRR-sequence towards the C-terminus of the peptide could function as a nuclear localisation signal. To continue from these observations, the aim was to establish the relevance of this signal for pVI protein during adenovirus infection and to assess whether this signal could be responsible for the nuclear import of the protease.

2. Materials and Methods

2.1.1 Plasmids

The gene encoding Ad2 protease had been previously cloned into pET11c (Novagen) vector (Anderson, 1990), referred to as p175 construct. The pGEX-2T vector (Amersham Biosciences) was a gift from L-N. Chen. The pEGFP-C1/23K plasmid was a gift from T. Vaughan. The pcDNA3.1(Invitrogen)-based vector, pdf20 was a kind gift from P. de Felipe, as were the Clontech-vectors pDsRed2-C1, pEGFP-C1 and pHcRed1-C1, the full description of which is available from the BD Biosciences website (http://www.bdbiosciences.com/clontech/). The oligonucleotide sequences used for the generation of different constructs are included in the Appendix (section 6).

2.1.2 Bacteria

Escherichia coli strain DH5α was used as a non-expressing host for plasmid preparations whilst *E. coli* strain BL21(DE3) was used as a host for the expression of recombinant AVP and pVI.

2.1.3 Mammalian cells

$HeLa^{CD}$ (Catherine Dargemont, Universités Paris) and COS-7 cell lines were used for eukaryotic transfections and infections with Ad2.

2.1.4 Antibodies

A rabbit antiserum, raised against the N-terminal region of the Ad2 protease [sequence MGSSEQELKAIVKDLGC coupled to human serum albumin) (Webster & Kemp, 1993)], was used for the detection of protease in Western blotting (at 1:4000 dilution). A mouse monoclonal anti-GFP antibody (Roche), a gift from P. de Felipe, was used for the detection of EGFP-fusion proteins (used at 1:1000 dilution in Western Blotting). A rabbit polyclonal anti-VI serum raised against the residues 94-170 was used for detecting pVI/iVI/VI (a gift from W.C. Russell). This antiserum was pre-adsorbed against uninfected, fixed and permeablised HeLa cells and used at 1:80 dilution for immunofluorescence.

The secondary antibodies, anti-rabbit IgG and anti-mouse IgG (Amersham) were used at 1:4000 dilution in Western blotting, whilst the anti-mouse and anti-rabbit fluorescein isothiocyanate (FITC)-conjugated antibodies (Oxford Biotechnology) were

used at 1:200 dilution for immunofluorescence.

2.2 Peptide synthesis

The peptides used in the experiments were synthesised by G. Kemp at the University of St Andrews according to the method of Atherton & Sheppard (1989) and by using a Pepsynthesiser II (Cambridge Research Biochemicals). The basic steps in solid phase peptide synthesis using fluorenyl-methoxycarbonyl-polyamide-chemistry (Fmoc) are: to immobilise the first amino acid to a polyamide resin, followed by the N-terminal elongation of the peptide by C-terminally activated, side chain protected amino acids. The newly synthesised and HPLC-purified peptides were also confirmed by mass spectrometry (University of St. Andrews).

2.2.1 Purification of peptides

Preparative reverse-phase High-Pressure Liquid Chromatography (HPLC) system (Gilson) was used to purify peptides after synthesis. Peptides were dissolved in 0.1% TFA in ddH_2O, injected onto a C18 column (Bio-Rad) pre-equilibrated with 0.1% TFA in ddH_2O and eluted by increasing concentrations of acetonitrile. The collected fractions were analysed by Mass Spectrometry and the correct fractions were freeze-dried using a Modulyo-drier.

2.2.2 Synthesis and preparation of fluorescein-tagged peptide, pVIct-F

A peptide with a fluorescein tag on the lysine residue of GVQSLKRRRCF was synthesised for *in vivo* assays whereby the peptide localisation could be followed in cells. The pVIct-F peptide was synthesised according to procedure by Hoogerhout *et al.* (1999). Standard Fmoc-polyamide chemistry was performed apart from the lysine residue being protected with piperdine-stable ivDDE group and also the glycine residue was protected with acid-labile Boc group, not with the usual piperdine sensitive Fmoc. Following the synthesis, the peptide was maintained attached to a hydrazine-treated resin. 40 μmol of 5-(and-6)-carboxyfluorescein succinimidyl ester (Molecular probes) in 0.5 ml of DMF was added to 0.25 g of peptide-containing resin, in order to label free ϵ-group of lysine. Together with 40 μl of di-isopropylethylamine, the mixture was sealed, protected from light and mixed using a rotator for 3 h at room temperature.

Sampling for MALDI-TOF (*m*atrix-*a*ssisted *l*aser *d*esorption/*i*onisation, *t*ime *o*f *f*light) mass spectrometry was first performed after 2 h, and every 0.5 h thereafter until finally the peptide was cleaved off the resin by TFA. The fluorescein-tagged peptide was purified as described previously, freeze-dried and stored at -20°C.

2.2.3 Determination of peptide concentration

Peptide concentrations were determined by comparison of electropherogram areas resulting from capillary electrophoresis to areas of peptides of known concentrations, according to method by Cabrita (1997).

2.3 Prokaryotic expression of recombinant adenovirus protease (AVP)

2.3.1 Expression of protease

A medium sized colony from p175 master plate was resuspended in 1 ml of water and absorbance at 600 nm was checked. The volume of cells was adjusted accordingly: if A_{600} was 0.1, 10 µl of cell suspension was resuspended in 1 ml water. 300 µl of the resulting suspension was spread onto LA/carbenicillin plates and incubated overnight at 37°C.

The colonies from the overnight plates were scraped into 10 ml Luria Bertani (LB), 0.5% (w/v) carbenicillin and centrifuged at 3,000 rpm for 10 min (3K10 Sigma). The resulting pellet was resuspended in 20 ml LB/carbenicillin. 20 µl of this cell suspension was diluted in 1 ml water and absorbance was checked. The volume of the cell suspension added to 500 ml of DMEM [supplemented with 2.5 ml of 10 mg ml^{-1} carbenicillin and sterile-filtered 25 mM HEPES, pH 7.5] was determined according to the following formula: Vol = 1.5 : A_{600}, in order to obtain a starting OD of 0.15. The culture was grown at 37°C till A_{600} reached 0.4-0.6 after which the expression of protease was induced by the addition of 2 ml of 0.15 M IPTG (Isopropyl-β-D-thiogalactopyranoside). The expression was left to proceed for 3 h at 37°C. The culture was centrifuged at 10,000 rpm (Beckman J2-21) for 5 min and the resulting pellet was washed and resuspended in suspension buffer (50 mM Tris-HCl, 5 mM EDTA, 4% glycerol, pH 8), and finally stored at -20°C.

2.3.2 Extraction of protease

To extract the protease expressed in the bacterial cells and to break the bacterial cell wall, samples were incubated at 37°C for 15 min in the presence lysozyme (100 µl of 10 mg ml^{-1} stock), followed by freeze-thawing in liquid nitrogen (x3). The DNA was broken down by adding 100 µl of 1M $MgSO_4$ and 100 µl of DNAase I (2 mg ml^{-1} stock) to the cell suspension, and incubating at 37°C for 15 min. Finally, the lysate was centrifuged at 13000 rpm (MSE Micro Centaur centrifuge) for 5 min to separate cell debris from the supernatant. The protease retained in the supernatant was stored at -20°C until purification.

2.3.3 Purification of protease

Single step purification of recombinant protease, method of Pollard (2001), was carried out with ion-exchange columns and using a Pharmacia P-500 system. Parameters of the apparatus were set as follows: pump A with buffer A (50 mM Tris, pH 8), pump B with buffer B (50 mM Tris, 1 M NaCl, pH 8), chart recorder set at 0.25 cm $min^{-1}$and flow rate set at 1 ml min^{-1}.

The extract containing the protease was applied to a 10 ml superloop and the sample was first passed through a 1 cm x 30 cm Diethylaminoethyl (DEAE) Sepharose column, equilibrated with buffer A and eluted with equilibration buffer at 1 ml min^{-1}. After 20 ml had been passed through DEAE column, pre-equilibrated Heparin-Sepharose (1 cm x 10 cm) and Carboxymethyl-Sepharose (1 cm x 3 cm) columns were connected and eluted with further 20 ml of buffer A. Finally the protease was eluted from the Carboxymethyl-Sepharose column by passing through 50 mM Tris, 0.2 M NaCl (20% buffer B). The collected 1 ml fractions were stored at -20°C until analysed on SDS-PAGE mini gels and by Western blotting. Protease-containing fractions were pooled and stored at -70°C.

2.4 Gel electrophoresis

2.4.1 SDS-Polyacrylamide gel electrophoresis (PAGE)

Sodium dodecyl sulphate polyacrylamide gel electrophoresis, SDS-PAGE was performed with Bio-Rad Mini Gel-equipment. First the separating gel was prepared [15% gel: 5.6 ml 40% (v/v) acrylamide, 0.65 ml 2% (v/v) bis-acrylamide, 5.6 ml 1 M

Tris/HCl pH 8.7, 2.9 ml ddH_2O, 0.15 ml 10% (w/v) SDS, 12.5 µl TEMED (N,N,N',N'-Tetramethylethylenediamine) and 50 µl of 0.1 mg ml^{-1} ammonium persulphate (APS)]. The separating gel mixture was poured in between 2 assembled glass plates and left to polymerise with overlaid saturated butanol. Prior to loading the stacking gel, [consisting of 1.3 ml 40% (v/v) acrylamide, 0.7 ml 2% (v/v) bisacrylamide, 1.25 ml 1M Tris-HCl pH 6.9, 6.75 ml water, 0.1 ml 10% (w/v) SDS, 25 µl TEMED and 50 µl of 0.1 mg ml^{-1} APS], the butanol was removed and the top of the gel rinsed with 70% ethanol. After the stacking gel polymerised, the comb was removed and the wells were washed with water to remove any unpolymerised acrylamide. The SDS-PAGE Bio-Rad apparatus was then assembled and filled with chamber buffer [0.3% (w/v) Tris, 1.44% (w/v) Glycine, 0.1% (w/v) SDS]. Samples were loaded into the wells after being boiled for 2 min with gel loading buffer [25% (v/v) β-mercaptoethanol, 7.5% (w/v) SDS, 18.75% (v/v) glycerol, 0.1875 M Tris, pH 6.9 and 0.0375% (w/v) Bromophenol blue]. Electrophoresis was carried out at 180V for 45 min or until sufficient separation was obtained using Bio-Rad Power Pac 3000.

2.4.2 Staining of gels

After performing a SDS-PAGE, the gels were stained with Coomassie blue, unless further used for Western blotting. After Coomassie blue-staining [0.2% (w/v) Coomassie brilliant blue R250, 50% (v/v) methanol and 10% (v/v) acetic acid], the gels were destained using 25% (v/v) methanol, 7.5% (v/v) acetic acid to visualize bands and to remove excess background. During both the staining and destaining procedures, the gels were placed onto an orbital shaker.

2.4.3 Determination of protein concentration

The concentration of the purified protease sample was determined from a standard curve obtained with 0.05-1.5 µg of Soybean Trypsin Inhibitor (SBTI) on a 20% SDS-PAGE. Bradford reagent (Bio-Rad) was also used to estimate protein concentration by measuring the absorbance at 595 nm and by comparison to prepared standards (Bradford, 1976).

2.4.4 Western blotting

Protein samples were electroblotted to a Hybond PVDF membrane after separation using SDS-PAGE. The PVDF membrane (pre-soaked in methanol for 2 minutes) was placed on top of the gel, which in turn was placed between two 3 mm papers (Whatman) soaked in transfer buffer [48 mM Tris, 39 mM glycine, 20% (v/v) Methanol & 0.00375% (w/v) SDS] and two fibrous pads. The transfer, using Bio-Rad Mini Gel equipment, proceeded at a constant current of 300 mA for 2 h.

The resulting membrane was incubated at room temperature in 20 ml of blocking buffer [5% (w/v) dried milk powder, 0.1% (v/v) Tween 20 in PBS] for 10 min. The primary antibody was added and incubation continued for 30 min, with shaking. The excess primary antibody was removed by washing with blocking buffer (3 x 10 min washes), after which the secondary antibody was added and incubation continued for 30 min. The membrane was washed in blocking buffer (3 x 10 min) and in TTBS (0.1% (v/v) Tween 20 in PBS) to reduce the background. Finally the blot was incubated in 1ml of each ECL reagent [reagent ^{1}: 2.5 mM luminol, 0.369 mM coumaric acid, 0.1 M Tris/HCl pH 8 and reagent ^{2}: 0.0192 % (v/v) H_2O_2 and 0.1 M Tris-HCl pH 8.5], placed between acetate sheets and exposed to Fuji X-ray film. The film was developed using Kodak M35 X-OMAT processor.

2.4.5 Non-denaturing, native gel electrophoresis

The non-denaturing, native gel electrophoresis method for AVP and peptide variants was adapted from Goldenberg (1989). The SDS-PAGE Mini Gel apparatus was assembled according to manufacturer's instructions and as described earlier in 2.4.1. The major difference between a non-denaturing, non-reducing native gel compared to a standard SDS-PAGE is the absence of SDS, sample preparation, and the gel polymerisation, in the case of riboflavin-based native gels.

2.4.6 Riboflavin native gel electrophoresis

A 15% separating gel consisting of 5.47 ml 40% (v/v) acrylamide, 3.0 ml 2% (v/v) bis-acrylamide, 1.53 ml ddH_2O, 2.5 ml riboflavin (0.004%), 10 µl TEMED and 2.5 ml separating gel buffer [48% (v/v) 1 M KOH, 17.2% (v/v) glacial acetic acid, pH 4.3] was prepared. The stacking gel mixture [0.91 ml 40% (v/v) acrylamide, 0.5 ml 2% (v/v)

bisacrylamide, 4.09 ml ddH_2O, 2.0 ml riboflavin (0.004%), 15 µl TEMED and 2.5 ml stacking gel buffer (48% (v/v) 1 M KOH, 2.9% (v/v) glacial acetic acid, pH 6.8)] was laid on the top of the separating gel with the well-forming comb. The polymerisation of the gels was started by exposing the gels to light using two RRB Illuminator light boxes. Electrophoresis was carried out in electrode buffer [3.12% (w/v) β-alanine, 0.8% glacial acetic acid, pH 4.5].

2.4.7 Ammonium persulphate native gel electrophoresis

The ammonium persulphate (APS)-containing native gel mixture consisted of [(15% gel): 4.5 ml 40% (v/v) acrylamide, 2.4 ml 2% (v/v) bisacrylamide, 3.45 ml ddH_2O, 10 µl TEMED, 150 µl 10% APS] and 1.5 ml separating gel buffer [12.8% (v/v) glacial acetic acid, 1% (v/v) TEMED, 1M KOH to pH 4]. The stacking gel mixture for APS native gel was prepared [1 ml 40% (v/v) acrylamide, 0.56 ml 2% (v/v) bisacrylamide, 5.2 ml ddH_2O, 10 µl TEMED, 200 µl 10% APS] and used together with 1 ml stacking gel buffer [4.3% (v/v) glacial acetic acid, 0.46% (v/v) TEMED, 1M KOH to pH 5.0]. Electrophoresis was carried out in electrode buffer [1.42% (w/v) β-alanine, acetic acid to pH 4.0].

With both types of non-denaturing gels, the gel-mixtures were degassed using water suction prior to the addition of APS or riboflavin with TEMED.

2.4.8 Binding assay mixture

The reaction mixture for the native gels consisted of 75 µl of purified protease sample to which 2.5 µl of 4 mg ml^{-1} lysozyme was added to serve as an internal standard of the loadings. 4 µl of the protease/lysozyme mixture was further added to 5 µl doubling dilutions of 1 mM peptide in water. Finally 12.5 µl of assay buffer (50 mM Tris, 10 mM EDTA, 2 mM β-mercaptoethanol, pH 8.0) and 10 µl glycerol-tracking dye solution [0.2% (w/v) methyl green, 50% (w/v) glycerol] was added and 20 µl of each sample was loaded per well. Electrophoresis was carried out towards the cathode at 40 mA for 45-60 min using Bio-Rad Power Pac 3000, after which the gels were stained with Coomassie blue for analysis.

2.4.9 Analysis of protein bands from native gel electrophoresis

The native gels were scanned using CanoScan FB 636U and the intensity of the heterodimer complex formation between the peptides and AVP was analysed by NIH image 1.62 software. The lysozyme added to the binding assay functioned as an internal standard of the loadings. To obtain equilibrium dissociation constant, K_d, the concentrations of Bound peptide, $[pVIct]_{bound}$ and Free peptide, $[pVIct]_{free}$ were calculated: $[pVIct]_{bound} = [AVP](I_0/I_{max})$

$$[pVIct]_{free} = [pVIct]_{initial} - [pVIct]_{bound}$$

where [AVP] is the initial protease concentration, I_0 the intensity of heterodimer band at a certain peptide concentration and I_{max} the maximum intensity for 100% bound- dimer. From Scatchard-plot analysis ($[pVIct]_{bound}/ [pVIct]_{free}$ v $[pVIct]_{bound}$), the K_d value could be determined [slope = $-1/K_d$].

2.5 Activity and binding experiments

2.5.1 Isometric Titration Calorimetry (ITC)

A VP-ITC MicroCalorimeter (MicroCal^{TM}) was used to measure binding between the protease and peptide variants. ITC is a technique by which both the magnitude of binding affinity and the magnitude of the enthalpy (ΔH) and entropy (ΔS) changes can be measured.

In a typical experiment 0.5-1 mM of activating peptide in a 250 μl syringe was injected to the 1.8 ml sample cell of MicroCalorimeter, containing 5-10 μM of purified AVP. The buffer, in which the protease and peptide were dissolved, was identical in terms of pH and concentration of buffer solvents. To minimise any heat effects associated with differences in buffer concentration, the AVP was dialyzed overnight against 50 mM Tris/HCl, 10mM EDTA, pH 8 (with or without 2 mM β-mercaptoethanol), in which the peptide was later dissolved. Prior to loading the peptide and AVP into the syringe and sample cell, respectively, the samples were degassed at 1-5 degrees below the intended experimental temperature using ThermoVac-system (MicroCal^{TM}). Using the VP viewer software, 21 injections of 10 μl of peptide were selected with a spacing of 150 sec. The constant temperature during the experiment was kept at 25°C, 30°C or 37°C, with an initial delay of data collection of 60 sec and a stirring speed of 300 rpm.

2.5.2 Protease activity assay with peptide substrate

2.5.2.1 Standard protease activity assay

The method has been described previously in Cabrita *et al.* (1997). 10 µl of purified protease (at 0.1-0.2 mg ml^{-1}) was incubated with 10 µl of activating peptide (100 µg ml^{-1} in ddH_2O) and with 25 µl of assay buffer (50 mM Tris, 10 mM EDTA, 2 mM β-mercaptoethanol, pH 8.0) at 37°C for 10 minutes. 5 µl of 2 mg ml^{-1} Ac-LRGAGRSR substrate (peptide with acetylated N-terminus) was then added to the reaction mixture and incubation was continued at 37°C. 10 µl samples were removed at 5, 10, 15 and 30 min time points. The reaction was terminated by the addition of 10 µl 1% (v/v) TFA and the samples were stored at -20°C until analysis by the BioFocus 3000 Capillary electrophoresis (CE) system.

2.5.2.2 Sample preparation and analysis

An additional 80 µl of filtered ddH_2O was added to the cleavage samples prior to the analysis with BioFocus 3000 system. The samples were separated by an electric field (from positive to negative electrode) in 0.1M phosphate buffer, pH 2.5 (Bio-Rad) within a capillary cartridge of 24 cm x 25 µm, at constant voltage 10 kV and at 20 PSI x sec pressure injection. The absorbance was set at 200 nm and the electropherograms were collected using BioFocus V3.10 software (Bio-Rad). The spectra were further analysed using Integrator V3.01 software (Bio-Rad) and the observed peaks were manually edited after conversion to ACQ (Acquisition files).

The relative specific activities were calculated according to the method by Cabrita (1997). The data [including time point, percentage of substrate remaining (S/S_0) and $\ln(S/S_0)$] were plotted in Microsoft Excel program. By employing the array formula {linest($\ln(S/S_0)^{5min}$: $\ln(S/S_0)^{30min}$, time point^{5min}:time point^{30min}, False, True)}, the initial rate of substrate digestion was obtained from the linear graph (-k), together with standard error and correlation coefficient.

2.5.3 Fluorescent-substrate assay

2.5.3.1 Kinetic data for AVP activated by pVIct variants

Binding and activation data for AVP and peptide mutants were obtained by conducting activity assays with a fluorescent substrate (benzyloxycarbonyl) z-Leu-Arg-Gly-Gly-

AMC (*a*mino*m*ethyl*c*oumarin) (Bachem). The experiments were performed using Perkin-Elmer Luminescence Spectrometer LS 50B and 10 mm light path fluorimeter cuvets (Sigma). The absorbance of the released cleaved product was measured at excitation wavelength 370 nm and emission wavelength 460 nm (slit width set at 2.5 nm at both occasions). Each experiment was performed in triplicate. Prior to adding the pre-incubated AVP and peptide to the substrate containing solution, the background for the substrate itself was recorded.

2.5.3.2 Rate constant experiments

The experiments for the determination of k_{cat} and K_m values were conducted as described previously apart from peptide concentration being kept at 2 μM whilst the substrate concentration was altered from 15.6 μM to 200 μM. The peptide concentration used was the same for all the peptide variants and for those with very high K_d values, the concentrations of peptides in the solution were less than saturating. Therefore, the concentration of active AVP/pVIct-complex present in the assay was determined according to the K_d of the peptide variant, according to method by Baniecki *et al.* (2001) and using the equation: $[pVIct]_0 [AVP]_0 / [pVIct]_0 + K_d$

where $[pVIct]_0$ and $[AVP]_0$ are the concentration of peptide and protease used, respectively, and K_d is the equilibrium dissociation constant of the peptide, as determined by the native gel electrophoresis.

2.5.3.3 Equilibrium dissociation constant (K_d) experiments

26 nmol of purified AVP and the varying concentrations of peptides (0.3-4 μM) were incubated in assay buffer [50 mM Tris, 10 mM EDTA, 2 mM β-mercaptoethanol (pH 8)] at 37°C for 10 min prior to the addition of the substrate (62.5μM). The assays were left to run for 10 min at 37°C. Data interval was set at 0.0017 and response time at 4 sec.

2.5.3.4 Analysis of data

The raw data obtained from the Perkin-Elmer Luminescence LS50 B was analysed using Igor Pro 3.12 software. The data points were converted to seconds and the fluorescence units to product formation after calculating the molar extinction coefficient

for 7-amino-4-methylcoumarin (AMC), which is the released fluorescent product after the cleavage by AVP. The rate of substrate hydrolysis was derived from a linear graph [rate v time] and all rates were finally plotted as a rectangular hyperbola, V_0 v [S].

For the binding-experiments, the fluorescence units were converted to product formation, as described above. Then to obtain the K_d, the concentrations of Bound peptide, $[pVIct]_{bound}$ and Free peptide, $[pVIct]_{free}$ were calculated:

$$[pVIct]_{bound} = [AVP](V_0/V_{max})$$

$$[pVIct]_{free} = [pVIct]_{initial} - [pVIct]_{bound}$$

where [AVP] is the concentration of the enzyme in the assay, V_0 the recorded rate, V_{max} the estimated maximum rate and $[pVIct]_{initial}$ the initial concentration of peptide added to the assay. By plotting the ratio of $[pVIct]_{bound}/[pVIct]_{free}$ versus $[pVIct]_{bound}$, one can obtain a Scatchard plot and the K_d value from the negative reciprocal of the slope [slope $= -1/K_d$].

2.6 Eukaryotic expression of proteins

2.6.1 Maintenance of mammalian cells

Human cervical cancer cells, $HeLa^{CD}$ and African Green Monkey kidney cells, COS-7 were maintained at 37°C and in 5% CO_2 atmosphere in Dulbecco's modified Eagle's medium, D-MEM (Gibco) supplemented with 10% foetal calf serum, FCS (Gibco), glutamine (4 mM), penicillin (100 $\mu g\ ml^{-1}$) and streptomycin (100 $\mu g\ ml^{-1}$). Cells were passaged at around 80-90% confluence of the cell monolayer. Medium of the cells was removed, monolayer was washed twice with 5 ml of warm PBS and the cells incubated for 2 min with 2 ml of trypsin. The trypsin was inactivated by addition of D-MEM/10% FCS, after which the cells were centrifuged at 1200 rpm for 3 min (Beckman GS15 centrifuge), resuspended in D-MEM /10% FCS and aliquoted into 75 cm^2 flat flasks (Cellstar®).

2.6.2 Transfections of mammalian cells

Transient transfection of mammalian cells was mediated either by electroporation (adapted from Neumann *et al.,* 1982), calcium phosphate method (adapted from Graham and van der Eb, 1973) or by using FuGENE 6 (Roche) transfection reagent.

2.6.2.1 Calcium Phosphate transfection

Calcium phosphate transfections were performed using sterile 2x HBS buffer (280 mM NaCl, 1.5 mM Na_2HPO_4, 50 mM HEPES pH 7.05) and sterile 2 M $CaCl_2$. Approximately 1 x 10^5 HeLa cells were plated onto each well in a 12-well dish (Nunclon™) 24 h prior to the transfection. (The DNA used in the transfection was diluted to a final concentration of 0.2-1 μg μl^{-1}.) First, 6-12 μg of the DNA was mixed with 37 μl 2 M $CaCl_2$, which was made up to 0.3 ml with water. This was added dropwise with continuous tapping to an equal volume of 2x HBS buffer. The solution was left at room temperature for 10-30 min before being added dropwise to the cells. The plate was incubated at 37°C for 24 h, after which the medium of the cells was changed to D-MEM/10% FCS and the plate incubated for further 24 h.

2.6.2.2 Electroporation

The electroporation- transfections were performed using Genepulser II (Bio-Rad). The cells were given fresh D-MEM medium enriched with 10% FCS 1 h prior to the transfection. After trypsin-treatment, the cells were resuspended in 15 mM HEPES/D-MEM. 200 μl of the cell suspension (5 x 10^6 cells per ml of medium) together with 210 mM NaCl and 5 μg of DNA in ddH_2O was electroporated in a 4 mm (EquiBio) cuvette at 950 mFD, 240 V for a ≥ 30 msec impulse. The cells were resuspended in 4 ml of D-MEM/10% FCS. 1 ml of this cell suspension was aliquoted to a well in a 12-well dish (Nunclon™) containing sterile coverslips and incubated at 37°C.

2.6.2.3 FuGENE transfection

FuGENE (Roche) is a multi-component lipid-based transfection reagent that complexes and transports DNA into the cell with very low cytotoxicity (Roche manual 5/2001).

To transfect a well of a 12-well dish (Nunclon™) with a monolayer of cells (1-3 x 10^5), 3 μl of FuGENE reagent was added to 97 μl of Optimem (Gibco). This solution was mixed thoroughly prior to the addition of 0.25-1 μg of DNA. The tube was gently tapped to mix and left at room temperature for 45-60 min. The mixture was then added dropwise to cells (in Optimem), which were incubated at 37°C for the required time. The amount of each component used was proportionally increased when performing larger scale transfection assays.

2.6.3 Addition of peptide to the culture medium

Monolayers of HeLa cells, on sterile coverslips in 12-well dishes (Nunclon™), were grown at 37°C in D-MEM/10% FCS. The culture medium was removed, cells washed (x3) in PBS and the culture medium was replaced with Optimem containing 1 μM or 10 μM of unlabelled or fluorescein-labelled peptide. The cells were incubated for 15-60 min in presence of the peptides at 37°C, after which the cells were either fixed for fluorescence imaging (see 2.6.4) or washed (x3) in PBS and incubated further at 37°C in Optimem (live-imaging). The protocol for the addition of peptides to transfected cells, between16-24 h post-transfection, was the same (as detailed above).

2.6.4 Fixing the cells

The transfected and/or infected coverslips were washed a few times in PBS containing 0.5 mM $CaCl_2$ and 1 mM $MgCl_2$ and fixed with 4% paraformaldehyde/PBS for 10 min. The coverslips were further washed with PBS and with 0.1 M Glycine/PBS for 15 min and left in PBS overnight at 4°C. Alternatively, the coverslips were washed with PBS and cells fixed with 1 ml of cold 95% (v/v) Methanol-5% PBS (kept at -20°C) at room temperature for 10 min (Morin *et al.*, 1989), or with cold, 1:1 (v/v) Acetone-Methanol (Matthews & Russell, 1998), after which they were rehydrated in PBS. Mowiol solution [2.4 g mowiol G488, 6 ml of glycerol, 6 ml ddH_2O, 12 ml of 0.2 M Tris (pH 8.5), 2.5% (v/v) DABCO and DAPI to 1.5 μg ml^{-1} (4',6-Diamidino-2-phenylindole)] was used to fix the coverlips onto slides. The slides were stored at 4°C.

2.6.5 Immunofluorescence

The cells fixed onto the coverslips were permeablised using 0.1% Triton X-100 in PBS and blocked using PBS (v/v) 0.5% Donkey Serum (DS). The primary antibody was added in PBS/DS and left to incubate for 1 hour. The primary antibody was washed off by PBS/DS. The coverslips were incubated for 1 h in the presence of anti-mouse or anti-rabbit FITC conjugated antibody (used at 1:200 dilution). Coverslips were mounted on the slides using moviol/DAPI (described above).

2.6.6 Microscopy

Coverslips were examined under 40x or 100x oil immersion with a Nikon Microphot-FXA microscope. Multiple fluorescence images were acquired using a *DeltaVision* Restoration Microscope system (Applied Precision, Issaquah, MA, USA), which consists of an inverted microscope (Olympus IX70, Tokyo, Japan) with 60x or 100x oil immersion objective and photometric CH300 CCD camera. Images were processed with *softWoRx*- software (Applied Precision).

2.6.7 Lysis of mammalian cells

The cell monolayer was washed twice with ice cold PBS and the cells were lysed using RIPA (Radio-Immunoprecipitation Assay) lysis buffer [150 mM NaCl, 1% Nonidet P-40, 0.5% sodium deoxycholate, 0.1% SDS, 50 mM Tris, (pH 8), 100 μg ml^{-1} phenylmethylsulfonyl fluoride, 1 μg ml^{-1} aprotinin, 1 mM ethylenediaminetetraacetic acid, 5 μg ml^{-1} leupeptin] (Sambrook *et al.*, 1989). The cold RIPA buffer was added to cell monolayer (500 μl per 60 mm well) and left for 20 min on ice at 4°C. The samples were collected with a cell scraper, centrifuged (at 13,000 rpm for 5 min) and supernatant collected for analysis by SDS-gel electrophoresis and Western blotting (see section 2.4.1).

2.6.8 Cytoplasmic and nuclear extracts of transfected mammalian cells

A larger scale transfection of HeLa cells was performed to obtain separate cytoplasmic and nuclear extracts of the cells. The transfected cells were removed from the 6-well plate (Cellstar®) or 25 cm^2 plates using a cell scraper at 24-30 hpt and resuspended in 200 μl buffer A [10 mM Hepes (pH 8), 50 mM NaCl, 0.5 M Sucrose, 1 mM EDTA, 0.5 mM spermidine, 0.15 mM spermine, 0.2% Triton X-100]. The lysate was left on ice for 6 min and centrifuged at 6500 rpm for 3 min at 4°C using Sigma 3K10 centrifuge. The resulting supernatant was stored at –70°C as a cytoplasmic fraction. The pellet was further washed with 200 μl of buffer B [50 mM NaCl, 10 mM Hepes, 25% (v/v) glycerol, 0.1 mM EDTA, 0.5 mM spermidine, 0.15 mM spermine] and centrifuged at 6500 rpm for 3 min at 4°C after which the supernatant was discarded. The pellet was carefully resuspended in 100 μl of buffer C [350 mM NaCl, 10 mM Hepes, 25% (v/v) glycerol, 0.1 mM EDTA, 0.5 mM spermidine, 0.15 mM spermine] and left on ice for 30

min, with regular mixing. The lysate was centrifuged at 6500 rpm for 20 min at 4°C. The resulting supernatant was stored at –70°C as a nuclear extract until further analysis. Buffers A-C all contained a mix of protease inhibitors added freshly before use.

2.6.9 Liquid nitrogen stocks of mammalian cells

A 75 cm^2 flask of cells was grown at 37°C, 5% CO_2 to 90% confluence. The cells were removed from the flask by trypsin/EDTA-treatment, centrifuged at 1200 rpm for 3 min and the pellet resuspended in 2 ml of freezing mix [10% dimethyl sulphoxide (DMSO), 30% FCS and 60% D-MEM]. The cells were aliquoted into 1 ml sterile vials and placed inside a polystyrene container overnight at -70°C. Next day the vials were frozen in liquid nitrogen.

2.6.10 Establishing stable cell lines

This method was used for the establishment of cell lines that constitutively expressed EYFP and ECFP-tagged proteins. After characterising the expression of the fusion proteins in HeLa cells, a standard FuGENE-transfection in 25 cm^2 flask was performed (described in 2.6.2.3). The following day, the standard media was replaced with Optimem/10% FCS containing 1.5 μg puromycin (Sigma) per ml medium, which over time selected for cells with stable incorporation of the construct in their genomic DNA. (The amount of puromycin required to kill non-expressing cells varied from one cell line to another.) The antibiotic medium was replaced every other day. Once the cell death of non-expressing cells was obtained, the remaining colonies were picked into 24-well dishes (Nunclon™) and checked separately for fluorescence. Single colonies were picked using a Gilson P100 pipette with a sterile tip, which was lowered to the surface of the cell, scraped and sucked gently and transferred to a separate well, in the presence of a small amount of trypsin/EDTA. After obtaining stable cells of interest, a lower concentration of puromycin was used. Also a stock of stable cell lines expressing the gene(s) of interest were prepared and stored at –70°C (as described in 2.6.9).

2.7 Adenovirus type 2 preparations

2.7.1 Preparation and purification of Ad2

The preparation and purification of Ad2 by CsCl-gradient centrifugation was performed as described previously by Russell and Blair (1977). 6 litres of HeLa spinner cells were grown in Jokliks/7.5% Newborn Calf Serum (NCS). The cells were pelleted by centrifugation at 4,000 rpm for 10 min (Beckham ultracentrifuge J6-HC) and resuspended in 250 ml Jokliks without serum. The cells were infected using 1 ml of Arcton-extract of previously purified virus. The infection was left to proceed for 5 h in the warm room, after which the cells were given another 4 l of Jokliks medium. The following day, another 2 l of Jokliks/ 2% NCS was added and the infection was left to proceed altogether for 72 h. The infected cells were then centrifuged at 4,000 rpm for 30 min using Beckham J6-HC. The resulting pellets were washed three times using sterile PBS before resuspending in 8 ml of sterile 10 mM Tris/HCl, pH 7.5 per each litre of infected cells. Each tube with 12 ml of cell suspension was mixed with 15 ml of Arcton (1,1,2-Trichlorotrifluoroethane) and the tubes were sealed prior to applying a wrist action shaker to disrupt the cells (shaken at full speed for 30 min in the cold room). The mixture was centrifuged at 4,000 rpm for 30 min and the top layer consisting of Arcton was removed. To obtain pure Ad2, 2 ml of sterile 2 M CsCl was pipetted into 4 cm^3 Beckham ultracentrifuge tubes. To the bottom of the tubes, 3 ml of 3 M CsCl was carefully injected, whilst the Arcton was pipetted onto the top of the gradient. Care was taken to ensure that the tubes were full in order to prevent collapse of the gradient. The tubes were centrifuged at 30,000 rpm for 2 h at 20°C using Beckham L-60 ultracentrifuge. After the centrifugation, the viral band (blue/white in colour) was collected carefully following the removal of the top, soluble antigen layer by pipetting. The purified virus was mixed in an equal volume of glycerol and stored at -70°C.

2.7.2 Plaque assay for virus titre

To estimate the titre for the purified virus, plaque assays were conducted using a monolayer of HeLa cells in 9.4 cm^2 plates (6-well plates, Cellstar®). First, a dilution series of the virus from 10^{-5} to 10^{-10} ml was prepared in D-MEM. The dilutions of the virus were added to the cell monolayer, which was incubated on a vertical shaker in the

warm room for 1.5 h. After allowing the virus particles to adsorb to the cells, the medium of the cells was replaced with a warm mixture of 18 ml of D-MEM/2% FCS, 100 μl of 1 M $MgCl_2$ and 7 ml of 3% low-melting agarose. This mixture was left to set on top of the infected monolayer at room temperature for 30 min, after which the plates were incubated at 37°C until observable plaque formation. To aid in the visualisation of the plaque forming units (pfu), the cells were stained with neutral red, a dye taken up by living cells.

2.7.3 Infections of HeLa cells by Ad2

Viral infections of HeLa cells were performed at a multiplicity of 5 to 10 pfu per cell. In general, the virus was added in D-MEM or Optimem (Gibco), without additional serum, to cells and left to incubate in the warm room, on slow shaking for 1-1.5 h. Afterwards, the medium of the cells was replaced with D-MEM or Optimem supplemented with 2% FCS. The percentage of serum was increased to 10% after 6 h, and the infection was left to proceed for another 18-40 h at 37°C prior to fixing the coverslips for immunofluorescence. Optimem medium was used in infections of transiently or stably expressing fluorescent-protein fusions.

2.8 Cloning

2.8.1 DNA sequencing

All generated plasmids were sequenced by ABI PRISM 377™ Applied Biosystems Sequencer at the University of St. Andrews DNA sequencing unit.

2.8.2 Polymerase Chain Reaction (PCR)

PCR reactions were carried out using Applied Biosystems' GeneAmp PCR System 2400 and the following cycle conditions: initial denaturing at 95°C for 2 min, 30 cycles of amplification (denaturing at 94°C for 30 sec, annealing at 50°C for 45 sec, extension at 72°C for 1 min), final extension at 72°C for 7 min. The PCR cycle conditions were adjusted according to the melting temperature of the primers and the size of the amplified fragment. A typical PCR reaction mixture consisted of 0.2-1.0 μg of template DNA, 2-5 μl of each oligonucleotide to final concentration of 1 μM (purchased from Oswel), 10 μl of 10x Vent polymerase buffer, 0.5-1.0 μl (0.5-1 units) of Vent DNA

polymerase (New England Biolabs), 2 μl of dNTP mixture from stock solution (10 mM of dATP, dCTP, dGTP and dTTP) and nuclease-free water, up to 100 μl.

2.8.3 Restriction digestions

A standard single restriction digestion mixture consisted of: 1 μg DNA sample in ddH_2O, 2 μl 10x restriction enzyme buffer, 2 μl acetylated BSA (1 mg ml^{-1}), 1 μl Promega® restriction enzyme (2-10 units) and ddH_2O to final volume of 20 μl. The reaction was left to proceed at 37°C for 2-4 h after which the digested fragments were analysed by agarose gel electrophoresis.

2.8.4 Ligation

Isolated and purified DNA samples were ligated using T4 DNA ligase (Promega®). A typical ligation reaction consisted of 5 μl water, 3 μl fragment, 1 μl linearized plasmid, 1 μl 10x ligase buffer (100 μl solution: 25 μl 1 M Tris-HCl pH 7.8, 10 μl 1 M $MgCl_2$, 5 μl 1 M β-mercaptoethanol, 6 μl 0.1 M ATP and 54 μl water) and 1 μl T4 DNA ligase (3 units μl^{-1}). Ligation reactions were incubated at 4°C overnight or alternatively on bench for 1-3 h. Control ligation reactions were performed alongside with cut vector. The insert/template ratio in ligations ranged from 3:1 to 10:1.

2.8.5 Agarose gel electrophoresis

Electrophoretic analyses and preparative purification of DNA (including amplified PCR products) were performed using Bio-Rad (Power Pac 3000) gel electrophoresis apparatus together with the appropriate agarose gel electrophoresis rigs (Bioscience Services). Preparative 0.9% agarose gels consisted of [0.45 g agarose, 50 ml 1x TBE buffer (10.8 g Tris, 5.5 g boric acid, 4 ml 0.5 M EDTA, pH 8) and 2.5 μl ethidium bromide at 10 mg ml^{-1}]. Agarose gel electrophoresis was carried out at 60-80 V until sufficient separation was obtained.

2.8.6 Isolation of DNA

2.8.6.1 Isolation of DNA from agarose gels

DNA bands were isolated from agarose gels by migration into autoclaved filter paper. The wet filter paper was placed inside a 500 μl Eppendorf (with a hole in the bottom of

the tube), which was placed inside a 1.5 ml Eppendorf. The tubes were centrifuged at 13,000 rpm for 1 min using MicroCentaur centrifuge. The recovery of DNA into the 1.5 ml Eppendorf was confirmed under UV lamp and samples stored at -20°C.

2.8.6.2 Gel extraction

Alternatively, the DNA bands were extracted and purified from agarose gel according to the QIAquick gel extraction kit (QIAGEN) protocol (QIAquick spin handbook March 2001). The DNA fragment was excised from the gel with a scalpel and weighed in a 1.5 ml Eppendorf tube. 3 volumes of QG buffer were added per 100 mg gel slice (or adjusted accordingly) and the tube incubated at 50°C for 10 min. Following that, one gel volume of isopropanol was added to the sample, which was mixed and applied onto a QIAquick column. The column was centrifuged for 1 min at 13,000 rpm using MicroCentaur centrifuge. The column was washed with 0.5 ml buffer QG, followed by 0.75 ml buffer PE. The DNA was finally eluted off the column by the addition of 50 μl of ddH_2O or EB buffer (10 mM Tris/HCl, pH 8.5) and by centrifugation at 13,000 rpm for 1 min.

2.8.7 Competent cells

Competent *E.coli* strain DH5α cells were used for routine plasmid DNA preparation. First, 5 ml of LB was inoculated with a single colony of DH5α and left to grow overnight at 37°C. The 5 ml culture was used to inoculate a further 100 ml of LB the following day. The bacteria were left to grow at 37°C until the absorbance at 600 (A_{600}) reached 0.4. The culture was then transferred into sterile 50 ml tubes and kept on ice for 30 min at 4°C. The cells were centrifuged at 3600 rpm for 5 min at 4°C using Sigma 3K10 centrifuge. The bacterial pellet was resuspended carefully in sterile, cold, 25 ml of (100 mM $CaCl_2$, 40 mM $MgSO_4$) and kept on ice for 30 min. The cells were centrifuged at 3600 rpm for 5 min at 4°C and resuspended in cold 5 ml of [100 mM $CaCl_2$, 40 mM $MgSO_4$, 10% (v/v) autoclaved glycerol]. The cell suspension was then aliquoted into 200 µl sets, quick frozen on dry ice and stored at -70°C. Cells were considered competent if 10^6 colonies were obtained per 1.0 µg circular plasmid.

2.8.8 Transformation

2-10 µl of the ligation mixture or 0.2-1 µg circular plasmid was transformed by heat shock method into 100 µl of *E.coli* strain DH5α competent cells. First the cells were kept on ice for 30 min, followed by 45 sec at 42°C before being placed back on ice for 1-2 min. The cells were left to recover with 500 µl LB at 37°C for 30 min. Prior plating out the cells onto LB-agar plates supplemented with the appropriate antibiotic, the cells were harvested by centrifugation at 13,000 rpm for 10 sec. 400 µl of the supernatant was removed whilst the remaining 200 µl of resuspended cells was spread onto the plates (supplemented with correct antibiotic). The plates were incubated at 37°C overnight. Positive colonies from the plates were used to inoculate 5 ml of LB, supplemented with the appropriate antibiotic. Plasmid DNA was isolated using the QIAGEN miniprep spin protocol.

2.8.9 Glycerol stocks of plasmids

Glycerol stocks of the plasmids were prepared in DH5α (Stratagene®) cell line designed for DNA purification. A single colony was used for inoculating 2 ml of LB supplemented with the appropriate antibiotic and grown overnight at 37°C. Following day, 2 ml of 80% glycerol was added to the culture and 1 ml aliquots stored at -70°C.

2.8.10 Purification of plasmid DNA

2.8.10.1 QIAGEN Miniprep

The method is based on the procedure of alkaline lysis of bacterial cells (described by Birboim & Doly, 1979), followed by the adsorption of the DNA onto silica QIAprep membrane in the presence of high salt. This protocol was followed according to QIAprep Handbook 10/2001, designed for the purification of up to 20 µg of circular plasmid DNA. First, 1-5 ml of overnight culture of *E.coli* in LB was centrifuged for 3 min at 13,000 rpm. The resulting cell pellet was resuspended in 250 µl buffer P1 (RNase-containing) and another 250 µl of (lysis) buffer P2 was added to the Eppendorf tube. The tube was inverted gently and left at room temperature for 5 min. 350 µl of (neutralising) buffer N3 was added to the lysate, the tube inverted several times before centrifugation at 13,000 rpm for 10 min. The resulting supernatant was applied to a QIAprep spin column and the column centrifuged at 13,000 rpm for 1 min. The column

was washed in 500 µl buffer PB and 750 µl buffer PE and centrifuged after each addition. The DNA was finally eluted off the column by the addition of either ddH_2O or buffer EB (10 mM Tris/HCl, pH 8.5), and by centrifugation of the column at 13,000 rpm for 1 min.

2.8.10.2 QIAGEN Maxiprep

As mentioned previously in the Qiagen Miniprep method, Maxi-preparation of circular plasmid DNA is also based on modified alkaline lysis procedure. The maxi protocol has been designed for the purification of up to 500 µg of high-or low-copy number plasmid (Maxiprep-handbook 10/2001).

First, a single colony was picked from a plate (supplemented with antibiotic), used to inoculate 5 ml of LB (with antibiotic), and left to grow at 37°C for 8 h. This culture was then used to inoculate 100 ml of LB (with antibiotic), which was grown at 37°C overnight. The following morning, the cells were centrifuged at 6000x g for 15 min at 4°C using Sigma 3K10. The resulting pellet was resuspended in 10 ml buffer P1. To this, 10 ml buffer P2 was added and the tube was gently inverted to mix and left at room temperature for 5 min. 10 ml of chilled buffer P3 was then added to the lysate, the tube inverted and centrifuged at 20,000x g for 30 min at 4°C. The supernatant containing the DNA was removed carefully and re-centrifuged at 20,000x g for 15 min at 4°C. The supernatant was then applied to a QIAGEN-tip 500 column (equilibrated with buffer QBT) and allowed to enter by gravity flow. The column was washed after the loading of the supernatant using 60 ml buffer QC. To elute the DNA off the column, 15 ml of buffer QF was passed and the eluate collected into a glass Corex® tube. The DNA was precipitated by the addition of 10.5 ml room-temperature isopropanol. The sample was quickly mixed and centrifuged at 12,000x g for 30 min at 4°C to obtain a glassy appearing pellet. The pellet was further washed in 70% ethanol at 12,000x g for 10 min. The pellet was finally air-dried and re-dissolved in appropriate volume of ddH_2O.

2.8.11 Determination of DNA concentration

The quantification of DNA was performed by Spectrophotometric analysis according to Sambrook *et al.* (1989). The first reading at 260 nm was used to calculate the concentration of nucleic acid [OD 1 corresponding to 50 µg ml^{-1} for dsDNA, 40 µg ml^{-1}

for ssDNA and RNA]. An estimate for the purity of the sample was obtained by calculating the ratio of readings at 260 nm and 280 nm [pure preparations of DNA or RNA having OD_{260}/OD_{280} around 1.8-2.0].

2.9 In vitro transcription/ translation experiments

2.9.1 TNT® Quick coupled transcription/translation

Cell-free *in vitro* expression of proteins from pdf20 clones containing a T7 promoter cloned genes was obtained by using TNT® Quick coupled transcription/translation system (Promega). The TNT® Quick system combines the RNA polymerase, nucleotides, salts and recombinant Rnasin® ribonuclease inhibitor with the rabbit reticulocyte lysate, also known as the Master mix.

The reactions were conducted according to manufacturer's instructions (Roche). Briefly, in a standard reaction 40 μl of master mix (from -70°C) was combined with 2 μl [^{35}S] methionine (1,000 Ci/mmol at 10mCi/ml), 1 μg plasmid DNA and nuclease-free water to a final volume of 50 μl. Often smaller scale reactions were performed by proportionally reducing the volumes of all assay components. The reaction mixture was incubated at 30°C for 60-90 min, after which the synthesised proteins were analysed by SDS-polyacrylamide gel electrophoresis (SDS-PAGE). The resulting gel was dried onto 3 mm paper using BIO-RAD 583 gel-dryer (at 80°C for 40 min) and exposed to Kodak-MR film. Alternatively, the gels were exposed to Phosphor-imager screen and analysed using Fujifilm FLA-5000 scanner and Image Reader software.

2.9.2 In vitro cleavage of TNT products by AVP

To assess the efficiency at which purified AVP was able to cleave the various pdf-protein constructs, the TNT-translation products were incubated at 37°C in the presence of protease for various timepoints. The cleavage assay consisted of 10 μl assay buffer [50 mM Tris, 10 mM EDTA and 2 mM β-mercaptoethanol], 5 μl TNT-translation product, 5 μl AVP at 0.1 mg ml^{-1} and 0.2 μg pVIct. After the incubation in the presence of AVP, the cleavage reaction was terminated by the addition of gel loading buffer [5% (v/v) β-mercaptoethanol, 2% (w/v) SDS, 2.5% (v/v) glycerol, 50 mM Tris, pH 6.9 and 0.001% (w/v) Bromophenol blue] and samples were boiled for a few minutes. The

cleaved products were analysed on a 12.5% SDS-gel and by Phosphor-imaging as described above.

2.9.3 Analysis of cleavage

The Image Gauge v3.45 programme was used for the quantification of the protein bands. The Profile/MW-mode was used, automated peak search selected and background was subtracted from the intensity of the protein bands. The percentage of substrate cleavage was calculated according to method by Hughes (2003):

Intensity of protein band/ Methionine-content of protein band = Actual protein intensity

(Actual intensity of cleaved fragment/ Actual intensity of uncleaved template) x 100

= % cleaved product.

3. Results: Activation and binding between protease and its cofactor peptide

3.1 Objectives of the study

Previous results have shown that binding of the peptide to the protease resulted in a conformational change, observed by intrinsic tryptophan fluorescence (Jones *et al.*, 1996). Furthermore, mutational analysis on the well-conserved Glycine'1 and Valine'2 showed that this N-terminal dipeptide was, together with the thiol-bridge forming Cysteine'10, an important component of AVP stimulation and for bringing about the conformational change (Cabrita *et al.*, 1997).

What is the significance of the other C-terminal residues along the peptide? The four cationic residues (the KRRR-motif) are well conserved throughout human adenovirus serotypes (see alignment of pVI C-terminal sequences, Figure 6). Also the presence of an aromatic amino acid at the 11^{th} position is apparent. The aim of this study was to investigate the importance of these residues to the binding of pVIct to the protease and to the stimulation of protease activity.

Figure 6. Alignment of known adenoviral pVI sequences. The protease cleavage sites are shown with a dashed line and the conservation of the C-terminal peptide residues, studied in this thesis, are shown in blue. The protein sequences were obtained from Protein Data Bank, and the alignment was performed with Clustal W (1.82) multiple sequence alignment.

```
P6_CanineC      MDAVNFSILAPRYGSHPMMSAWSGIGTSDMNGGAFNWGGIWSGIK----NFGSNVKNWGS 56
P6_CanineR      MDAVNFSILAPRYGSHPMMSAWSGIGTSDMNGGAFNWGGIWSGIK----NFGSNVKNWGS 56
P6_Bovine       MEGINFSALAPRYGSRPMLSSWSDIGTSSMNGGAFNWGSLWSG---------------- 43
P6_Human2       MEDINFASLAPRHGSRPFMGNWQDIGTSNMSGGAFSWGSLWSGIK----NFGSTIKNYGS 56
P6_Human5       MEDINFASLAPRHGSRPFMGNWQDIGTSNMSGGAFSWGSLWSGIK----NFGSTVKNYGS 56
P6_Human11      MEDINFSSLAPRHGTKPYMGTWSDIGTSQLNGGAFNWSSIWSGLK----NFGSTIKTYGN 56
P6_Human40      MEDINFASLAPRHGSRPFMGTWNEIGTSQLNGGAFSWSSLWSGIK----NFGSSIKSFGN 56
P6_Human41      MEDINFASLAPRHGSRPFMGTWNEIGTSQLNGGAFSWSSLWSGIK----NFGSSIKSFGN 56
P6_Human12      MEDINFSSLAPRHGTRPYMGTWNEIGTSQLNGGAFNWNSIWSGLK----NFGSTIKTYGT 56
P6_Mouse        MDDP-FSTLAPRRGTQPLLSNWATIGISELHGGALGWGSWWSNLSRLGSSFGSNLKNLGL 59
P6_Frog         ----MYSMLAPHMGQTTFSGYD--IGTSELRGGKINWGALGSSISNAFKTTGRFIGSAAN 54
P6_Turkey       ----MFSNLAPRLGHTSFSTVS--VGSAELRGGKINWGSLGSSISNALRTTGRYLGQKAT 54
P6_CELO         ---MDYAALSPHLGGWALRDHH--IGDSSLRGGAINWGNLGSRITSALNSTGRWLYNTGN 55
P6_EDS          ---MAFARLAPHCGLTPVYGLR--IGNSDMRGG-FSWASLGSSLSSGLSRIGSAVANTAR 54
P6_Snake        ---MAYSRLAPHCGL-PVYGHH--IGNSEMSGG-FSWSSLGSSLSSGLSRIGSFLGSTAQ 53

P6_CanineC      RAWNSQTGKLLRQKLNDTKVREKLVEGISTGVHGALDIANQEIAKQIERRLER------- 109
P6_CanineR      RAWNSQTGKLLRQKLNDTKVREKLVEGISTGVHGALDIANQEIAKQIERRLER------- 109
P6_Bovine       ------------------------------------------------------------
P6_Human2       KAWNSSTGQMLRDKLKEQNFQQKVVDGLASGISGVVDLANQAVQNKINSKLD-------- 108
P6_Human5       KAWNSSTGQMLRDKLKEQNFQQKVVDGLASGISGVVDLANQAVQNKINSKLD-------- 108
P6_Human11      KAWNSSTGQALRNKLKDQNFQQKVVDGIASGINGVVDLANQAVQKKINSRLD-------- 108
P6_Human40      KAWNSNTGQMLRDKLKDQNFQQKVVDGLASGINGVVDIANQALQNQINQRLENSRQPPVA 116
P6_Human41      KAWNSNTGQMLRDKLKDQNFQQKVVDGLASGINGVVDIANQALQNQINQRLENSRQPPVA 116
P6_Human12      KAWNSQTGQMLRDKLKDQNFQQKVVDGLASGINGVVDIANQAVQKKIANRLE-------- 108
P6_Mouse        KAWNSSTGQALRQHLKDTNLQHKVVEGLSTGIHGAVDIARQEVDRQLAKRLEN------- 112
P6_Frog         KFAKSKAFADIKQGLNDSGIARNVAALAGETLNNLVDIGRTRLQQDLDDLREK------- 107
P6_Turkey       KFANSKTFSDIKAGIQDSGLVRNVAGLAGQTLNSLVDIGRFKVESELQKLRDR------- 107
P6_CELO         RFVHSNTFNQIKQGIQDSGVIRNVANLAGETLGALTDIGRLKLQQDLEKLRRK------- 108
P6_EDS          QIGNSQAFQQAKSGFLQSGILENVGQLAGQAVSSLVDVGRIKLEQDVQNLRDK------- 107
P6_Snake        RIGNSQGFQQAKEGFLKSGVLENVGSLAGQTVSSLADIGRLKLESDLQKLRER------- 106

P6_Caninec      ------HEPLEPEVEEETVETKSEA-KAPLVVEMPLKRPRDEDLVITADEPPSYEETIKT 162
P6_CanineR      ------QQPLEPEVEEETVETKSEA-KAPLVVEMPLKRPRDEDLVITADEPPSYEETIKT 162
P6_Bovine       ------------------------------------------------------------
P6_Human2       --------PRPPVE-EPPPAVETVS--PEGRGEKRPRPDREETLVTQIDEPPSYEEALKQ 157
P6_Human5       --------PRPPVE-EPPPAVETVS--PEGRGEKRPRPDREETLVTQIDEPPSYEEALKQ 157
P6_Human11      --------PPPATPGEMQVEEEIPP--PEKRGDKRPRPDLEETLVTRVDEPPSYEEATKL 158
P6_Human40      LQQRPPPKVEEVEVEEKLPPLEVAP-PLPSKGEKRPRPDLEETLVVESREPPSYEQALKE 175
P6_Human41      LKQRPTPEPEEVEVEEKLPPLETAP-PLPSKGEKRPRPELEETLVVESREPPSYEQALKE 175
P6_Human12      ------PRPDEVMVEEKLPPLETVPGSVPTKGEKRPRPDAEETLVTHTTEPPSYEEAIKQ 162
P6_Mouse        -----YEPPRVASTEETVDDVKTVA--LPSKED-----ESERVLVTKIREPPPPYDAVFG 160
P6_Frog         --------ALKKE-ALSPDKMIELLMRYQDSVSPAPLPA---------LPSPSPQIVELE 149
P6_Turkey       --------VLN---TIPADQLAQILLNYQQTHDQVPMPVTPGD--AIPLPPPPPAAIEPR 154
P6_CELO         --------ALGEEGPATQAELQALIQALQAQVAAGEPPAAP------AAPAPAPPLVP-T 153
P6_EDS          --------VLGERQQHQGHPMPYPHIVQPPPEPIVRPPALPPVPALPALPPPIPLPPPAV 159
P6_Snake        --------ALG-AQQQQLPPLTQEQLAQLLASTQTELPSSAPAVPMP-IPAPVP-PLVTG 155

P6_CanineC      MAP----LVPMTRPHPSMARPVIAD----RPTTLELKP-------------SDQPPPYSP 201
P6_CanineR      MAP----LVPMTRPHPSMARPVIAD----RPTTLELKP-------------SDQPPPYSP 201
P6_Bovine       ------------------------------------------------------------
P6_Human2       GLP-------TTRPIAPMATGVLG---QHTPVTLDLPP-PADTQQKP--VLPGPSAVVVT 204
P6_Human5       GLP-------TTRPIAPMATGVLG---QHTPVTLDLPP-PADTQQKP--VLPGPTAVVVT 204
P6_Human11      GMP-------TTRPIAPMATGVMKPSQLHRPVTLDLPP-PPAAT-----AVPASKPVAAP 205
P6_Human40      GASP----YPMTKPIGSMARPVYGK--ESKPVTLELPP-PVPTVP------PMPAPTLGT 222
P6_Human41      GAS-----YPMTRPIGSMARPVYGK--EKTPVTLELPP-PAPTVP------PMPTPTLGT 221
P6_Human12      GAALSPTTYPMTKPILPMATRVYGKN-ENVPMTLELPPLPEPTIADPVGSVPVASVPVAS 221
P6_Mouse        PAP-----SAETNKKQKFEETLQNAG------LVSSPP------------APIAAPAAIA 197
P6_Frog         SEP--------PLPAVSVPALPSTS---------------------------KRPLEVE 173
P6_Turkey       KRPYVEEIDDNPNDAEVVIDTPALS-----------------------------TVPAIPA 186
P6_CELO         TRP--------IPEMVTEVKPPVTS---------------------------SAPAVPV 177
P6_EDS          VEPPV----VAPAIAAPSLAAPVEA---------------------------DMPPASE 187
P6_Snake        VRPGQ----MRPEVLPPDRGVALG-----------------------------PLIEE 180

P6_CanineC      QSSNMPVTAP---------VRSRGWQGTLANIVGVGLSNVKRRRCF 238
P6_CanineR      QSSNMPVTAP---------VRSRGWQGTLANIVGVGLSNVKRRRCF 238
P6_Bovine       ------------------------------------------------
P6_Human2       RPSRASLRRAASGPRSMRPVASGNWQSTLNSIVGLGVQSLKRRRCF 250
P6_Human5       RPSRASLRRAASGPRSLRPVASGNWQSTLNSIVGLGVQSLKRRRCF 250
P6_Human11      KPVAVARSRPGGAPR-----PNAHWQNTLNSIVGLGVQSVKRRRCF 246
P6_Human40      AVSRPTAPTVAVATP-ARRPRGANWQSTLNSIVGLGVKSLKRRRCY 267
P6_Human41      NVPRLAAPTVAVATP-ARRVRGANWQSTLNSIVGLGVKSLKRRRCY 266
P6_Human12      TVSRPAVRPVAVAS--LRNPRSSNWQSTLNSIVGLGVKSLKRRRCY 265
P6_Mouse        VPAQTTMSHPASSR------RRHHWQGTLDSIMGLGLQPIKRRRCF 237
P6_Frog         EMQVQSFVPSRKR--FRGTGVNSAWRQKLNEIVGSGVNYSTLSRCY 217
P6_Turkey       PPPTVAFVPSIKRPRIRGTGE-SEWQTHLNKMLGQGVRFTSTNQCY 231
P6_CELO         DVPTTLEMRPPPPKRRRKRARPGQWRARLDSLSGTGVATATRRMCY 223
P6_EDS          PVADTVVDRRRRN---KKRKRVSGWGAALDSMVGDGVRYGSQRYCY 230
P6_Snake        PAPRPIAVPGSRP---RKRKRVRGWGSALEDMLGDGVCYRSKRYCY 223
```

3.2 Activation studies with peptide variants

Activating peptides were synthesised containing single Alanine-substitutions along the wild-type peptide sequence [GVQSLKRRRCF (wild-type or wt), GVQSL**A**RRRCF, GVQSLK**A**RRCF, GVQSLKR**A**RCF, GVQSLKRR**A**CF, GVQSLKRRRC**A**, GVQSLKRRRC**Y**, GVQSLKRRRC] according to the method by Atherton & Sheppard (1989). In addition, a wt activating peptide with a fluorescein-tag on its lysine residue was synthesised as outlined in method 2.2.2 for *in vivo* experiments (discussed later in section 4). Two peptide sequences corresponding to the last 11 residues from the pVI sequences of fowl adenovirus type 1 or Chick Embryo Lethal Orphan (CELO) virus and that of the Egg Drop Syndrome (EDS) virus, belonging to the *Aviadenoviridae* and *Atadenoviridae* genus, respectively, were also generated. It was thought of interest to assess whether the EDS peptide (GVRYGSQRYCY) and CELO peptide (GVATATRRMCY) were capable of activating an evolutionary distant, human adenovirus serotype 2 protease.

For the *in vitro* activation and binding experiments performed in this study, recombinant protease was purified according to method 2.3. In brief, the recombinant wt AVP in pET 11c vector was expressed and extracted from *E. coli* BL21 cells according to the method outlined in section 2.3.1 and 2.3.2. The protease was purified by a single step purification method (Pollard, 2001) by passing the extract through the Diethylaminoethyl (DEAE) Sepharose column, Heparin-Sepharose and Carboxymethyl-Sepharose columns. The yield of protease, determined by Bradford assay and by comparison to SBTI standards on 20% SDS-PAGE, was approximately 1 mg l^{-1} of cell culture. Figure 7 (A-C) shows the general purification profile of the protease through the different exchange columns and the protease fractions obtained from purification, confirmed by Western blotting following SDS-PAGE.

The specific activity of protease with the peptide variants was conducted using the Ac-LRGAGRSR-peptide substrate (a synthetic peptide with acetylated N-terminus). The assays were performed essentially as described previously by Webster *et al.* (1989b) and Cabrita *et al.* (1997). The initial rates of substrate digestion were calculated from integrated peak areas (of Ac-LRGA and GRSR products and of un-cleaved substrate) using Integrator V3.01 software (Bio-Rad). The data was analysed according to a method by Cabrita (1997) as summarised in method 2.5.2.2.

The relative activation efficiencies for the peptide variants, presented in Figure 7D, were collected from a minimum of three determinations, with correlation coefficients of ≥0.9. Due to the differences in activity between protease batches used, each assay with a peptide variant was performed alongside wild-type pVIct. Subsequently, the results were normalised by expressing the activation rates as a percentage of that obtained with wt pVIct.

The overall trend for the activation ability of the Alanine-mutants of KRRR-motif was an approximately 40-50% reduction in activity to that of the wt pVIct. The KARR, KRAR and KRRA-mutants displayed very similar rates of substrate hydrolysis (50.2±6.6, 56.7±11.7 and 50.1±10.2 % of wt, respectively). The Lysine-6 mutant, ARRR displayed slightly lower activity than the Arginine counterparts (44.3±9.5 % of wt).

The pVIct-F, peptide with a fluorescein-tagged lysine residue, was capable of activating the protease relatively efficiently (60.1±9.1 % of wt). This peptide was synthesised for cell culture work, and it is discussed in more detail in Chapter 4 (nuclear localisation experiments).

The C-terminal mutation, F'11A on the other hand caused the highest reduction in activity (15.0±5.2 % of wt), together with the deleted version F'10 peptide (10.4±4.6 % of wt), lacking the eleventh residue. Surprisingly, the tyrosine peptide (F'11Y) was not as efficient in activation (52.0±4.3 % of wt) as the wt, Phenylalanine-bearing pVIct. Given that the tyrosine is present in the sequence of several adenoviral pVI serotypes, it was expected to easily substitute for the phenylalanine without an effect on the activation.

The peptides from the distant avian adenoviral serotypes are capable of activating protease from human adenovirus type 2. The CELO and EDS peptides displayed activities of 25±5.6 and 23.7±4.0 % of that obtained with the wt peptide, respectively.

Figure 7 (A)-(C). The purification profile of AVP (A). The protein extract was applied to DEAE-Sepharose, Heparin-Sepharose, and Carboxymethyl-Sepharose columns. At position I, only DEAE-column was connected, after which all three columns were connected (II). Finally, only Carboxymethyl-Sepharose column was connected and the protease was eluted using 0.2 M NaCl (III). Purified AVP fractions were separated on a 15% SDS-gel (B), and further confirmed by Western blotting using an antiserum raised against the N-terminal 17 residues of the Ad2 protease and coupled to human serum albumin (HSA) (C). S refers to protein molecular weight markers (note that HSA was included and hence the band appearing in the Western blot) and p-AVP refers to a previously purified protease sample.

Figure 7 (D). Relative specific activity of peptide variants, determined by cleavage of the peptide-substrate Ac-LRGAGRSR. Rates are expressed as a percentage of that obtained by the wt peptide. The activity of the protease in the presence of wt pVIct was 5-10 mmol product min^{-1} $mmol^{-1}$ protease. Values plotted are the mean values (± standard error) derived from minimum of three determinations.

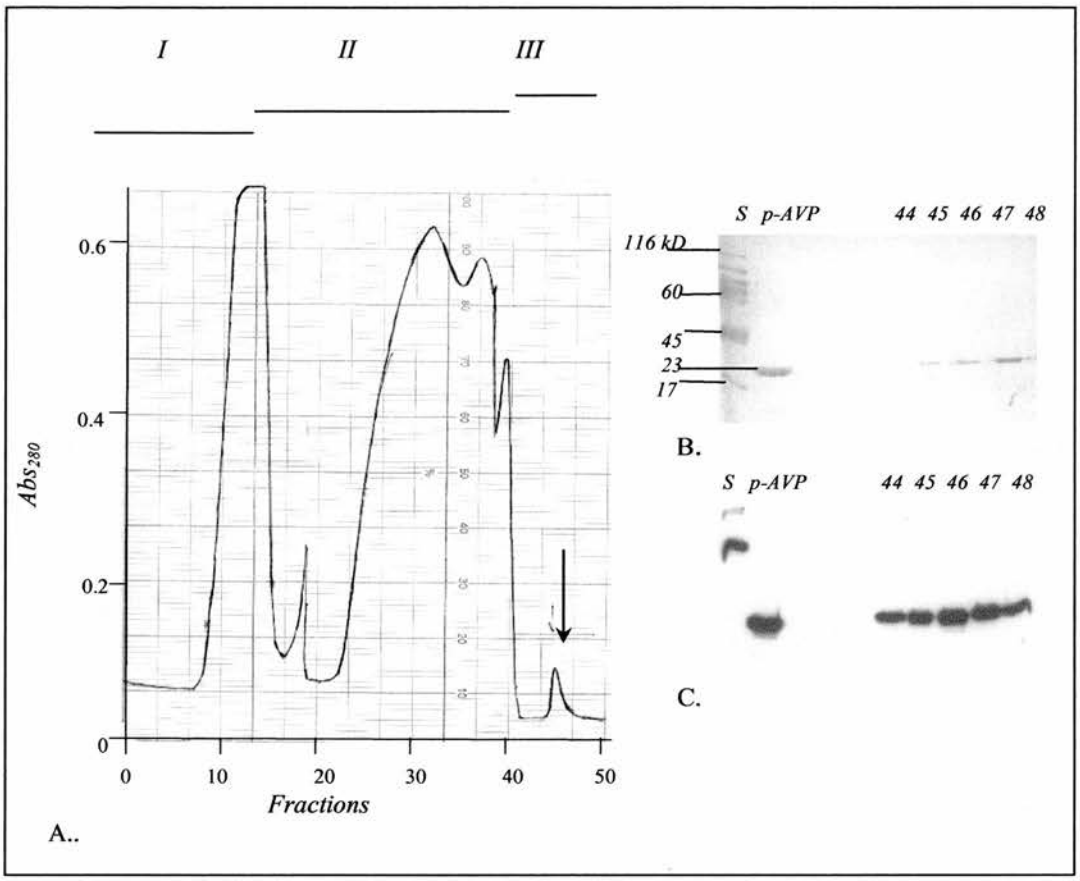
I
II
III
0.6
0.4
0.2
0
Abs280
0
10
20
30
40
50
Fractions
A..
S p-AVP
44 45 46 47 48
116 kD
60
45
23
17
B.
S p-AVP
44 45 46 47 48
C.

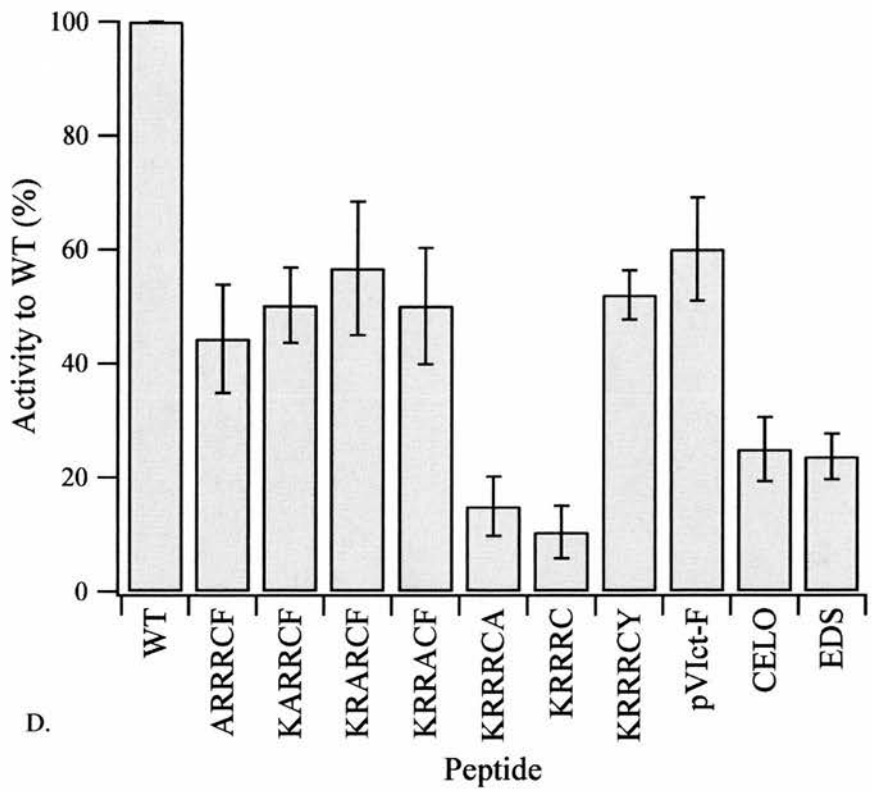
100
80
60
40
20
0
Activity to WT (%)
WT
ARRRCF
KARRCF
KRARCF
KRRACF
KRRRCA
KRRRC
KRRRCY
pVIct-F
CELO
EDS
Peptide
D.

3.3 Binding experiments with native gel electrophoresis

Non-denaturing, 'native' gel electrophoresis, performed in the absence of SDS and near neutral pH, can be used to study protein-protein interactions and protein conformations whilst the protein is found in its native conformation. Unlike SDS-PAGE, during native electrophoresis the mobility of proteins depends on their charge, hydrodynamic size and the folded conformation of the protein, not on their molecular mass (Goldenberg, 1989).

In this study, the native gel electrophoresis for basic proteins (an adapted method from Goldenberg, 1989) was used to study binding between adenovirus protease and peptide. Essentially, the binding assay mixture (described in section 2.4.8) with purified recombinant protease and doubling dilutions of 1 mM peptide was prepared with assay buffer and gel tracking solution, prior to being loaded onto a 15% native riboflavin gel, which was separated as detailed in Methods. Lysozyme was added to the assay to function as an internal standard. Following native gel electrophoresis, the gels were stained with Coomassie blue, destained, scanned and the band intensities were measured using NIH Image 1.62 software (developed at the U.S National Institutes of Health).

The data from native gel electrophoresis assays were used for Scatchard-plot analysis. For the calculation of equilibrium dissociation constant, K_d, 1:1 binding ratio for the peptide and protease is assumed. The published crystal structure supports the concept that the protease behaves as a heterodimer and that only one pVIct molecule binds to one AVP molecule (Ding *et al.*, 1996). To obtain equilibrium dissociation constant, K_d, for pVIct variants the concentrations of Bound peptide, $[pVIct]_{bound}$ and Free peptide, $[pVIct]_{free}$ were calculated, as detailed in method 2.4.9. The K_d value was determined from the negative reciprocal of the slope [slope = $-1/K_d$] in Scatchard-plot analysis ($[pVIct]_{bound}/ [pVIct]_{free}$ v $[pVIct]_{bound}$).

The representative native gel in Figure 8A (lane B) indicates the two bands subject to analysis. The upper band represents the formation of a protease/activating peptide heterodimer-complex, whilst the lower band is that of the lysozyme. With the doubling dilution series of the peptides (final concentration ~140 μM to 2 μM), the intensity of the protease/peptide complex decreases (Figure 8B). As a control, native gels were performed without the inclusion of peptide. From Figure 8A (lane A), it can be seen that

in the absence of the peptide, there was no visible band for the AVP itself but rather a smearing or ladder-effect, emphasising the importance of pVIct for the formation of the active complex.

Table 2 shows the mean values of binding data together with standard deviations for each peptide variant (data from minimum of three determinations). According to the binding dissociation constants derived from the native gel electrophoresis, Alanine-mutants to the KRRR-motif displayed affinities similar to that of the wt pVIct (K_d 1.28±0.19). From those four peptide variants, Lysine to Alanine mutation caused the biggest increase in the K_d value (2.88±1.51). The differences between the mean binding affinities of GVQSLKRARCF, GVQSLKRRACF and GVQSLKARRCF peptides however, were small.

Following the analysis, the C-terminal mutant F'11A and the peptide lacking the 11^{th} residue (GVQSLKRRRC) exhibited the weakest binding affinities compared to that of the wt pVIct, apparent from the approximate 4.6 and 7.5-fold increase in K_d values, respectively. If however, the C-terminal Phenylalanine was substituted with Tyrosine, which is very similar in nature, binding was restored close to that obtained with wt (2.04±0.40).

The fluorescent peptide pVIct indicated relatively good binding ability (1.8±0.57) while the two avian peptides CELO and EDS demonstrated similar binding affinities (3.3±0.34 and 2.9±0.8, respectively).

Overall, these experiments showed that this method could be successfully used as a means of obtaining binding information and repeatable data, and in this case binding affinities between a peptide and a protease. However, when conducting native gel electrophoresis, and to obtain consistent data, variables such as the enzyme preparation used and its age, should be kept to a minimum. In this study, photo-polymerisation with riboflavin was preferred since it leaves less reactive compounds in the gels offering perhaps the most native conditions for proteins.

Table 2. Binding data for peptide variants obtained from native gel electrophoresis. The data for the peptide variants was derived from a minimum of three determinations, the standard deviations are shown (±).

Figure 8 (A). Representative native gel showing the AVP/pVIct-complex. Lane A shows the protease (adenain) in the absence of peptide while lane B shows the dimer-complex formed in the presence of a 300-fold molar excess of pVIct.[Figure courtesy of G. Kemp, (Honkavuori *et al.,* 2004)].

Figure 8 (B). Representative riboflavin-based native gels for the determination of binding affinities. [1] Protease with doubling dilutions (140 μM–2 μM) of wt pVI-CT. [2] Protease with doubling dilutions (140 μM–2 μM) of peptide mutant GVQSLKRRACF. Native gel electrophoresis and analysis were performed as described in Methods, with lysozyme as an internal standard. 100%-lane refers to undiluted peptide sample (280 μM) in the presence of 0.8 μM protease.

Figure 8 (C). Representative binding data for peptide GVQSLKRRRCA and GVQSLKRARCF. Concentration of protease used in assay was 0.8 μM.

Table 2. Binding dissociation constants

Peptide	K_d *(μM)*
GVQSLKRRRCF	1.28±0.19
GVQSLARRRCF	2.82±1.51
GVQSLKARRCF	1.45±0.12
GVQSLKRARCF	1.55±0.3
GVQSLKRRACF	1.47±0.27
GVQSLKRRRCA	5.88±0.28
GVQSLKRRRC	9.56±2.13
GVQSLKRRRCY	2.04±0.40
pVIct-F	1.80±0.57
EDS	2.9±0.80
CELO	3.3±0.34

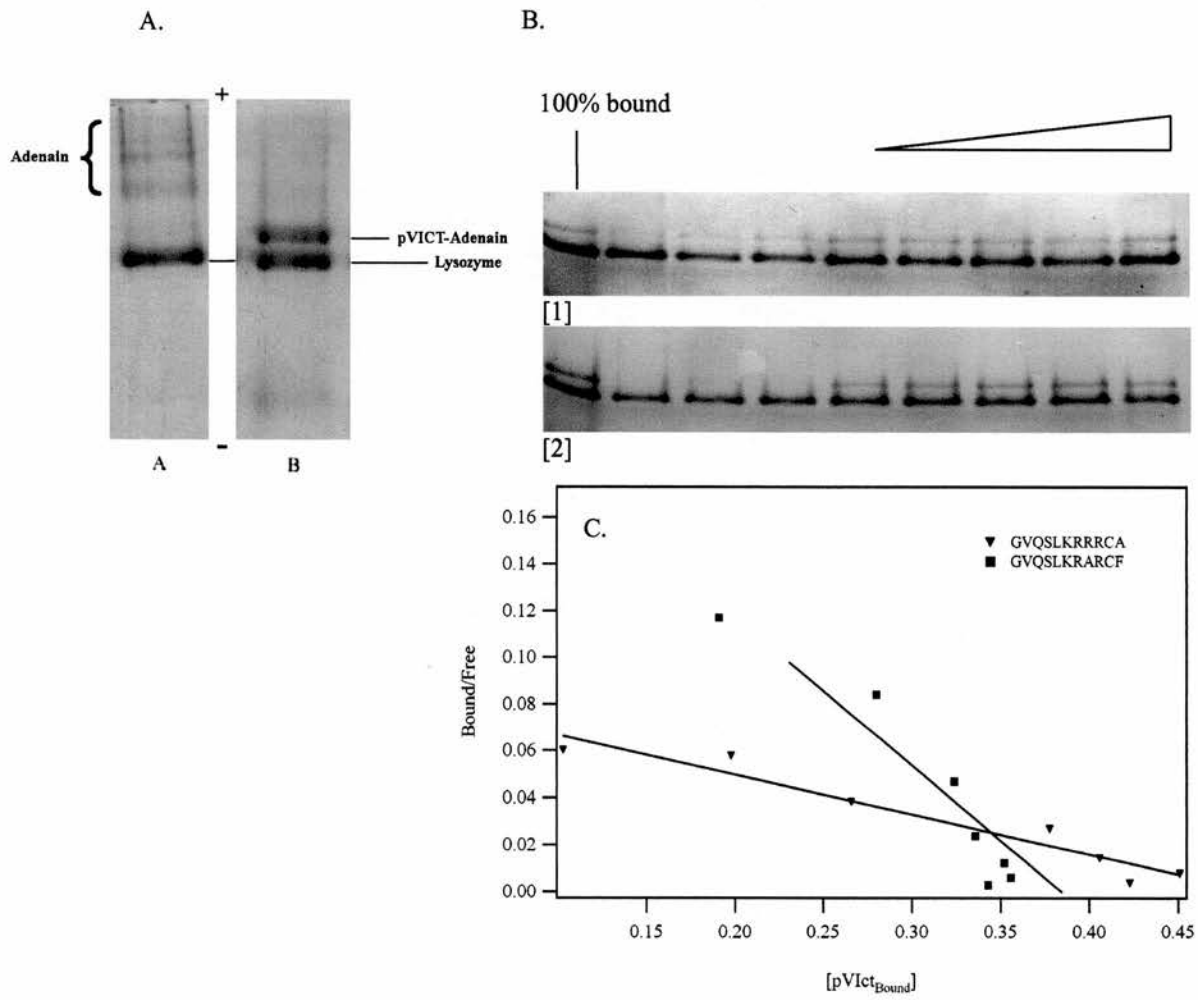

3.4 Fluorescent-substrate assays: binding and activation

In order to measure both the binding and activation abilities of the peptide mutants, expressed as the Michaelis constant (K_m), catalytic rate constant (k_{cat}) and the equilibrium dissociation constant (K_d), I opted for the use of a fluorogenic substrate, which is commercially available and previously used for the confirmation of protease activity (Balakirev *et al.*, 2002).

The experiments were performed with a fluorescent substrate z(benzyloxycarbonyl)-Leu-Arg-Gly-Gly-AMC (7-*a*mino-4-*m*ethyl*c*oumarin) (Bachem) and using a Perkin-Elmer Luminescence Spectrometer LS 50B. The adenovirus protease cleaves this peptide-AMC substrate following the second Glycine residue. The absorbance of the released cleaved product (AMC) was measured at an excitation wavelength of 370 nm and an emission wavelength of 460 nm. In the activity assays (k_{cat} and K_m experiments), varying fluorescent substrate concentrations were added to the pre-incubated 26 nM of AVP and 2 μM of peptide. In the K_d-experiments, the concentration of the peptide was varied (0.3-4 μM) while the substrate and protease concentration was kept at 62.5 μM and 26 nM, respectively. The concentration of components used in the assay was based upon the data published by Baniecki *et al.* (2001), where a similar synthetic substrate (Leu-Arg-Gly-Gly-NH)$_2$-Rhodamine was employed to evaluate the binding and activation abilities of peptide mutants. Conducting experiments in this manner also allowed for easier comparison with the corresponding data of Baniecki *et al.*

The data obtained was analysed using Igor Pro 3.12 software, and as described in Methods. The catalytic rate constants, Michaelis constants and the binding data from the experiments with the fluorogenic substrate are summarised in Table 3. For the calculation of k_{cat}, the concentration of active complex present in the assay needed to be considered. Since the assays were conducted in the presence of 2 μM peptide variant, the concentrations of the active AVP/pVIct-complex were less than saturating. Therefore, the concentration of active complex in each experiment was calculated on the basis of the K_d values obtained from the native gel electrophoresis, as explained in method 2.5.3.2, and according to the example by Baniecki *et al.* (2001).

The k_{cat} for the wt pVIct was 0.0283 sec^{-1}; the highest catalytic rate constant obtained from all the peptide variants assayed. The Alanine mutants of the KRRR-sequence

exhibited a catalytic rate 57-71% of that by the wild-type, with K_m values varying from 60-135 μM.

The most crucial residue according to these experiments, which if mutated lead to a dramatic decrease in both binding and activation of the protease, was the Phenylalanine-11. The Phenylalanine to Alanine mutant displayed a 3.8-fold reduction in activity as well as a 4.6-fold reduction in binding ability. When, in this study, the Phenylalanine was substituted with a Tyrosine, the binding affinity was restored, although the catalytic rate constant was still only approximately half of that obtained with the wt pVIct.

Since the excitation and emission spectra, at which AMC-product formation was measured overlaps with the spectrum for fluorescein, the data for the fluorescein-tagged peptide should be treated merely as an approximation (although here there was no indication that the peptide caused interference with its fluorescein-tag to the measurement of product formation). The rate of substrate hydrolysis for this peptide was approximately 46% of that obtained with the wt peptide. According to the AMC-substrate experiments, the pVIct-F and GVQSLARRRCF peptides showed that a mutation to or a tag on the Lysine residue affected slightly the binding to the protease (K_d ~2.5), but overall these peptides were capable of stimulating protease activity reasonably well when compared to the wt peptide.

With the AMC-based substrate, the rates of hydrolysis with the two distant avian peptides, were ~5% (EDS) and ~6% (CELO) of that obtained with the wild-type peptide Considering the reduced sequence similarity between the avian strains with that of the human serotype 2, the approximately two-fold increase in K_d values and their poorer ability to activate protease were perhaps expected.

Table 3. Activation and binding data for peptide variants using a fluorogenic substrate. The assays were performed using z-Leu-Arg-Gly-Gly-AMC-substrate as described in Methods. In brief, in the K_d experiments 26 nmol of purified AVP and the varying concentrations of peptides (0.3-4 μM) were incubated in assay buffer [50 mM Tris, 10 mM EDTA, 2 mM β-mercaptoethanol (pH 8)] at 37°C for 10 min prior to the addition of the substrate (62.5μM). The experiments for the determination of k_{cat} and K_m values were conducted as described previously apart from peptide concentration being kept at 2 μM whilst the substrate concentration was altered from 15.6 μM to 200 μM. Each experiment was performed in triplicate and standard errors are shown (±). The concentrations of active AVP/pVIct-complex used for the determination of k_{cat} values was calculated according to method by Baniecki *et al.* (2001).

Figure 9. Binding of wt peptide to AVP, shown as $[pVIct]_{bound}$ v $[pVIct]_{free}$ (A) and as a Scatchard-plot (insert) (B). The K_d values for the peptides were obtained from Scatchard-plot analysis. The assays were performed using the aforementioned fluorogenic substrate, 26 nM of recombinant AVP and assay conditions as described in Methods.

Table 3. Activation and binding data for pVIct variants

Peptide	K_d *(μM)*	K_m *(μM)*	k_{cat} s^{-1}
GVQSLKRRRCF	1.62±0.16	49.1±16.5	0.0283±0.004
GVQSLARRRCF	2.5±0.4	135±44.4	0.0202±0.0038
GVQSLKARRCF	1.34±0.39	98.55±15.5	0.017±0.0014
GVQSLKRARCF	2.19±0.18	61.6±21	0.0161±0.0024
GVQSLKRRACF	1.01±0.30	60.9±12.7	0.0173±0.0016
GVQSLKRRRCA	7.46±1.64	200±92.9	0.0075±0.0022
GVQSLKRRRC	9.09±2.48	171.1±121	0.0015±0.0005
GVQSLKRRRCY	0.86±0.2	34.55±11.4	0.0117±0.0009
pVIct-F	2.52±0.15	109.8±54.3	0.013±0.0033
EDS	3.00±0.35	79.63±20.1	0.0013±0.0002
CELO	4.19±0.56	169.1±26.2	0.0018±0.0002

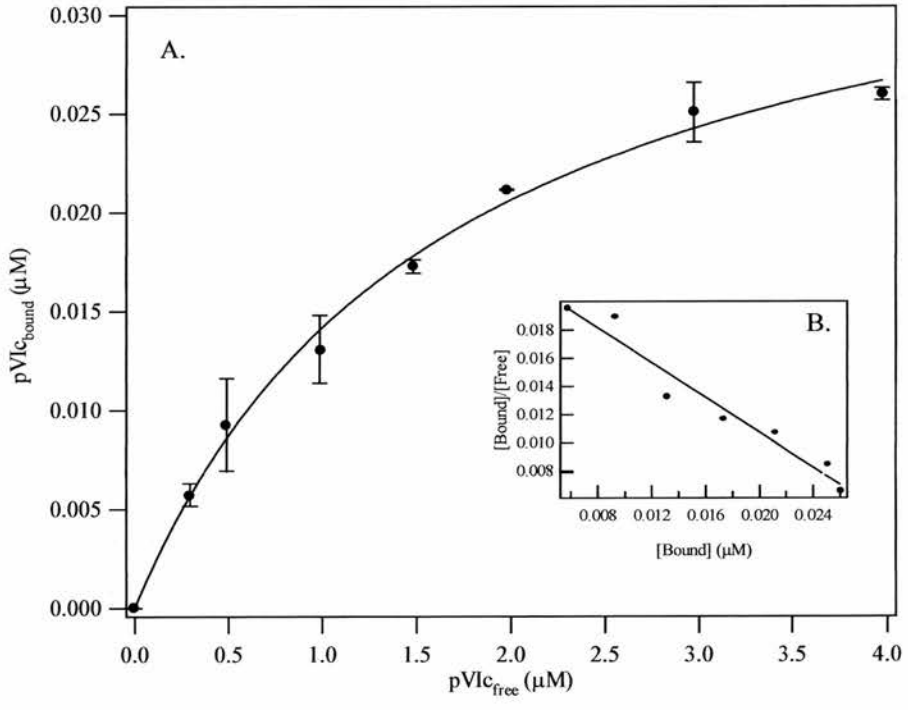

3.5 Discussion

3.5.1 Crucial interactions between pVIct and AVP

Within experimental error the binding affinities, whether determined by native gel electrophoresis or by using the fluorescent substrate, are comparable (Table 2 & 3). The K_d for the wt pVIct is 1.62 μM and 1.28 μM as determined by the fluorescent substrate assay and native gel electrophoresis, respectively. In the case of the mutants GVQSLARRRCF, GVQSLKARRCF, GVQSLKRARCF and GVQSLKRRACF, K_d values vary from 1.01 to 2.5 μM with the fluorescent assays and from 1.45 to 2.82 μM with native gel electrophoresis. Another conserved residue, hydrophobic Phenylalanine'11, however, if mutated resulted in approximately 4.5-fold increase in K_d. Both the native gel electrophoresis and fluorescent substrate assays gave similar fold-increases in K_d values for this mutant when compared to that of the wild-type.

Likewise, the relative specific activities obtained using Ac-LRGAGRSR-substrate and the catalytic rate constants derived from the use of the AMC-fluorogenic substrate, displayed the same trend for the peptide variants. The Alanine-mutants to the KRRR-motif exhibited around 50-70% activity to that of the wt pVIct and the most dramatic decrease in activity was obtained with the C-terminal mutants F'11A and the peptide lacking the 11^{th} residue.

Overall, the experiments demonstrated that the binding to AVP was not dramatically affected by mutating any of the cationic residues along pVIct. Yet, in addition to the important residues of Cysteine'10, Valine'2 and Glycine'1 previously reported from this laboratory (Cabrita *et al.*, 1997), Phenylalanine'11 from the C-terminus of the peptide is another crucial component contributing to the binding between pVIct and AVP and to the stimulation of activity. Mutation to this last residue seemed to be poorly tolerated, as shown by the F'11A mutant, unless substituted with another aromatic residue.

Does the 3-dimensional structure of the protease/peptide-complex reveal potential roles for the individual residues on the C-terminus of pVIct? At least partly, there are interactions and contacts made by the components, which are apparent from the structure modelling and can help interpret the results obtained from the Alanine-scanning mutagenesis.

A closer look at the C-terminus of the pVIct structure complexed with the protease domain provides a potential insight to the importance of the 11th residue (Figure 10A-C). As the final residue along the peptide, the aromatic, hydrophobic Phenylalanine seems to be buried within a pocket formed by the residues Glu'89, Leu'92, Arg'93, Ile'97, Arg'103 and Ile'105 of the protease (some of which are indicated in Figure 10B). Also, Arg'9 of the peptide, which potentially forms a salt-bridge with Glu'89 of the protease, turns towards the Phenylalanine and contributes to the hydrophobic pocket. Thus, if Phe'11 is removed or substituted with a small amino acid such as Alanine, the hydrophobic pocket would subsequently become exposed, resulting in a disruption between the binding of the C-terminus of pVIct and AVP, as observed by an increase in K_d and decrease in k_{cat}.

Surprisingly, the Tyrosine peptide (Tyr'11) was unable to activate or bind Ad2 protease as well as Phe'11 peptide, despite its similarity to Phenylalanine. On the basis of the structure of the pVIct C-terminus, it could be that a Tyrosine with its extra hydroxyl group does not fit in as comfortably as the Phenylalanine in the space available or disturbs the Arg'9-Glu'89 interaction. In addition, it could be that the adenovirus serotypes bearing the Tyrosine have slightly different order of protease residues lining the hydrophobic pocket, and for an optimal fitting, Tyrosine residue is preferred. In fact, sequence alignment of protease residues (not shown here) reveals that Ad40, Ad41 and EDS possess a Lysine residue in the place of an Arginine at position 93 of the protease. Furthermore, Ad40 and Ad41 encode for a Histidine residue instead of an Arginine at the position 103 of the protease. Together these changes in the residues, although small, could allow for a different formation in the protease pocket, which might explain the preference for the Tyrosine at the 11th position in pVIct sequences of the abovementioned serotypes.

Ad12 peptide, with an identical sequence (GVKSLKRRRCY) to Ad40 and Ad41, has been shown to stimulate the cleavage-activity of Ad2 AVP to a similar level as Ad2 pVIct while in the presence of Ad2 DNA and a synthetic protein substrate, as examined by gel electrophoresis (Freimuth & Anderson, 1993). From the sequence alignment (Figure 6) it is apparent that Ad12, 40 and 41 do also carry a Lysine at position 3 of the pVIct sequence compared to Glutamine found in serotypes 2 and 5. While Ad12 is a

Figures 10 (A-C). Interactions between the Ad2 protease and its peptide. The images were generated using molecular visualisation and analysis program, VMD version 1.8.1. The protease molecule in all of the images has been presented in Surf, molecular surface solver-mode. In (A) colouration of the protease was performed according to the Pos-mode of the program, which is based on the distance of each atom to the center of the molecule (i.e blue indicates surface exposure while orange buried, core structure). The peptide is shown in silver with its termini labelled. (B) and (C) show the C-terminal residues studied, in a perspective view of the structure complex. The peptide residues are shown in turquoise and with single amino acid abbreviations whilst the interacting protease residues are shown in white and with three letter amino acid abbreviations.

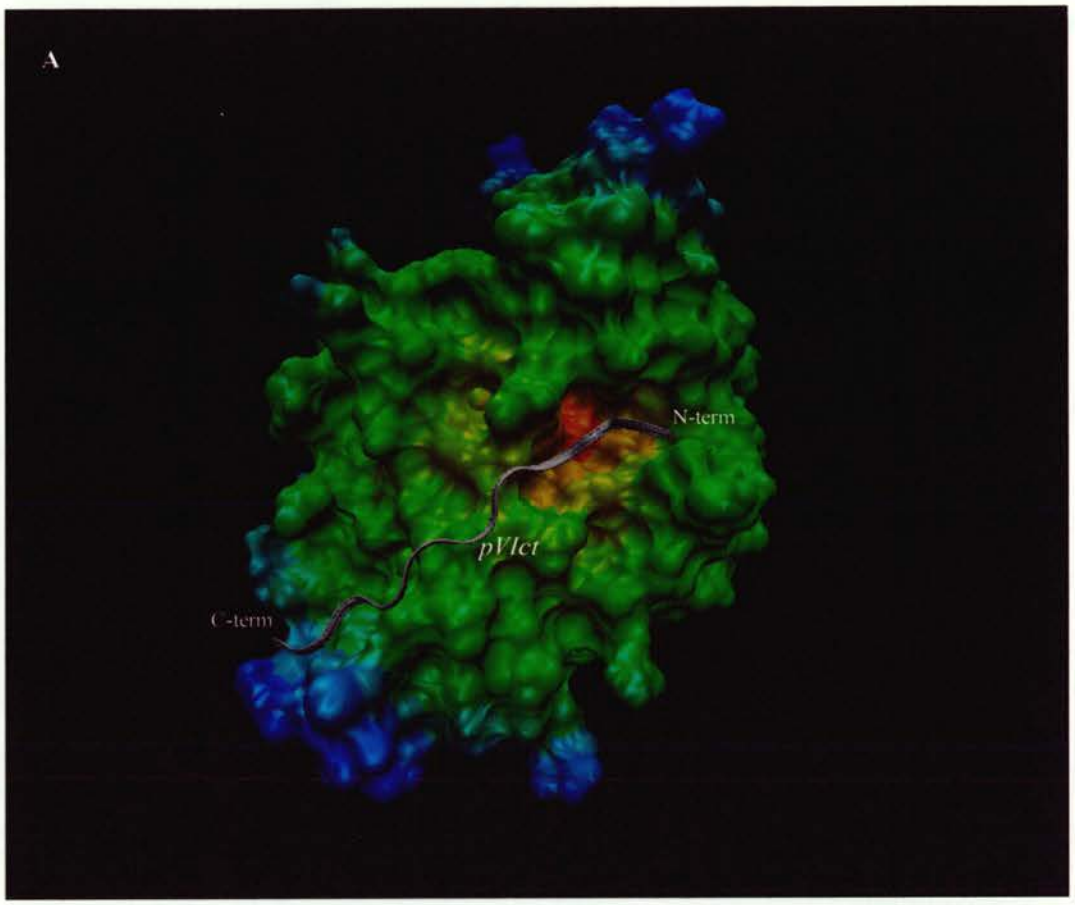
A
N-term
pVIct
C-term

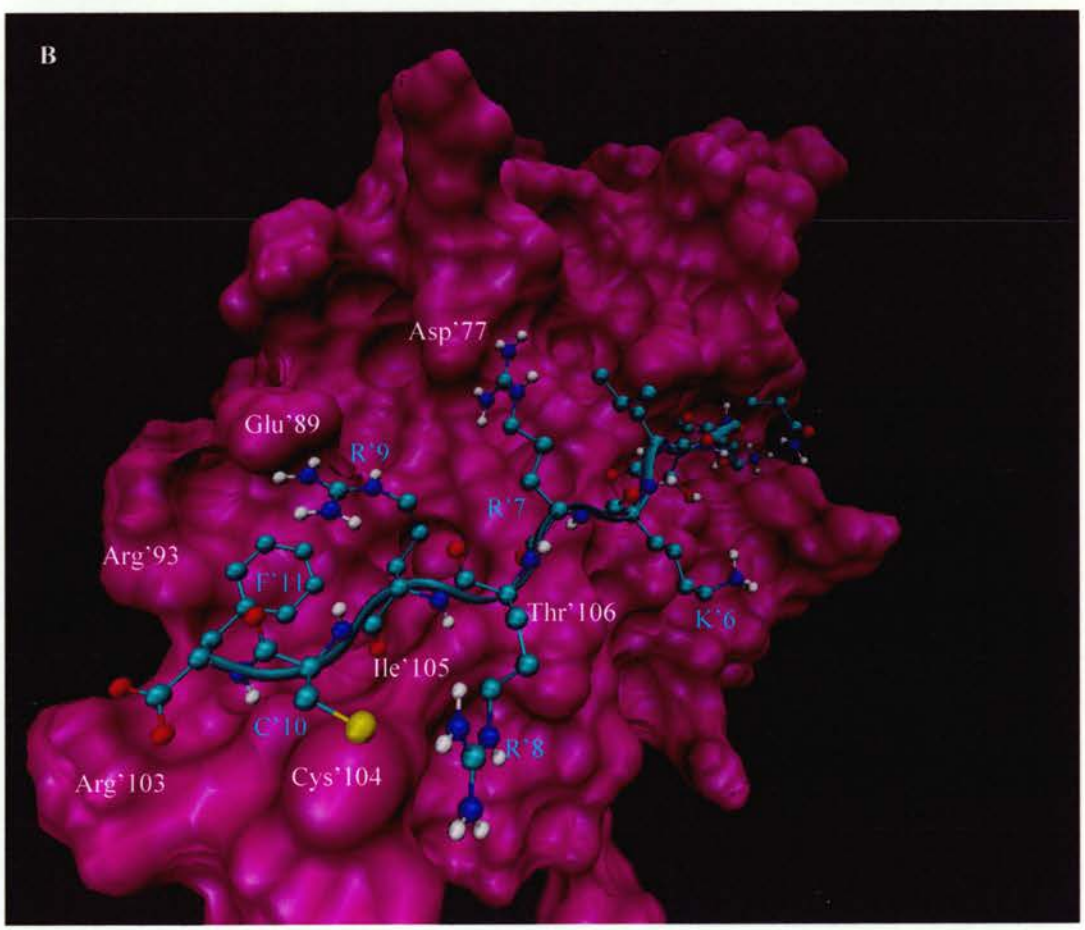
B
Asp'77
Glu'89
R'9
R'7
Arg'93
I'11
Thr'106
K'6
Ile'105
C'10
R'8
Arg'103
Cys'104

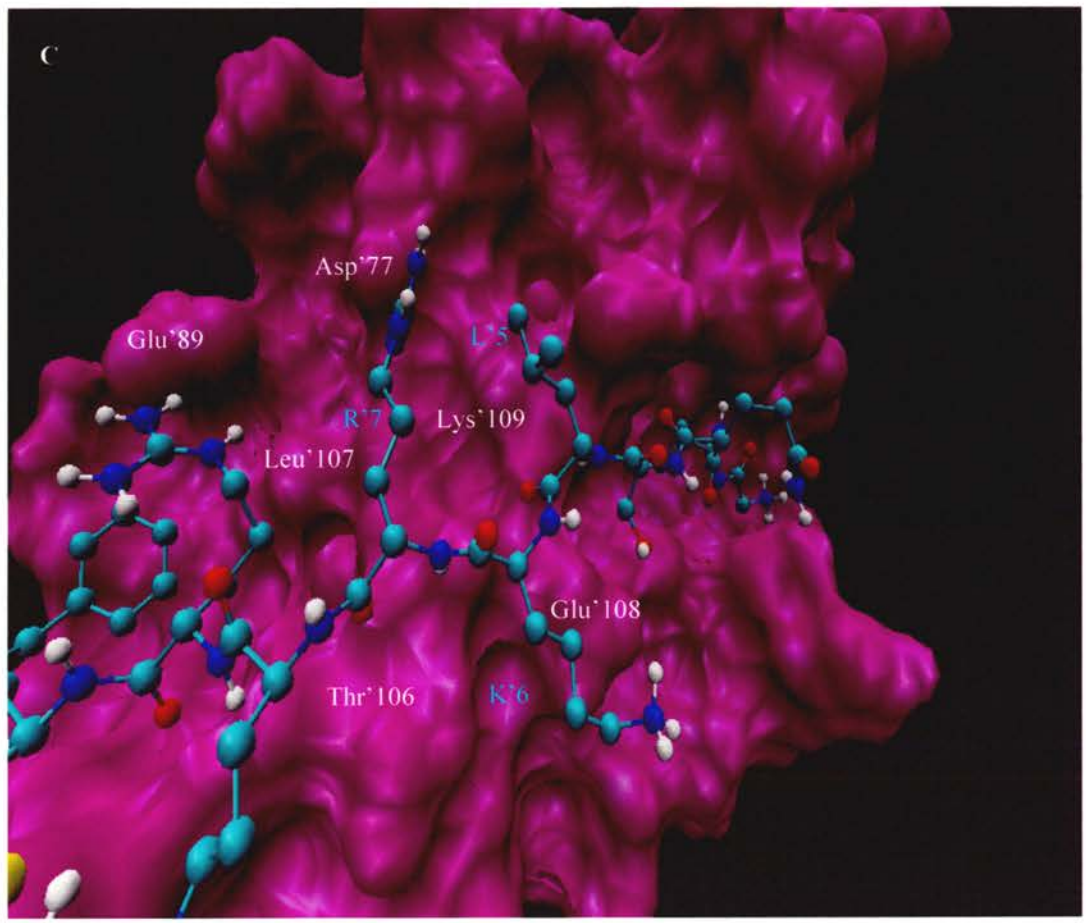
C
Asp'77
Glu'89
L'5
R'7
Lys'109
Leu'107
Glu'108
Thr'106
K'6

serotype bearing a Tyr at position eleven on its peptide, it contains Arg at position 93 and 103 in its protease sequence, similar to Ad2 AVP. However, slight differences can be found at positions 99-101 where, instead of Ser-Ser-Pro-stretch, Ad12 displays Ala-Thr-Lys. These changes could potentially lead to variations in the structure of the hydrophobic pocket. In addition, it should be mentioned that there is no peptide sequence identified amongst the Ad serotypes and their pVI sequences identical to the GVQSLKRRRCY synthesised and used in this study, which could be taken to mean that other small changes in the peptide sequence need to accompany the Tyrosine-preference.

Moving further towards the N-terminus of the peptide, the disulphide bond between Cysteine'104 of the protease and C'10 of the peptide forms on the side of the Phenylalanine and 'underneath' the Arginine'9. Arginine'9 is facing the side of the protease molecule whilst Arginine'8 points away from the β-sheet of the protease, towards the Cys'104 and in the vicinity of Thr'106 of the protease (Figure 10B). The third Arginine ('7) of pVIct again extends to the side of the protease molecule, close to Lys'109 and Asp'77, and potentially forms a salt-bridge with Asp'77.

Lysine'6 of the peptide, in the same way as Arg'8, twists away from the protease having Glu'108 of the protease located underneath. Given that Lys'6 seems to push away from the peptide backbone (Figure 10C), the fluorescein-tag on that specific residue should not critically interfere with the binding of the peptide to the protease. This is supported by the activation and binding ability of pVIct-F.

Overall, the structure of the C-terminus of the peptide shows an alternating trend: every other residue essentially points away from the main structure of the protease molecule. Hence, it would be expected that the residues not facing the side of the protease (i.e. Arg'8) are not as important for optimal binding as those that do (i.e. Arg'9). However, taken as a whole, the small differences in the binding and activation data between the Alanine mutants to these cationic residues imply that the residues can be comfortably mutated to small nonpolar residues (even Arg'9 and Arg'7, which potentially form salt-bridges). Therefore, interactions formed by these residues are not crucial; residues with the same general character (size and charge) should be able to substitute for the KRRR-motif and follow the general line of residues forming the peptide β-sheet.

The sequences from the two distant avian serotypes, EDS and CELO, do in fact display the minimum requirement of conserved residues needed for binding and activation of the Ad2 protease. Both of these peptides contain the essential Glycine'1, Valine'2, Cysteine'10 as well as the aromatic 11th residue Tyrosine in their sequences [GVRYGSQRYCY (EDS) and GVATATRRMCY (CELO)] and were able to stimulate protease activity according to the assays conducted in this thesis. Other than the conservation at the very N-and C-terminus, the avian peptides lacked the 'QSLK'-stretch of residues present in human adenovirus serotypes. Despite the fact that both of the peptides carry one or two Arginines, the cationic motif is not strictly conserved in these peptides.

Similar to the C-terminus of the peptide, the N-terminus seems to comfortably 'occupy' a pocket at the other side of the protease structure, as is evident from Figure 10A. Hence, the collective role of the conserved residues at both termini of pVIct is probably to bind and 'tie' two separate domains of the protease into a more compact structure required for catalysis, as proposed by Cabrita *et al.* (1997).

3.5.2 Comparison of results

Baniecki *et al.* (2001) published their Alanine-scanning mutagenesis studies on the peptide residues and their importance to the stimulation of protease activity. To compare their data, obtained using (Leu-Arg-Gly-Gly-NH)$_2$-Rhodamine substrate (R110) and the data presented here with the z-LRGG-AMC substrate, the specificity constants, i.e. the ratios of k_{cat}/K_m were calculated. Using this ratio, the specificity of different synthetic substrates for the same enzyme can be evaluated.

In the presence of wt pVIct, the k_{cat}/K_m ratio for the substrate used in this study was 5.8 x10^2 (M^{-1} s^{-1}) compared to 5.1 x 10^5 (M^{-1} s^{-1}) in the study of Baniecki *et al.* Evidently their substrate is preferred by the protease as displayed by a better turn-over number. In fact their catalytic rate constant, obtained using the rhodamine-based fluorescent substrate, is approximately 38-fold higher than that found in this study (1.08 s^{-1} and 0.0283 s^{-1}, respectively). This is surprising considering that the substrates possess the same, type[1] consensus cleavage site [(M, I, L) XGG-X] with an identical peptide sequence and differ only in the type fluorophore present (rhodamine or amino methylcoumarin). A thousand-fold difference between the k_{cat}/K_m ratios of the substrates

suggests that the rhodamine-tag itself could have affinity for the protease or that the AMC-tag is somehow a hindrance.

Previously Leytus *et al.* (1983) noted that a rhodamine-based peptide substrate for bovine trypsin, human and dog plasmin and for human trombin was substantially more active than an equivalent 7-amino-4-methylcoumarin-substrate. This has been explained in that the Rhodamine is a better leaving group, which could also confer optimal orientation of the substrate at the active site, seen as improved efficacy in catalysis. The differences between the K_m values obtained in this study with an AMC-substrate (~50 μM for wt pVIct) and those of Baniecki *et al.* with R110-substrate (2 μM for wt pVIct) do imply that the fluorophores affect the binding and orientation of the substrate in the active site of the enzyme.

Another study, in which different AVP synthetic substrates were used, also noted the high efficiency of the R110-substrate (Diouri *et al.*, 1995). The somewhat unexpected turnover number of R110 by AVP has been rationalised on the basis of its energetically favourable electronic rearrangement that follows as the rhodamine amino groups are liberated. The fluorescence of this substrate results from a two-step process: non-fluorescent bisamide is cleaved to a fluorescent monoamide and a further conversion to free rhodamine 110, which results in further gain in fluorescence.

Thus, certain chromophoric or fluorophoric leaving groups on peptides may confer much improved substrate-binding properties. This has been shown to be the case with several other viral proteases and their substrates, such as those of HIV-1 (Matayoshi *et al.*, 1990).

3.5.3 Does viral DNA play a role as an activator of AVP?

There are reports suggesting that DNA functions as a second cofactor for AVP (Mangel *et al.*, 1993). According to this model, the ternary complex of adenoviral DNA, pVIct and AVP, is the fully active complex required during infection to perform proteolysis of precursor proteins.

Baniecki *et al.* reported that adenoviral DNA increases the k_{cat}/K_m ratio of substrate hydrolysis 34,000-fold in the presence of pVIct and AVP compared to that of AVP alone. DNA, according to the above authors, could also suppress the negative effect of an Alanine substitution along pVIct. This was evident from the approximately 17-fold

increase (from 0.41 s^{-1} to 6.79 s^{-1}) on the catalytic rate of GVASLKRRRCF peptide following the addition of 12-mer ssDNA (GACGACTAGGAT). Despite these reports, previous attempts by other groups have been unable to confirm that DNA, a polymer with high negative charge density, is a crucial cofactor in AVP stimulation (Webster *et al.*, 1994, Diouri *et al.*, 1995).

As proposed by McGrath *et al.* (2001a), the differences in the results for the role of DNA could be due to several factors such as the length of pre-incubation of AVP-pVIct complex, as well as the concentrations of DNA, substrate and enzyme used.

To evaluate the role of DNA, I repeated the assays with both the rhodamine-based substrate and the AMC-substrate. With the AMC-substrate and by using the assay buffer [10 mM Tris-HCl (pH 8), 5 mM octyl glucoside] and conditions described by Baniecki *et al.* (2001) I found no increase in activity in the presence of 1 μM ssDNA (with same GACGACTAGGAT sequence as used by the aforementioned authors). Following the proposal by McGrath *et al.* (2001a) that higher concentrations of substrate can be inhibitory and therefore deter the increase in activity mediated by DNA, the activity of AVP/pVIct/DNA at a lower substrate condition (3 μM) was also evaluated. However, with the use the AMC-substrate, the inclusion of DNA had no effect on the *in vitro* activity of the protease-peptide complex (rates not shown here). Contrary to this, with the rhodamine-substrate (and assay conditions described by Baniecki *et al.*, 2001), the inclusion of 12-mer ssDNA resulted in an apparent increase in AVP activity. Due to the limited amount of the rhodamine-substrate available, the experiments could not be performed in sufficient repeats to obtain kinetic constants. The preliminary results indicated approximately 1.9-fold increase in activity following the inclusion of DNA in the presence of wt pVIct.

Another assay specific concern is the addition of NaCl and whether elevated ionic strength does in fact stimulate the *in vitro* activity of AVP. According to the assay system of Baniecki *et al.* (and McGrath *et al.*, 2001a), 20 mM NaCl is included in assays performed in the absence of DNA. Whilst optimising their assay conditions with substrate (Leu-Arg-Gly-Gly)-NH_2, Mangel and coworkers (1996) discovered that half of the AVP activity was lost when 10 mM or 45 mM NaCl was included in the absence and in the presence of DNA, respectively. Therefore, the inclusion of 20 mM NaCl with the rhodamine-substrate could cause an unnecessary increase in the difference between

the respective catalytic rates in the absence and in the presence of DNA. However, these findings differ from those by Webster *et al.* (1994), which showed that with peptide substrate LSGGAFSW, the addition of 1 M NaCl enhanced substrate hydrolysis fivefold whilst the inclusion of DNA had no effect. Therefore, the effect of other assay components as factors causing variation between results cannot be ignored. Equally, the role of the ionic strength in stimulating AVP activity does seem to mainly depend upon the nature of the substrate.

Can overall conclusions be drawn from the different reports for the role of DNA? It seems that a crucial determinant in the *in vitro* AVP-assays is the substrate used, agreeing with the suggestion that DNA stimulation could be specific to the (Leu-Arg-Gly-Gly-NH_2)-rhodamine-substrate (Baniecki *et al.,* 2001). While the importance of DNA in stimulation of AVP activity can be argued on the basis of varying *in vitro* results, there is some *in vivo* data supporting a role for DNA. Mangel and coworkers (1993) showed that Dnase-treatment results in the loss of protease activity in virions, which is restored upon the addition of Ad2 DNA.

On the basis of the alanine-scanning mutagenesis performed in this study, the conservation of the cationic residues along pVIct cannot be reasoned solely by the activation role of the pVIct. McGrath *et al.* (2001a) have previously proposed a biological role for this sequence during the assembly phase of the infection; as the protease molecules enter the empty capsid bound to adenoviral DNA, the AVP-DNA complex comes into contact with pVI, whose C-terminal positive charge enhances the yield of pVIct. Furthermore, with pVIct bound to it, the protease reaches its maximal stimulation and the protease-peptide complex moves along the DNA cleaving viral precursor proteins. Their kinetic data support this theory, seen as the reduction in K_d values and an increase in k_{cat} following the systematic binding of each of the factors (Baniecki *et al.*, 2001). The charge-potential map of AVP-pVIct complex revealed five clusters of positive charge on the protease molecule, which the authors presented as putative binding sites for the negatively charged adenoviral DNA phosphate groups (Ding *et al.*, 1996). Also, the previous report of pVI possessing DNA binding ability (Russell and Precious, 1982) could support this theory by offering a way in which pVI could come into contact with AVP/DNA-complex prior to the cleavage of other adenoviral precursor proteins. However, what should also be considered is that the DNA

affinity of pVI may simply be a requirement for proper packaging during virion assembly: pVI is a hexon-associated cement protein and thought to be closely linked with viral DNA in the virion.

In order to obtain more specific binding data concerning affinity between the pVI protein and DNA, and to assess the activation ability of the whole pVI protein on AVP, expression of the full-length pVI protein in a pGEX-2T vector (Amersham Biosciences) in *E. coli* BL21 cells was attempted in this study (see Appendix for oligonucleotide sequences). However, no expression of the full-length pVI, as a C-terminal fusion to Glutathione S-transferase, was obtained. Previously, Matthews and Russell (1994) have conducted extensive studies into pVI and hexon interactions and while attempting to express and purify pVI/iVI/VI proteins as Histidine-fusions, noted that residues 38-48 of pVI contained a toxic region deterring the expression of the full-length pVI in bacteria. Therefore for future attempts, only N-terminal deletion mutants of the pVI protein are likely to be expressed in bacterial cells to sufficient levels for purification.

Alternatively, gel retardation and ethidium bromide exclusion assays or Isothermal Titration Calorimetry (ITC) assays could be conducted to assess whether the KRRR-stretch on pVIct has specific affinity to DNA. Attempts were made in this study to use a MicroCalorimeter (VP-ITC) to record more specific information concerning the binding energetics of protease-peptide interaction (method 2.5.1). Although these attempts were unsuccessful, this was most likely due to the overall low protease and peptide concentrations used and not because the interactions occurring between the peptide and protease are beyond the limits of calorimetric determination. Therefore, with further optimisation, peptide-DNA binding interactions should be attainable with ITC, as was recently demonstrated with peptideV (derived from adenovirus protein V) and plasmid DNA (Preuss *et al.*, 2003).

The discussion for an alternative or additional role for the KRRR-motif continues in section 4.

4. Results: Nuclear localisation studies on Adenovirus protease and pVI protein

4.1 Objectives of the study

The activity studies presented in this thesis support the idea that the KRRR sequence on the C-terminus of the activating peptide has an additional role during adenoviral infection. The individual residues of KRRR do not, if mutated, abolish AVP binding and activation ability.

On the basis of the nature of the motif, this sequence could function as a nuclear localisation signal (NLS). Previous results from this laboratory (Pollard, 2001) showed that the KRRR motif was able to confer nuclear accumulation of pyruvate kinase, an otherwise cytoplasmic protein. These experiments were conducted by fusing the peptide encoding sequence to the C-terminus of the pyruvate kinase gene and by observing the localisation of the fusion protein in transfected cells.

Furthermore, since the protease itself carries no apparent NLS on its sequence, and yet it requires to nuclear localise for the assembly events, one hypothesis is that it associates with the peptide for nuclear transport. The aim here was to further examine what function(s) this sequence could exhibit within the adenovirus replication cycle.

4.2 Studies with fluorescein-labelled peptide

4.2.1 Localisation of pVIct-F

A fluorescein-labelled peptide, pVIct-F, was synthesised in order to follow the localisation of the activating peptide in mammalian cells during transfections with the adenovirus protease, AVP. The GVQSLKRRRCF peptide was synthesised by standard Fmoc chemistry (Atherton & Sheppard, 1989), except for the labelling of the ϵ-group of lysine with 5-(and-6)-carboxyfluorescein succinimidyl ester (Molecular probes) (see method 2.2.2). The peptide was purified and quantified in the same manner as the other peptides used in this study (method 2.2.1). Labelling of the lysine residue and the structure of the fluorescent-tag is illustrated in the reaction scheme of Figure 12.

For fluorescence microscopy, 2-5 x 10^5 HeLa cells were cultured overnight on a glass coverslip in 30-mm plates. The cell monolayer was incubated with 10 μM of pVIct-F (in Optimem) for 15-60 min at 37°C, after which the medium was replaced with fresh Optimem and the incubation was continued at 37°C (method 2.6.3). The cells were fixed with 4% paraformaldehyde in PBS, as outlined in method 2.6.4, and the distribution of the fluorescein-tagged peptide was analysed on a *DeltaVision* microscope system (Applied Precision) using a 60x or 100x oil immersion objective. The images were acquired as 0.2-0.5 μm optical sections through the cells, which were subsequently deconvolved and compressed to one 'layer' (Quick Projection) to show the overall fluorescence pattern in cells, using *softWoRx*-software (Applied Precision). This applies to all fluorescence images shown in this thesis.

As apparent from Figure 11, one hour after the initial addition to the culture medium a punctate cytoplasmic and a dotted or diffuse nuclear distribution of the peptide was detected.

The translocation ability of cationic cell penetrating peptides, or CPPs, to the nucleus by direct transport through the lipid bilayer, and not by endocytosis, has been proposed in the literature (Derossi *et al.*, 1996, Vives *et al.*, 1997). However, a recent review of the mechanism of cell penetrating peptides (CPPs) introduced the problem of cell fixation used in fluorescence microscopy, which was found to lead to artifactual redistribution of CPPs in cells. Richard *et al.* (2003) noted that in unfixed cells the cationic peptide $Tat^{48\text{-}60}$ (GRKKRRQRRRPPQ from HIV-1 Tat protein) had an endosomal distribution compared to the nuclear localisation in fixed cells. According to

Figure 11 (A & B). Localisation of the fluorescein-labelled peptide, pVIct-F. DAPI-staining was used to visualise the nucleus and the cells were fixed 1 h after the addition of the peptide to the culture medium. The images shown [(A) closer view, (B) several cells] were acquired using a *DeltaVision* microscope and 100x and 60x oil immersion, respectively.

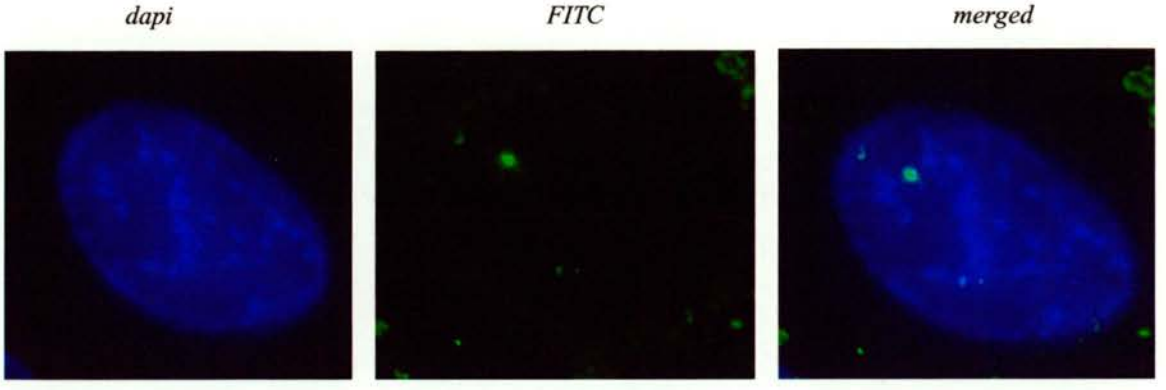

A.

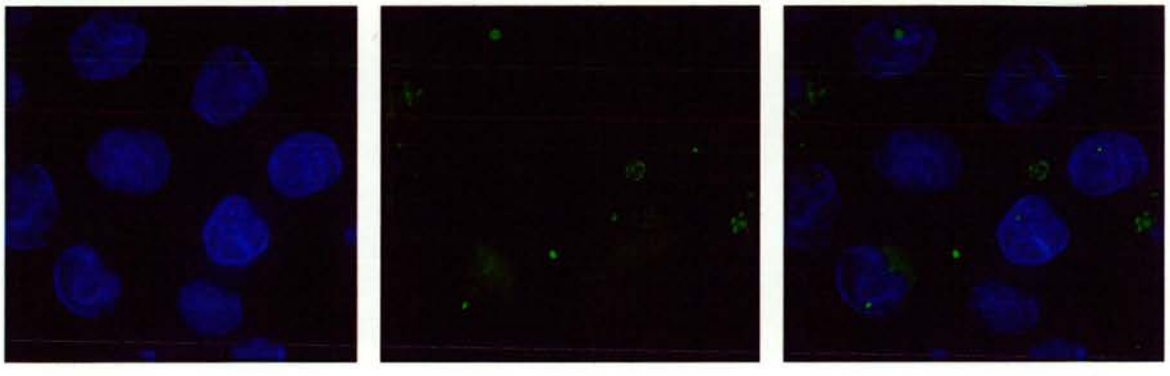

B.

the aforementioned authors, the artifact of nuclear localisation of CPPs could be related to their highly cationic nature. The charge on the peptides would cause them to bind to the negatively charged plasma membrane and following cell fixation CPPs, probably bound to nucleic acids, would accumulate in the nucleus.

In this study, the distribution of the fluorescein peptide was also followed in living, unfixed HeLa cells in glass-bottom WillCo-dishes® using a *DeltaVision* inverted microscope-system containing a built-in environmental chamber (Solent Scientific) with controlled temperature of 32.5°C and CO_2 enrichment. As evident from Figure 12 (B-C), the hourly images acquired display mainly a diffuse nuclear localisation for the peptide. In the fixed-experiment, pVIct-F caused a more punctated cytoplasmic distribution, characteristic of endocytic markers (Richard *et al.*, 2003), while nuclear accumulation was noted to a lesser extent and as a few singular dots. The ability of the peptide to concentrate in nuclei is obvious with the live-experiment. Therefore, it seems that cell fixation performed for fluorescence microscopy had, in the case of pVIct-F, a negative and not artifactual effect on the peptide nuclear accumulation.

4.2.2 Binding and activation of AVP by pVIct-F

On the basis of previous reports from this laboratory (Pollard, 2001), the main purpose for synthesising the pVIct-F peptide was to assess the hypothesis that the activating peptide could be responsible for the translocation of the protease to the nucleus. Confirmation that the fluorescein-tag on the lysine residue did not greatly interfere with the binding and activation of AVP by the peptide was therefore essential. As discussed in the previous results section (3), the activation and binding studies between the peptide variants and AVP were conducted using native gel electrophoresis, peptide-substrate assay and fluorescent substrate assay. I found that the attachment of the label to the lysine residue did not cause a severe detrimental effect on the binding and activation ability of the peptide (pages 63, 66 & 70).

4.2.3 Is pVIct-F able to traffic AVP to nucleus?

In order to examine whether pVIct-F could bind and transport protease molecules to the nucleus with it, the gene for the protease was inserted into a mammalian red fluorescent expression vector, pDsRed2-C1 (Clontech). The expression of the protease as a

Figure 12. Localisation of pVIct-F, fluorescein-tagged peptide in live, unfixed cells alone (B-C) and together with AVP/HcRed (D-F). (A) Structure and labelling of the lysine residue of pVIct with carboxy-fluorescein succinimidyl ester (created with ChemDraw 6.0). (B) and (C) show cells at 1 h and 2 h post-initial addition of 10 μM peptide into the culture medium, with PBS washes performed before the imaging, as briefed in Methods. The peptide was added to the (AVP/HcRed1-C1)-transfected cells at 24 hpt for 30 min. (D) shows peptide and protease distribution at 25 hpt [(E) & (F) show peptide and protease distribution alone, respectively]. Fluorescent images were acquired using a *DeltaVision* microscope system and a 60x oil immersion objective. The images shown were deconvolved and processed using *softWoRx*-software (Applied Precision) (scale bars 15 μm, as shown). Live, time-lapse experiments were performed within an environmental chamber (Solent Scientific) with controlled temperature and atmosphere.

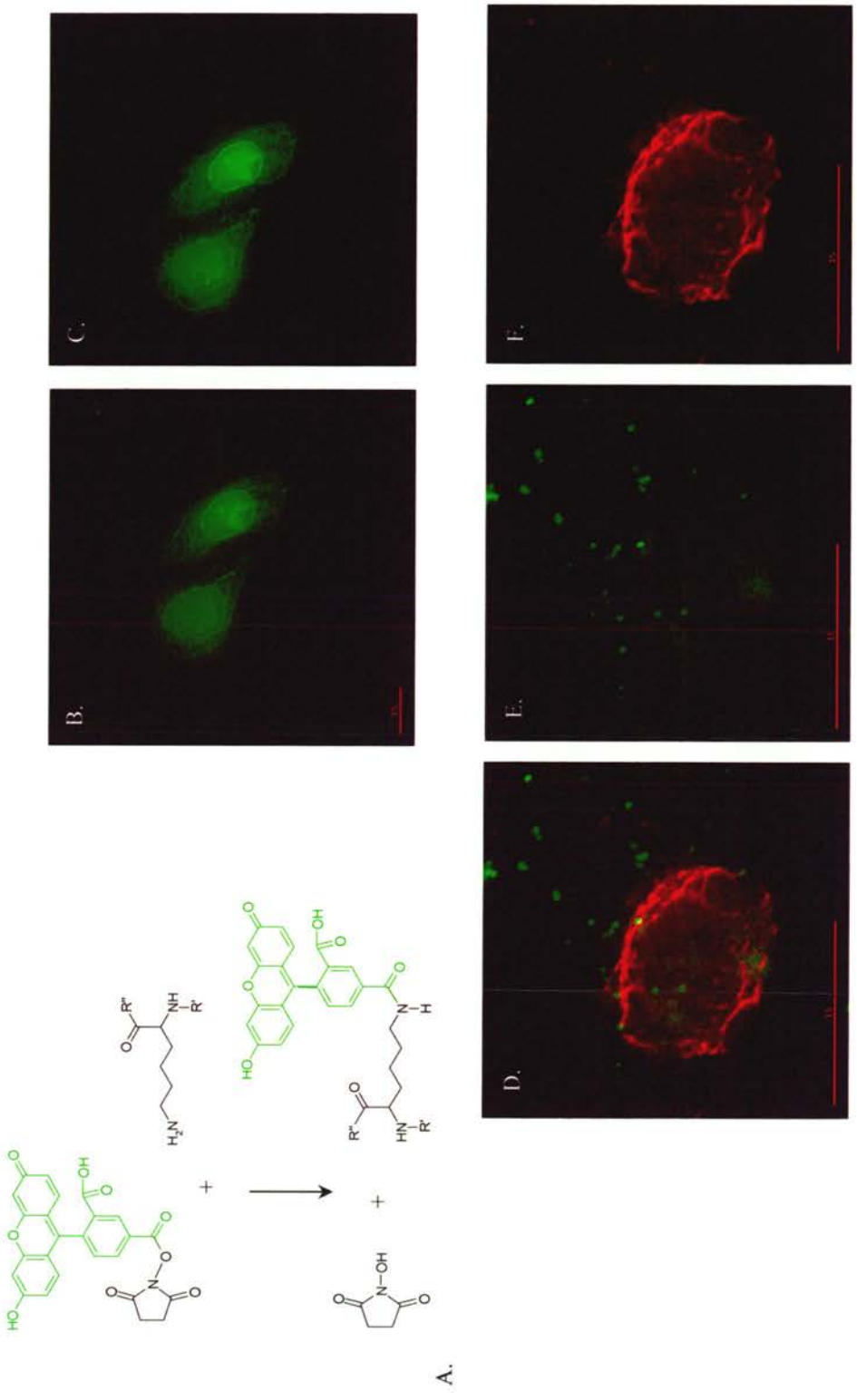
A.
B.
C.
D.
E.
F.

C-terminal fusion to the fluorescent protein could be easily detected *in vivo* and, moreover, in the presence of the peptide. In addition, two AVP mutants, C122G and C104A, were also assayed. They have previously been characterised as an active site mutant, C122G (specific activity <0.5% of that by wt) and a mutant unable to form a disulphide bond with the activating peptide, C104A (specific activity 3% of that by wt) (Grierson *et al.*, 1994, Jones *et al.*, 1996). The mutants C104A, C122G and wt AVP have been previously cloned into pET11c vector in this laboratory, sub-cloned into pEGFP-C1 by T. Vaughan, and in this study further sub-cloned into pDsRed2-C1 and pHcREd-C1 (Clontech) vectors by restriction digestion at the *Eco*RI/*Bam*HI-sites, found in multiple cloning site (MCS). After successful ligation, the fusion constructs were sequenced at the University of St. Andrews DNA Sequencing Unit.

Transient transfections of HeLa cells with the DsRed2-fluorescent constructs were performed by electroporation or by using the calcium phosphate technique, according to methods 2.6.2.2 and 2.6.2.1, respectively. Alongside, transfections with the DsRed2-fluorescent constructs were performed, to which pVIct-F was added at 24 hpt (hours post-transfection). The cells were fixed for fluorescence microscopy with 4% paraformaldehyde (method 2.6.4) and mounted with mowiol-solution containing 4',6-Diamidino-2-phenylindole (DAPI), which reacts with nucleic acids, hence highlighting the cell nuclei. The cells were checked for fluorescence with a Nikon Microphot-FXA microscope. The double fluorescent images were acquired with a *DeltaVision* microscope.

The wild-type protease and the cysteine mutants C122G and C104A, as fusions proteins with the fluorescent DsRed2, localised as thread-like structures and globules within the cytoplasm (Figure 13A). This is consistent with previous labelling experiments showing a cytokeratin-network distribution for the protease during transient transfection (Pollard, 2001, Brown *et al.*, 2002). In those cells, to which the peptide was added, the intracellular protease distribution seemed to be unaffected (Figure 13A). Co-localisation or interaction between the two components would have been visible as yellow colour (DsRed + FITC).

Subsequent to the fixed-transfection experiments, time-lapse experiments were performed to confirm that no co-localisation or interaction between the peptide and protease occurred, by acquiring hourly images of unfixed HeLa cells till 28 hpt. The

peptide was added at 20-24 hpt to the culture medium (Optimem) for 30 min, after which the medium was replaced. Figure 12 D-F show HcRed/AVP at 25 hpt, at which point peptide had been in the cells for 1 h. However, no co-localisation of the components was observed. Some peptide was visible in the nucleus (albeit to a lesser extent than in live-experiments with pVIct-F alone), whilst the AVP localised in its characteristic thread-like manner in the cytoplasm.

Confirmation of the localisation of the protease and mutants following the inclusion of the peptide was performed by subcellular fractionation of transiently transfected cells. The cells were fractionated into nuclear and cytoplasmic extracts using a lysis buffer procedure (method 2.6.8). The samples were further subject to SDS-PAGE and Western blotting and the expression of protease was detected using an antiserum raised against the N-terminal 17 residues of the Ad2 protease (Webster & Kemp, 1993). As illustrated in Figure 13 (B), the transfected protease, or mutants thereof, appeared in the cytoplasmic fractions before and after the addition of the peptide. Similarly to the cytoplasmic distribution visualised by fluorescence microscopy, the fractionation experiments did not indicate a change in the subcellular localisation of AVP by pVIct-F.

Despite the fact that the *in vitro* assays for pVIct-F indicated activation and binding ability, there was a need to ascertain that the fluorescein-label did not interfere with protease/peptide interactions *in vivo*. To address this, 10 μM of unlabelled wt pVIct was added to the culture medium of the cells transfected with AVP/DsRed2 at 24 h ptr. The results from the unlabelled peptide experiments were identical to those where pVIct-F was used in that the abundance of the protease and mutants within the cytokeratin network was prominent and there was no indication of protease nuclear accumulation following the inclusion of the peptide (images not shown here).

In conclusion, the fluorescein-labelled peptide seemed to be able to gain entry into cells and also, to a lesser extent, localise within the nucleus. However, there were some concerns about the validity of the observed peptide localisation due to the somewhat inconsistent distribution in non-transfected and AVP/HcRed-transfected cells (Figure 12). The transfection with the protease could have affected the uptake of pVIct-F by the cell, owing to the toxic nature of the protease. Furthermore, the inability to retrieve the peptide from the cells after its addition (the peptide could be degraded by cellular proteases or otherwise aggregated or modified within the cell into a form unable to bind

Figure 13 (A) & (B). Localisation of protease and mutants in the presence of pVIct-F and pVI. The AVP and mutants, and pVI were expressed as a C-terminal fusion with fluorescent proteins DsRed2 or EGFP, respectively, and used in transfections of mammalian cells. The peptide was added to the cells for 30-60 min at 24 hpt (hours post-transfection) and incubation of the cells was continued till 30 hpt. The cells were fixed for fluorescence microscopy at 25 hpt (images shown here) and every hour thereafter. The images were acquired using a *DeltaVision* microscope. For Western blotting of nuclear (N) and cytoplasmic (C) fractions of transfected cells (B), the expression of the protease and mutants was confirmed using the Ad2 protease antiserum (Webster & Kemp, 1993). A previously purified protease sample (p-AVP) was included as a size marker. The controls (C) and (N) refer to non-transfected cytoplasmic and nuclear fractions, respectively and DsRed refers to cells transfected with an empty pDsRed2-C1 vector.

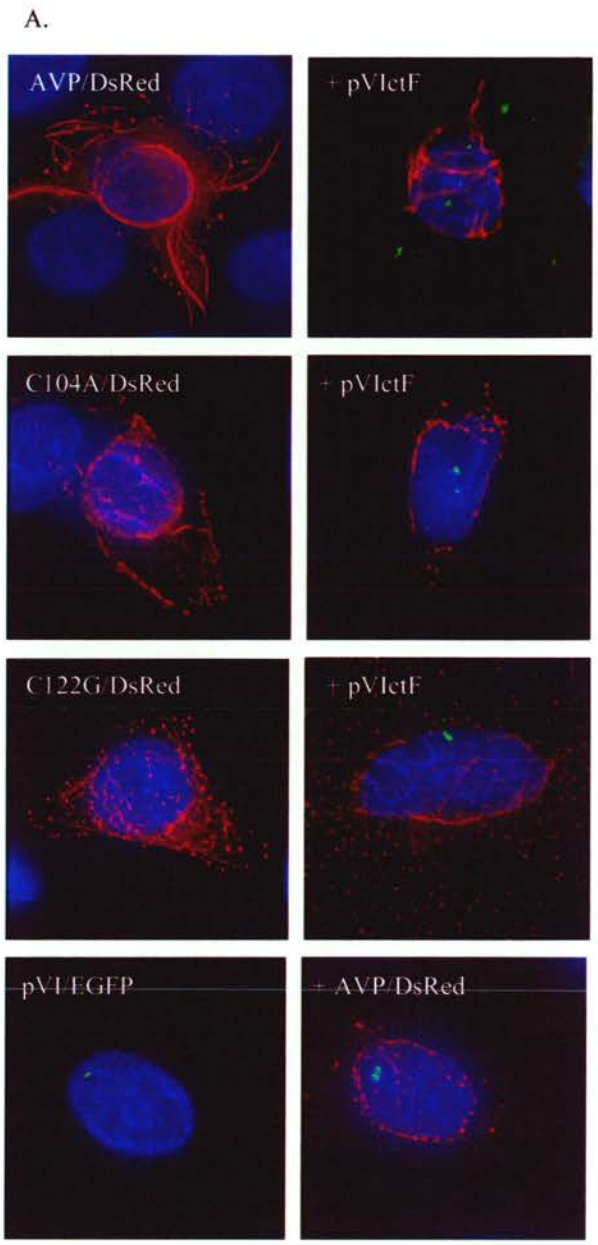
A.
AVP/DsRed
+ pVIctF
C104A/DsRed
+ pVIctF
C122G/DsRed
+ pVIctF
pVI-EGFP
+ AVP/DsRed

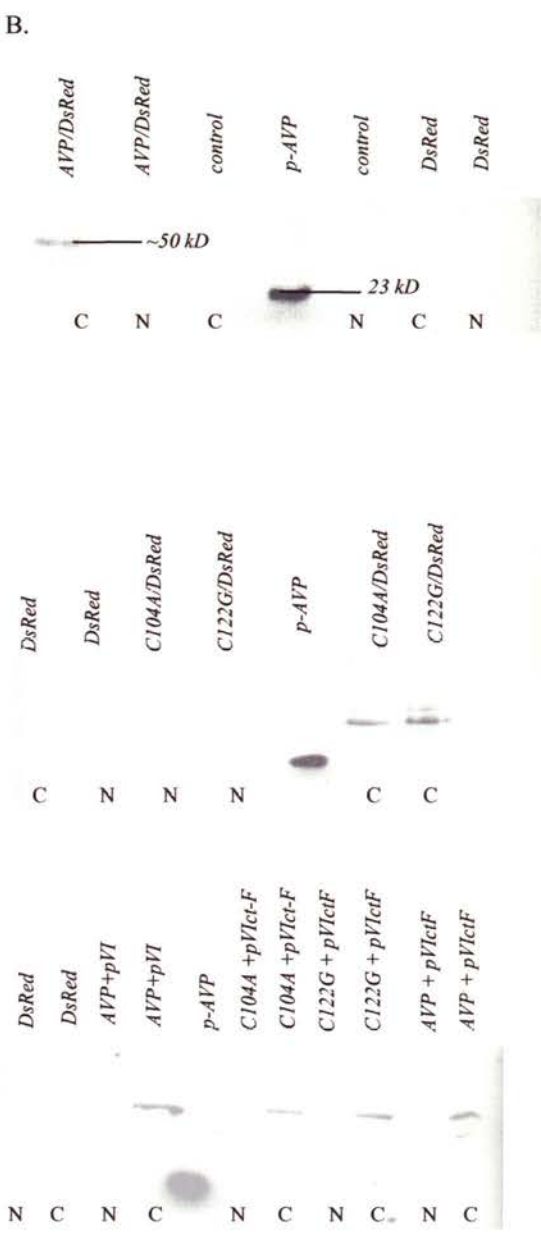
B.
AVP/DsRed
AVP/DsRed
control
p-AVP
control
DsRed
DsRed
~50 kD
23 kD
C N C N C N
DsRed
DsRed
C104A/DsRed
C122G/DsRed
p-AVP
C104A/DsRed
C122G/DsRed
C N N N C C
DsRed
DsRed
AVP+pVI
AVP+pVI
p-AVP
C104A +pVIct-F
C104A +pVIct-F
C122G + pVIctF
C122G + pVIctF
AVP + pVIctF
AVP + pVIctF
N C N C N C N C N C

AVP) prompted the development of an alternative assay for the *in vivo* detection of AVP/pVIct-interaction.

4.2.4 Protein-protein interaction required for nuclear localisation?

Some nuclear proteins, such as the adenoviral pre-terminal protein (pTP) in a complex with DNA polymerase (Zhao & Padmanabhan, 1988), have been reported to be capable of 'piggy-backing' other proteins to the nucleus. The fact that the peptide is cleaved off from the C-terminus of the pVI presented a hypothesis whereby the full-length pVI protein, rather than merely its C-terminus, could be required for AVP nuclear accumulation. To test this, the sequence encoding for pVI was amplified by PCR from pVI/pUHD10-3 plasmid (Pollard, 2001) with the oligonucleotides R1-N-P6 and R1-C-P6 (see Appendix), and cloned into pEGFP-C1 and pDsRed2-C1 fluorescent vectors (Clontech). Co-transfections with AVP/DsRed and pVI/EGFP constructs were subsequently performed according to the calcium phosphate transfection method (2.6.2.1).

Figure 13A shows the distribution of pVI/EGFP in transient transfection; pVI localised in the nucleus mainly as singular dots. In co-transfection experiments, the AVP/DsRed and pVI/EGFP localised independently of each other, AVP being cytokeratin-associated whilst pVI nuclear. In addition to the fluorescence microscopy, Western blotting of co-transfected nuclear and cytoplasmic fractions (where antiserum raised against the protease was used) failed to indicate that pVI protein could target AVP to the nucleus (Figure 13B). pVI/EGFP behaved in a similar manner as pVIct-F in that it was capable of nuclear translocation but incapable of altering the cytokeratin distribution of the protease.

4.3 Double-fluorescent constructs incorporated with sections from pVI protein

Following experiments with the fluorescein-labelled peptide, the aim was to obtain a fluorescent construct, within which the peptide sequence could be incorporated. Since the C-terminus of pVI is cleaved by the protease resulting in the release of the activating peptide, this section of the protein could be used for the construction of a cleavable fluorescent, *in vivo*-substrate. With this type of fluorescent construct, both co-transfections with AVP and infections with Ad2 could be performed in order to observe possible co-localisation of the peptide sequence with the protease. Furthermore, these assays would be more likely to mimic the real-life events present during Ad2 infection.

Various constructs were generated containing different length sequences from the C-terminus of pVI, which were introduced between enhanced yellow and cyan fluorescent proteins (EYFP and ECFP, respectively) or between EYFP and puromycin-resistance encoding gene, enabling efficient selection of transfected cells (puromycin N-acetyl transferase or pac). Pdf20, a pcDNA3.1 based-plasmid, which contains the human cytomegalovirus (CMV) immediate-early promoter allowing expression in mammalian cells, was used as the template for the constructs (a kind gift from P. de Felipe). Figure 14 shows the cloning procedure performed and the outcome and order of the gene inserts in the constructs 20.1-20.6. Rather than introducing the mere 11-residue peptide next to the EYFP and between EYFP/ECFP proteins, different length sequences from 34 amino acids (aa) and 79 aa to the full-length pVI (250 aa) were synthesised. This was performed in order to obtain an optimal, fluorescent *in vivo*-substrate for AVP; one whose KRRR-motif would not be buried, nor cleavage site inaccessible for the protease. This was a reasonable concern due to the large size (27 kD) of the cyan and yellow fluorescent proteins on both sides of the insert. To bring in further flexibility for the cleavage-site inserts, glycine residues were introduced to both N- and C-terminus of the pVI-inserts (see Appendix for the oligonucleotide sequences).

Given that the constructs 20.5 and 20.6 encode the gene for the full-length pVI, they carry on their sequence both protease cleavage sites (between residues 33-34 and 238-239). The pdf68 vector (constructed by P. de Felipe for picornavirus 2A-mediated experiments) was also assessed in this study: it contains the 79 aa sequence from the C-terminus of pVI and therefore a single protease cleavage site. The order of genes in pdf68 is shown in Figure 16.

Figure 14. Pdf-fluorescent constructs with pVI-inserts. The pdf20 vector (kindly donated by P. de Felipe) was modified, as outlined in the Figure, to contain different length sequences from the C-terminus of pVI (34 & 79 aa) to the full-length pVI (250 aa) insert. The pVI C-terminal sequences were amplified by PCR and using oligonucleotides, the sequences of which can be found in the Appendix. Arrows, unless otherwise stated, refer to specific restriction digestions.

CMVp = cytomegalovirus promoter
EYFP= yellow fluorescent protein
ECFP = cyan fluorescent protein
2A= self-cleaving picornavirus 2A protein
pac= Puro^{R}, puromycin-N-acetyl-transferase
pA= polyA tail
*C pVI = pVI C-terminal sequence, with AVP cleavage site
f-l pVI = full-length pVI sequence, includes 2 AVP cleavage sites

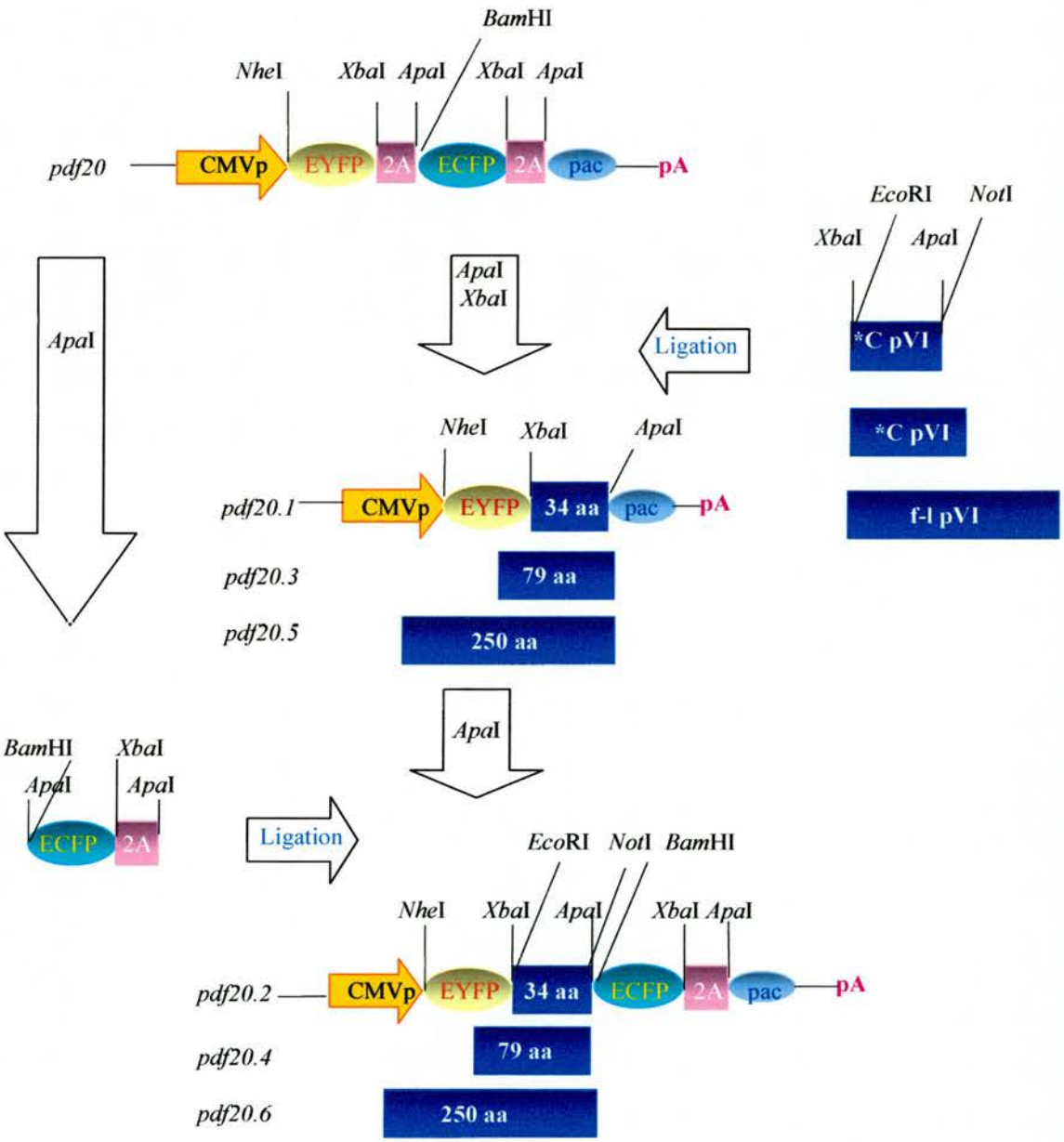

It should be emphasised that there were no potential nuclear localisation signals present on the pdf20-construct. The picornavirus 2A protein, an 18 amino-acid-long oligopeptide, which cleaves itself C-terminally and co-translationally, accumulates non-specifically in the cytoplasm and nucleus as a fusion with EYFP or ECFP (de Felipe & Ryan, 2004). Furthermore, ECFP and EYFP, derived by amino acid substitutions from the enhanced green fluorescent protein (EGFP), have been characterised as cytosolic proteins (Clontech Living Colours user manual, November 2001). Therefore, the pdf-constructs made here were also utilised to estimate the strength of the KRRR-signal.

4.3.1 Localisation of fluorescent pdf-constructs

The behaviour and competence of the pdf-constructs was measured by three different means: (1) by their ability to translocate during transfections, (2) by *in vitro* transcription-translation followed by cleavage assay with recombinant AVP and (3) by *in vivo* cleavage during co-transfections with AVP and during infections with Ad2.

First, the constructed EYFP and EYFP-ECFP plasmids were used to transiently transfect $HeLa^{CD}$ (Catherine Dargemont, Institutés Paris) and COS-7 cells with FuGENE (Roche), according to method 2.6.2.3. Both cell lines were used in order to confirm that the localisation of the fluorescent polyproteins was consistent. The localisation of the constructs was observed with a *DeltaVision* microscope (Applied Precision) using a 100x oil immersion objective. The yellow and cyan fluorescence were acquired with correct filters (EYFP λ_{ex}=500/20 & λ_{em}=535/30, ECFP λ_{ex}=436/10 & λ_{em}=470/30), however, for clarity of representation, yellow fluorescence is shown here in red while cyan is shown in green.

The successful nuclear accumulation was evident with all EYFP and EYFP-ECFP constructs with the exception of 20.2 (Figure 15). The construct 20.2, with 34 amino acids from the C-terminus of pVI, was found in both cytoplasm and nucleus. The likely explanation for this, considering the construct 20.1 was nuclear, is that the signal sequence is buried in between the two fluorescent proteins. While the pac-protein fused to the C-terminus does not seem to hinder the recognition of the KRRR-NLS (construct 20.1), the ECFP, presumably due to its size or structure, does (construct 20.2). Hence, this observation can be explained by the reports that the karyophilic domain needs to be

Figure 15. Localisation of pdf-constructs during transient transfection. HeLa cells were transfected with pdf-constructs, containing either 39 aa or 79 aa from the C-terminus of pVI or the full-length pVI (250 aa) either in between EYFP and pac-protein (20.1, 20.3, 20.5) or in between EYFP and ECFP fluorescent proteins (20.3, 20.4, 20.6). The pdf68 was constructed by P. de Felipe and contains 79 aa from the C-terminus of pVI in between ECFP and pac-protein. Transfections were performed using FuGENE-reagent according to manufacturer's instructions (Roche). The cells were fixed for imaging at 24 hpt with paraformaldehyde and as detailed in Methods. The images were acquired using a *DeltaVision* microscope.

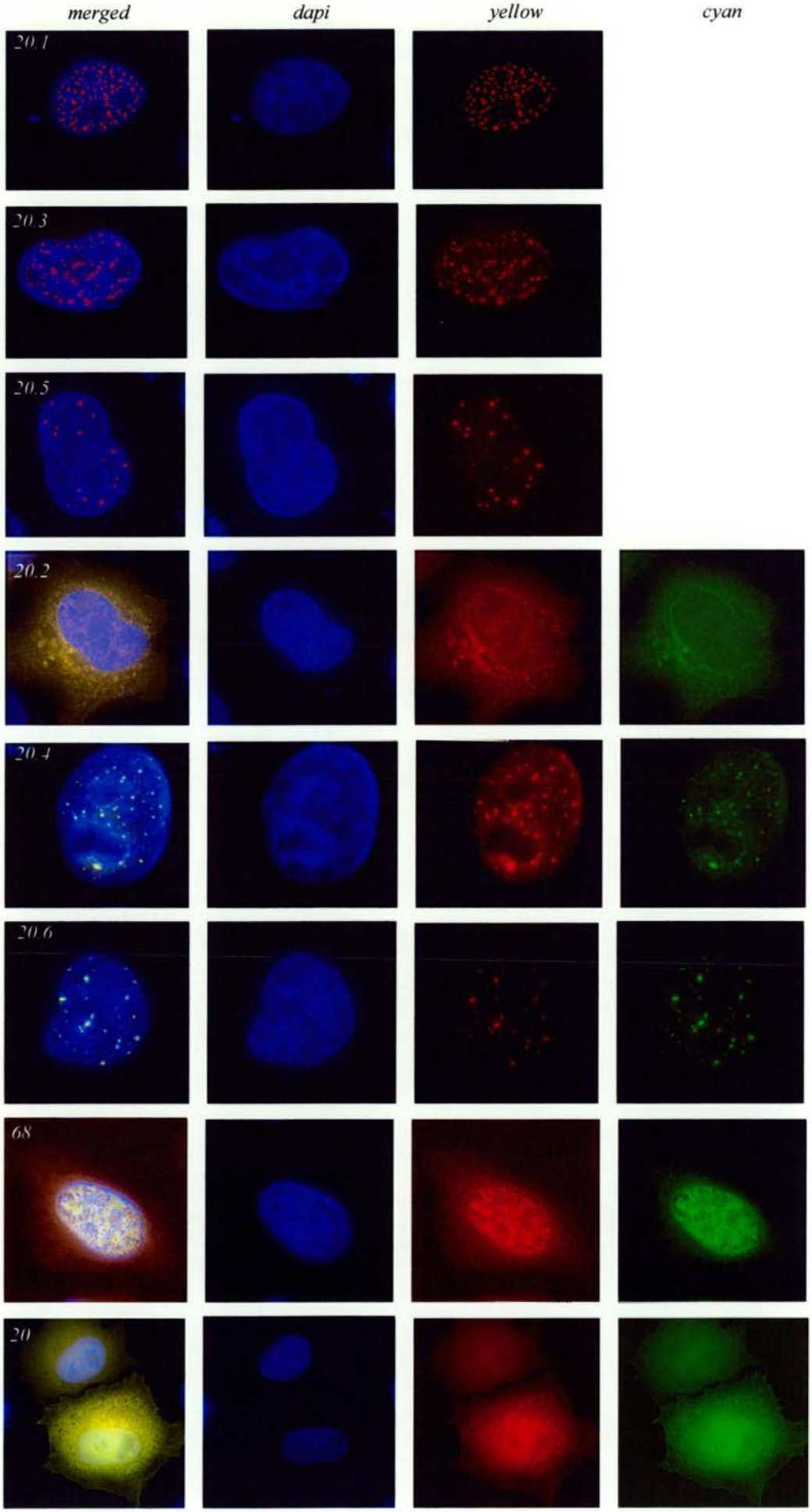
merged
dapi
yellow
cyan
20.1
20.3
20.5
20.2
20.4
20.6
68
20

exposed on the surface of the protein to function as an efficient NLS (Roberts *et al.*, 1987).

4.3.2 In vitro transcription/translation and cleavage of pdf-subtrates

Assessment of the cleavage efficiency of substrates 20.1-68 by recombinant AVP was made possible by the use of cell-free *in vitro* transcription and translation (TNT®) system (Promega). The plasmid DNA templates (constructs pdf 20-68 in this case) with a T7 promotor were expressed using rabbit reticulocyte lysate-mix and the production of the protein was followed by the addition and incorporation of a radioactive amino acid [^{35}S] methionine. Following the TNT-expression, the constructs were cleaved for various times by purified, activated AVP and separated on a 12.5% SDS-gel, according to method 2.9.2. The radioactive gel was exposed to a Phosphor-imager screen and the resulting bands were analysed by Image Reader software. The Profile/MW-mode was selected and the background was automatically subtracted from the intensity of the bands (method 2.9.3).

Figure 16A shows the representative translation profiles of the polyproteins and the products, which can be identified following cleavage by AVP. Construct pdf20 and its translated protein profile served as a reference for the other constructs. Since picornaviral 2A protein was present in some of the constructs, and the co-translational cleavage by 2A (of itself) was subject to variability throughout individual TNT-experiments, two values for the uncleaved template were used for the calculation of the initial maturation rates, if needed. For instance, in the case of construct 20.4, the cleavage by AVP would result in the [YFP][pVIC* -fragment. However, this cleavage product could be obtained from the uncleaved [YFP][pVI C*][CFP][2A][pac]-template and from the [YFP][pVI C*][CFP][2A]-template, mediated after co-translational 2A-cleavage.

The percentages of cleaved and uncleaved proteins were calculated in the following manner: $^{(1)}$ intensity of protein band/methionine-content of the protein band = actual intensity of the protein band, $^{(2)}$ actual intensity of a cleaved fragment/actual intensity of uncleaved template x 100 = % cleaved fragment. Since the constructs 20.5 and 20.6 contained two AVP cleavage sites (compared to one in all the others), only cleavage occurring at the C-terminal site was examined. This was performed in order to maintain

the analysis of the different substrates consistent, and also since the main interest of the experiments was to assess the release of peptide for potential nuclear accumulation of the protease. The cleaved protein bands *CFP][2A][pac] and *pac] in 20.6 and 20.5, respectively, could be identified by a comparison to the translation profile of other substrates. In Figure 16D, the protein bands used for calculations as the uncleaved template* and cleavage product*, have been labelled.

The cleavage-experiments with the fluorescent-substrates by AVP were performed in duplicate and therefore, the data presented here should be weighted accordingly. These maturation experiments were conducted in the hope of discovering an ideal substrate, which would consequently be preferred for the *in vivo*-cleavage experiments, and not to obtain exact values. The initial maturation rates shown in Figure 16C, are the mean values plotted.

The initial maturation rates from the *in vitro* experiments for 20.3, 20.4, 20.5, 20.6 and 68 were comparable, 5.5-7% per min, and all notably better than the maturation efficiency for 20.1 and 20.2 (under 1% cleavage per min). Taking under consideration the size (27 kD) of the two fluorescent proteins, namely ECFP and EYFP, it appeared, as no surprise that the size of the 'substrate-cleavage' insert was a determining factor in maturation. Here the substrates 20.1 and 20.2, containing the shortest pVI C-terminal sequence, exhibited the poorest cleavage efficiency.

On the whole, the results from the *in vitro* cleavages tied in together with those from the localisation experiments; the least efficient substrate 20.2 is also unable to accumulate solely in the nucleus, a problem not associated with the larger constructs. Thus, the KRRR-motif must be inaccessible together with the preceding cleavage site in the construct 20.2, whereas exposed in the construct 20.1.

4.3.3 Co-transfections of pdf-substrates with Avp/HcRed

To re-test the hypothesis that pVIct transports the protease to the nucleus, *in vivo*-maturation of the pdf-constructs by AVP was attempted. In order to visualise several fluorescent colours simultaneously, the pHcRed1-C1 (Clontech) vector was used. This is a far-red vector with distinct spectral properties beneficial for multicolour-labelling experiments, such as those in this study where cyan and yellow fluorescence was already employed. Due to the similarity in the multiple cloning sites in the fluorescent

Figure 16 (A.-D). *In vitro* cleavages of pdf-constructs. The pdf–constructs were expressed using TNT-system (Promega) in the presence of [S^{35}] methionine as outlined in the Methods. The expressed proteins and protein-complexed were cleaved by the activated protease (5 μl AVP at 0.1 mg ml^{-1} and 0.2 μg pVIct in a 20 μl reaction) at 37°C for various timepoints, separated by SDS-PAGE and following exposure to Phosphor-imager screen, analysis was carried out as briefed in Methods.

(A) TNT-profiles of pdf-constructs showing cleavage products in the presence AVP/pVIct (timepoints 10 and 20 min are shown). The uncleaved profiles of the constructs are shown on the right, together with molecular weight markers.

(B) Maturation over a time period for pdf 20.1-68. The pdf-constructs were incubated for 10, 20, 60 and 180 min in the presence of AVP/pVIct, and analysed as explained above. The experiments were performed in duplicate, (B) showing one such an experiment for the constructs.

(C) Initial maturation rates indicating the differences in cleavage efficiencies for pdf-constructs. Values calculated following the analysis of the samples incubated for 10 min with AVP/pVIct. Mean values are shown from the experiments performed in duplicate.

(D) Schematic diagram of the uncleaved template and the cleavage products used for the calculations of the values presented in (B) and (C).

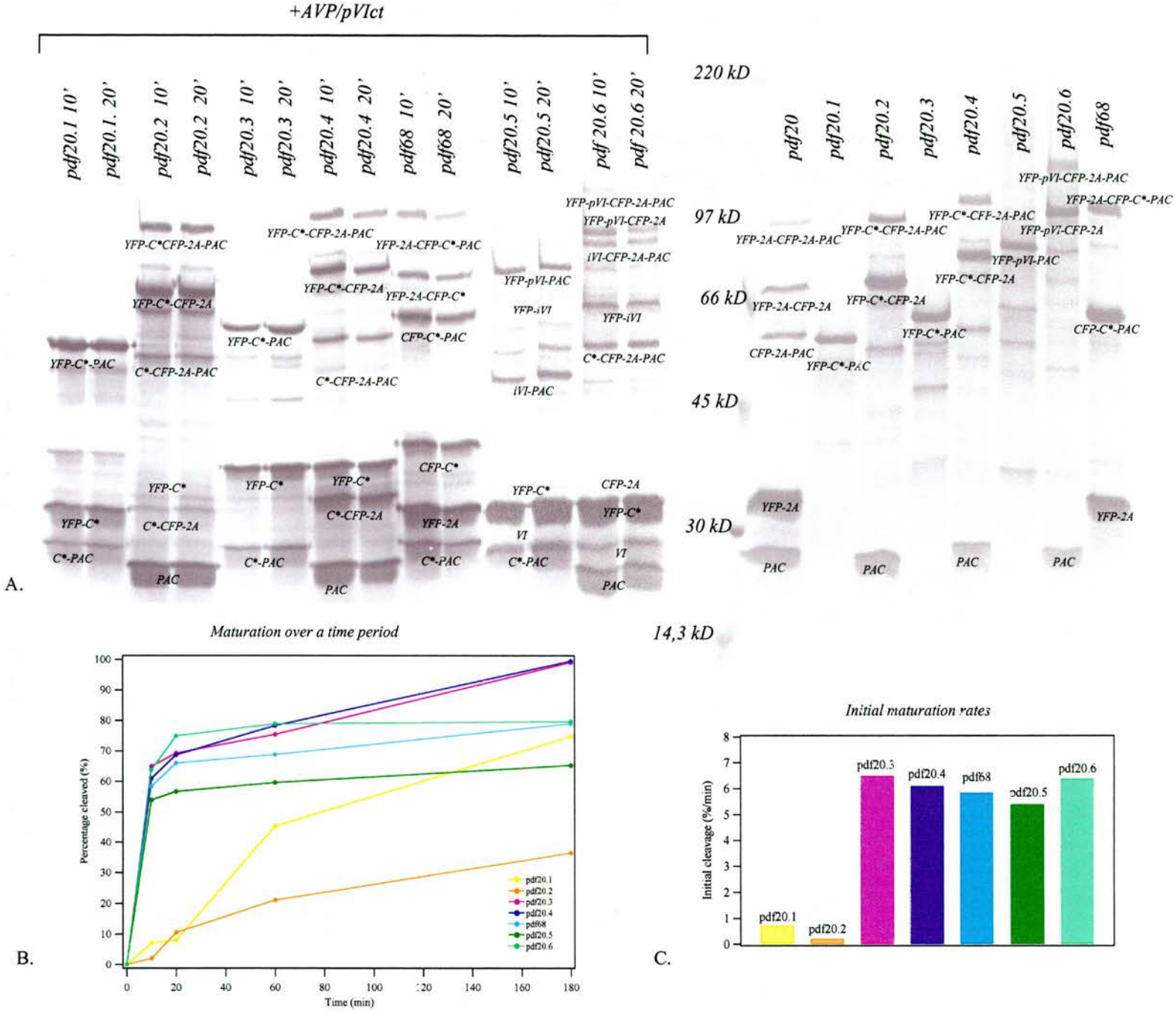
+AVP/pVIct
pdf20.1 10'
pdf20.1. 20'
pdf20.2 10'
pdf20.2 20'
pdf20.3 10'
pdf20.3 20'
pdf20.4 10'
pdf20.4 20'
pdf68 10'
pdf68 20'
pdf20.5 10'
pdf20.5 20'
pdf 20.6 10'
pdf 20.6 20'
YFP-C*-PAC
YFP-C*CFP-2A-PAC
YFP-C*-CFP-2A
C*-CFP-2A-PAC
YFP-C*-PAC
YFP-C*-CFP-2A-PAC
C*-CFP-2A-PAC
YFP-2A-CFP-C*-PAC
CFP-C*-PAC
YFP-pVI-PAC
YFP-iVI
iVI-PAC
YFP-pVI-CFP-2A-PAC
YFP-pVI-CFP-2A
iVI-CFP-2A-PAC
YFP-iVI
C*-CFP-2A-PAC
YFP-C*
C*-PAC
PAC
CFP-C*
YFP-2A
VI
CFP-2A
YFP-C*
VI
220 kD
97 kD
66 kD
45 kD
30 kD
14,3 kD
pdf20
pdf20.1
pdf20.2
pdf20.3
pdf20.4
pdf20.5
pdf20.6
pdf68
YFP-2A-CFP-2A-PAC
YFP-C*-CFP-2A-PAC
YFP-C*-CFP-2A-PAC
YFP-pVI-CFP-2A-PAC
YFP-2A-CFP-C*-PAC
YFP-pVI-CFP-2A
YFP-pVI-PAC
YFP-C*-CFP-2A
YFP-pVI-CFP-2A
YFP-2A-CFP-2A
YFP-C*-CFP-2A
YFP-C*-PAC
CFP-C*-PAC
CFP-2A-PAC
YFP-C*-PAC
YFP-2A
YFP-2A
PAC
PAC
PAC
PAC
A.
Maturation over a time period
Percentage cleaved (%)
Time (min)
pdf20.1
pdf20.2
pdf20.3
pdf20.4
pdf68
pdf20.5
pdf20.6
B.
Initial maturation rates
Initial cleavage (%/min)
pdf20.1
pdf20.2
pdf20.3
pdf20.4
pdf68
pdf20.5
pdf20.6
C.

D.

* *uncleaved template* **cleavage product used for calculations*

cleavage products refers to both 2A mediated co-translational cleavage and in vitro-AVP cleavage

vectors (Clontech), the gene encoding for AVP was simply sub-cloned into pHcRed1-C1 vector by restriction digestions with *Bam*HI and *Eco*RI from pDsRed2-C1 vector (see earlier section 4.2.3).

For fluorescence microscopy, approximately 1 x 10^5 cells seeded onto glass coverslips were transfected with 1 μg of each plasmid DNA (AVP/HcRed and pdf-plasmid) using FuGENE 6 transfection reagent. The expression of proteins was allowed to proceed up to 30 h, after which the cells were fixed for microscopy and the localisation of the fluorescent proteins was analysed with a *DeltaVision* microscope system, as described earlier.

The co-transfections did not, however, indicate cleavage by AVP/HcRed. The substrates were found in the nucleus while the protease was cytoplasmic, localising as observed with earlier transfections. The lack of cleavage during co-transfections could be due to the fluorescent substrates, bearing the nuclear signal(s), capable of rather quick localisation following their synthesis on the ribosomes. The protease and substrates may therefore not have had a chance to interact.

Co-transfections of 20.2 with AVP/HcRed were performed exactly for this reason; to allow for interaction between the substrate and enzyme. Although construct 20.2 was earlier noted to be a poorer substrate, it accumulated in both the cytoplasm and nucleus, and could therefore be available for AVP in the cytoplasm. Despite these efforts, no cleavage of substrate 20.2 was observed when co-transfecting with AVP/HcRed. The localisation of the substrate-constructs, although unaffected following co-transfections with the protease, is shown in Figure 17.

Another possibility for the lack of observable cleavage could have been impairment in AVP activity. The attachment of the fluorescent protein to the N-terminus of AVP could have disturbed its proteolytic ability. In addition, it cannot be confirmed that the structure of the protein following the pVI C-terminal insert (whether ECFP or pac, depending upon the construct) does not hinder *in vivo* the binding to AVP/HcRed. Compared to the *in vitro*-cleavage experiments, the protease used therein was untagged and purified, and therefore expectedly more active.

Figure 17. Co-transfections with pdf-constructs and AVP/HcRed. HeLa cells were transfected using FuGENE-reagent and fixed for microscopy with paraformaldehyde at 24 hpt as described in Methods. Images acquired using a *DeltaVision* microscope and 60x oil immersion objective. The multiple fluorescent images were processed with *softWoRx*-software (Applied Precision).

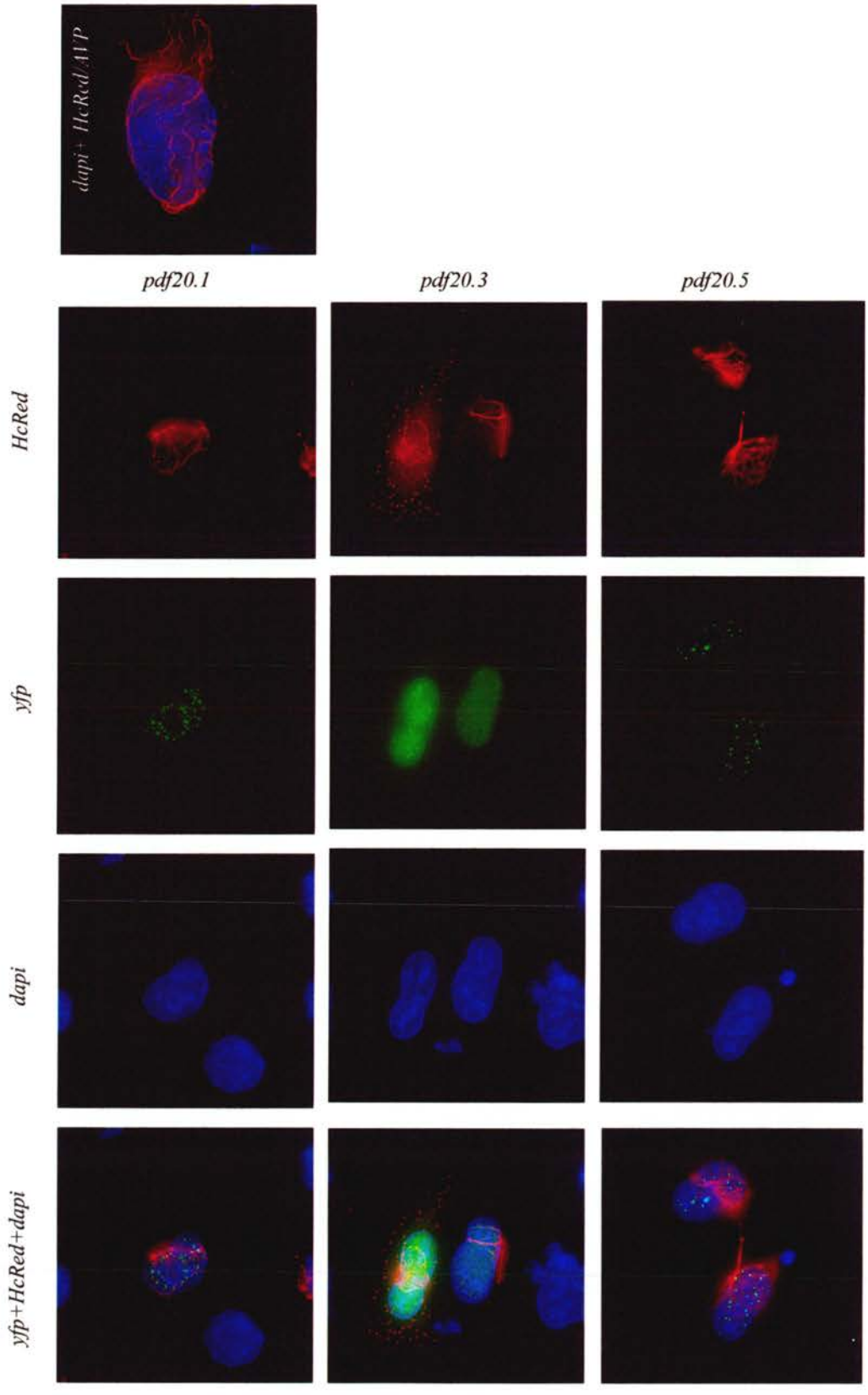
dapi+ HcRed/AVP
pdf20.1
pdf20.3
pdf20.5
HcRed
yfp
dapi
yfp+HcRed+dapi

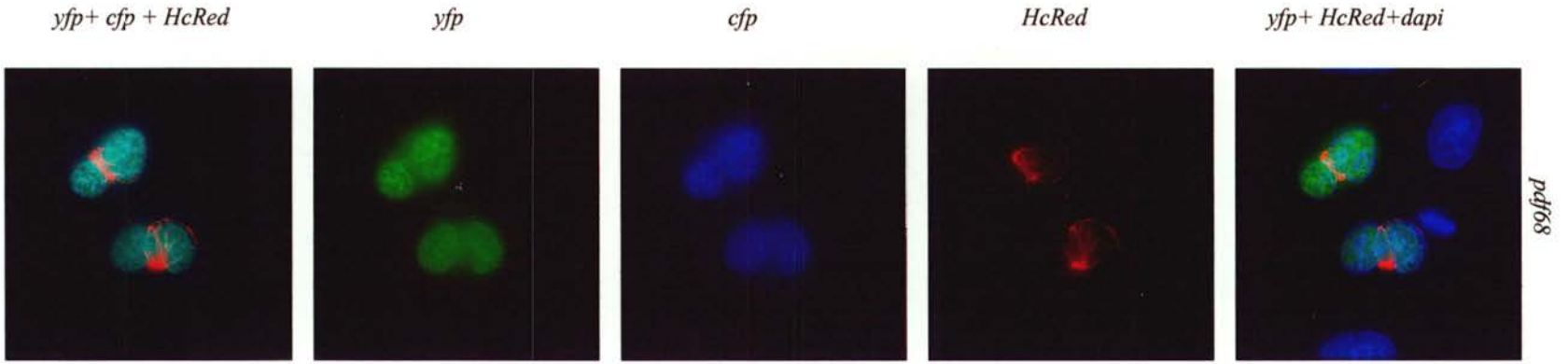

pdf68

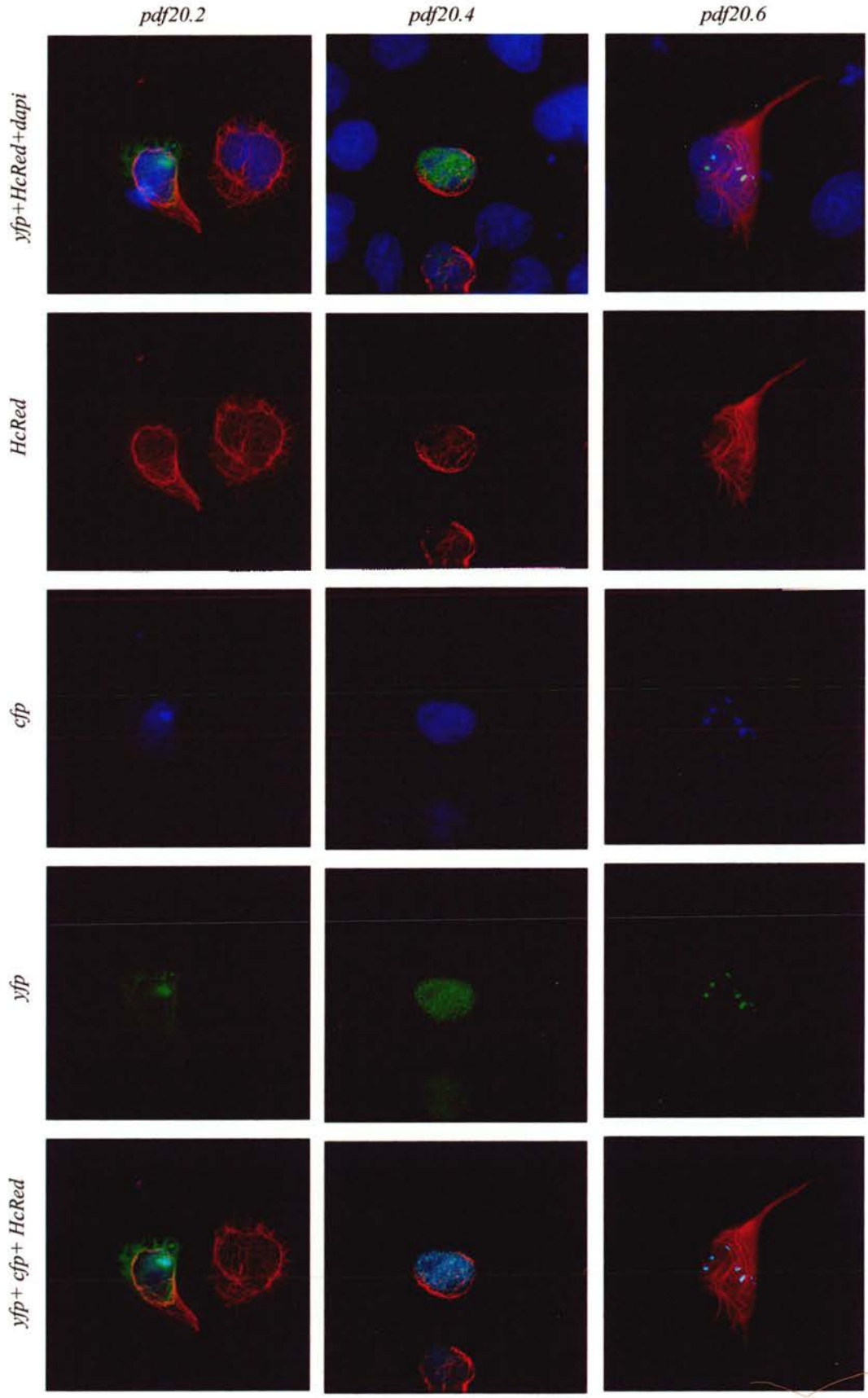
pdf20.2
pdf20.4
pdf20.6
yfp+HcRed+dapi
HcRed
cfp
yfp
yfp+ cfp+ HcRed

4.3.4 Cleavage of the pdf-constructs in stably expressing HeLa cells by Ad2

On the basis of the efficiency of maturation in TNT-cleavage experiments, 20.3, 20.4, 20.5 and 20.6 constructs were used to obtain stably expressing HeLa cells for the infection experiments. Cells stably expressing the fluorescent constructs were selected with puromycin (method 2.6.10). The fluorescence pattern seen in stably expressing cells was analogous that seen in transient transfections, although occasionally more 'diffuse', non-dotted nuclear distribution was observed. However, diffuse nuclear staining also occurred with extended transient transfections (≥30-48 h) (de Felipe & Ryan, 2004), and therefore this phenomenon is likely to be due to the expression of the fluorescent proteins simply increasing to such an extent that the 'singular', dotted distribution disappears.

The preparation and purification of Ad2 by CsCl gradient centrifugation was performed as described previously by Russell and Blair (1977). Viral infections of stable (or transfected) HeLa cells were performed at a multiplicity of 5 to 10 plaque-forming units (pfu) per cell, as described in method 2.7.3.

At 30-32 h post-infection (hpi), nuclear substrates 20.3 and 20.4 showed signs of maturation by the protease. In some cells, stably expressing the substrate pdf 20.3, the yellow fluorescence was visible in the cytoplasm following the infection with Ad2, as expected. The only NLS on 20.3 would, after cleavage, be separated from the EYFP, leading to the relocation of EYFP. The localisation of pVIct however, which was now only attached to pac-protein, could not be followed.

In cells stably expressing substrate 20.4 (Figure 18), the consequence of protease activity was evident at 32 h into an Ad2 infection with the appearance of two distinct, yellow and cyan, fluorescence areas in the nucleus (shown as red and green in the image, respectively). While the intact fusion-protein could be visualised as yellow fluorescence in the image (EYFP + ECFP), the separated [EYFP][C* and pVIct][ECFP][2A] could be seen as red and green dots (indicated with arrows). However, as the cleavage at the C-terminus of pVI between residues 238-239 (at the IVGL|G site, see Figure 5C) results in the KRRR-motif separation to the pVIct][ECFP][2A, with time the [EYFP][C* should relocate into the cytoplasm having lost the only NLS. pVIct][ECFP][2A] should retain itself in the nucleus.

Following the observation that the protease was proteolytically active in the nucleus at 30-32 hpi, *in vivo* cleavage of construct 20.2 was attempted in the hope of examining the timepoint, at which the protease is active in the cytoplasm. Unfortunately, no cleavage of pdf 20.2 was noted. Also, because of the two cleavage sites present on constructs pdf 20.5 and 20.6 analysing where the cleavage has occurred, according to a change in fluorescence pattern, would be impossible with these two larger constructs.

An additional drawback associated with the Ad2 infections of the stable cells was the inability to follow the localisation of the protease. Attempts were made to label the protease with an antiserum [OA10, raised against AVP (Vaughan, 1997)], during Ad2 infections, however, without success.

The localisation of pVI/iVI/VI during Ad2 infection was also assessed by the use of an antiserum raised against residues 94-170 of protein VI (a gift from W.C. Russell) and a secondary, anti-rabbit fluorescein isothiocyanate (FITC)-conjugated antibody. The localisation of the protein during infection (at 22 hpi) confirmed that the dotted pVI nuclear distribution, seen in cells transfected with pdf-constructs and pVI/EGFP, was not an artefact associated with the transfections or fluorescent proteins used (Figure 18).

The infection-experiments with pdf-constructs demonstrated the ability use synthetic substrates to assess protease activity during adenoviral infection. They also indicated that at 30-32 h post-initial infection protease mediated cleavage is detectable in the nucleus. Unfortunately though, by using infectious Ad2 virions, the other proteins and factors present during normal infection were not excluded. Hence, if the protease could access the pdf-substrates found in the nucleus, and was able to cleave them, at least some of the protease molecules were obviously nuclear localising independently of the peptide KRRR-motif present on the substrate. Therefore, these experiments could not provide an answer as to how the protease accesses the nucleus.

Figure 18. *In vivo* cleavage of pdf20.4 during Ad2 infection (A -C) and the localisation of pVI/iVI/VI in Ad2 infected HeLa cells (D). The distribution of the construct 20.4 and its cleavage products at 32 h post-initial infection in fixed cells, shown here with (A) and without (B) DAPI-staining. The image (C) shows a magnification of a section, (boxed in B) indicating the appearance of separate red (EYFP) and green (ECFP) fluorescence dots, as a result of cleavage by the protease. Image (D) shows the pVI/iVI/VI distribution at 22 h post-initial Ad2 infection, detected with a protein VI-antiserum together with a secondary FITC-conjugated antibody. All images acquired using a *DeltaVision* microscope and 100x oil immersion.

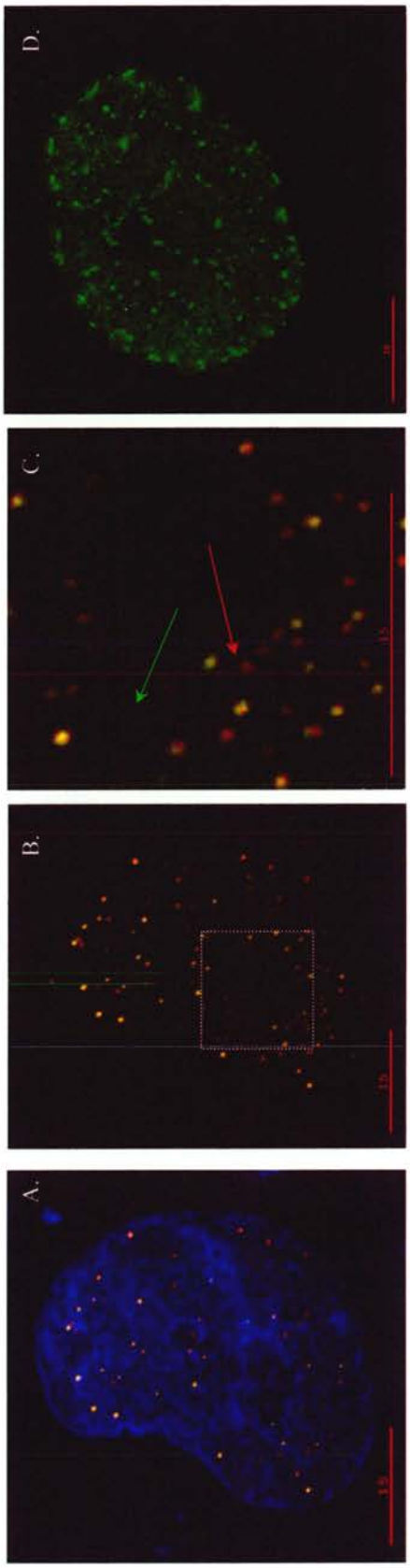
D.
C.
B.
A.

4.4 Studies on the nuclear localisation of pVI

Despite the efforts with the pVIct-F and pdf-substrate assays, I found no confirmation for the theory that pVIct or pVI translocates the protease to the nucleus. Interest, however, turned towards the nuclear accumulation of pVI protein itself. In fact, the sequence of pVI harbours two putative NLS: in addition to the KRRR $^{245-248}$ at the very C-terminus, another putative NLS is situated in the middle of the protein KRPRP $^{131-135}$. Several nuclear proteins are known to contain multiple NLS, which can function independently or act cooperatively to emphasize nuclear localisation. The sequence KRPRP is also highly conserved throughout adenovirus human serotypes (Figure 6, page 60). In addition, the KRPRP sequence has previously been identified as a NLS for adenoviral E1A protein (Lyons *et al.*, 1987), reconfirming the possibility that it is also a NLS for the adenoviral pVI protein.

To assess the importance of the KRPRP and KRRR sequences for the nuclear accumulation of pVI, they were mutated to five and four Alanines, respectively, using site-directed mutagenesis by PCR (see appendix for oligonucleotide sequences). Also a double mutant was constructed, in which both putative NLS signals were abolished. These are referred to as a middle-mutant (mm), C-terminal mutant (cm) and double-mutant (dm) in this thesis.

In addition, truncated versions of pVI (34-250, 1-239 and 34-239) were generated. These mutants are natural cleavage-site products of AVP: 1-239 and 34-250 intermediate forms (iVI), and 34-239 the mature VI.

The PCR-generated mutants of pVI protein were cloned to the C-terminus of both types of fluorescent proteins: enhanced green fluorescent protein (EGFP) and red-fluorescent protein (DsRed2). This was performed in order to confirm that the nuclear accumulation of this protein and its mutants was independent from the fluorescent tag, to which it was attached. Söling *et al.* (2002) reported that different fluorescent proteins affected the intracellular localisation of Herpes simplex virus type 1 thymidine kinase (TK). The aforementioned authors found that fusion proteins of the thymidine kinase with DsRed2-tag were unable to pass through the nuclear pores compared to the fusion proteins of TK with an EGFP-tag. While the first version of DsRed protein (DsRed1), isolated from *Discosoma* species, has been criticised for causing aggregates in cells

owing to its tendency to tetramerise, the successor variant DsRed2 does have reportedly a much improved solubility (Clontech Living Colours user manual, July 2001).

In this study, the intracellular distribution of the truncated pVI-proteins and that of the NLS mutants was assessed by fluorescence microscopy and by subcellular fractionation and Western blotting of transfected cells. In transient transfections of HeLa cells with empty DsRed2-C1 and EGFP-C1 plasmids, fluorescence was visible throughout cytoplasm and nucleus, as expected. Collectively, it can be concluded from images A-F (Figure 19) that the pVI protein and mutants of it localised in a similar manner whether expressed as a fusion with the fluorescent protein EGFP or DsRed2.

As evident from Figure 19, the cm and mm mutants were found in both the cytoplasm and the nucleus in a spot-like distribution. The dm, however, was mainly found in the cytoplasm. From the synthesised truncated versions, 1-239 (iVI) and 34-239 (VI) localised similarly, in both the cytoplasm and nucleus, having both lost one of their NLS. Surprisingly, the truncated version 34-250 was also incapable of complete nuclear accumulation despite possessing both putative NLS. This was presumably a consequence of a disruption to the protein conformation, after the deletion of the first 33 amino acids, and to such an extent that the NLS were not readily 'available' for recognition. None of the mutants, however, were capable of complete nuclear accumulation, similar to that observed with the wild-type pVI protein.

Subsequently, the fluorescence microscopy experiments were followed by fractionation of transfected cells (at 24 hpt) into cytoplasmic and nuclear extracts. The fractions were obtained following lysis-buffer (see method 2.6.8) and they were subject to SDS-PAGE electrophoresis and Western blotting. The antiserum raised against residues 74-190 of protein VI (a gift from W. C. Russell) and the anti-GFP-antibody (Roche) were used for detecting the expression of the fusion proteins.

The cytoplasmic and nuclear fractions (see Figure 19), revealed the localisation of the mutants to be very similar to that observed with fluorescence microscopy. Most of the truncated versions and NLS mutants were present in both fractions, in comparison to the wild-type pVI, which was solely nuclear. The cm, mm, iVI, VI and 34-250 proteins were all present in both nuclear and cytoplasmic fractions, compared to the dm, which was almost exclusively cytoplasmic.

Figure 19 (A-B). Localisation of the NLS mutants and truncated versions of pVI. The localisation of the proteins, expressed as C-terminal fusions with EGFP & DsRed2, was confirmed by fluorescent microscopy following standard transient transfection (method 2.6.2.3)(A) and by Western blotting of nuclear and cytoplasmic fractions of cells transfected with EGFP-fusions (B). Anti-GFP antibody (Roche) was used at 1:1000 dilution in Western blotting for the detection of the proteins. The cells were fixed for microscopy at 24 hpt and viewed using a *DeltaVision* microscope and 100x oil immersion.

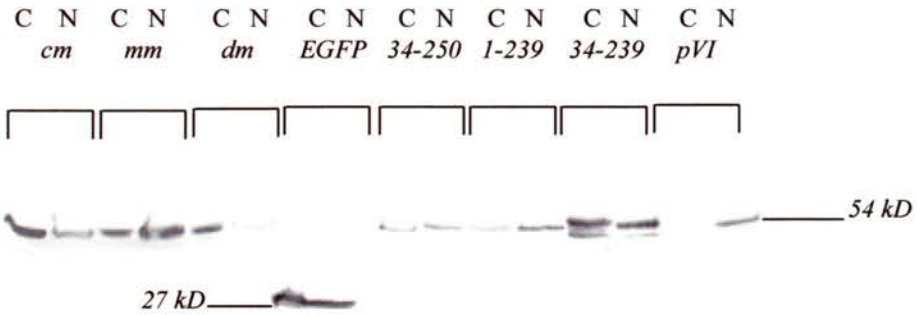
C N C N C N C N C N C N C N C N
cm mm dm EGFP 34-250 1-239 34-239 pVI
54 kD
27 kD

B.

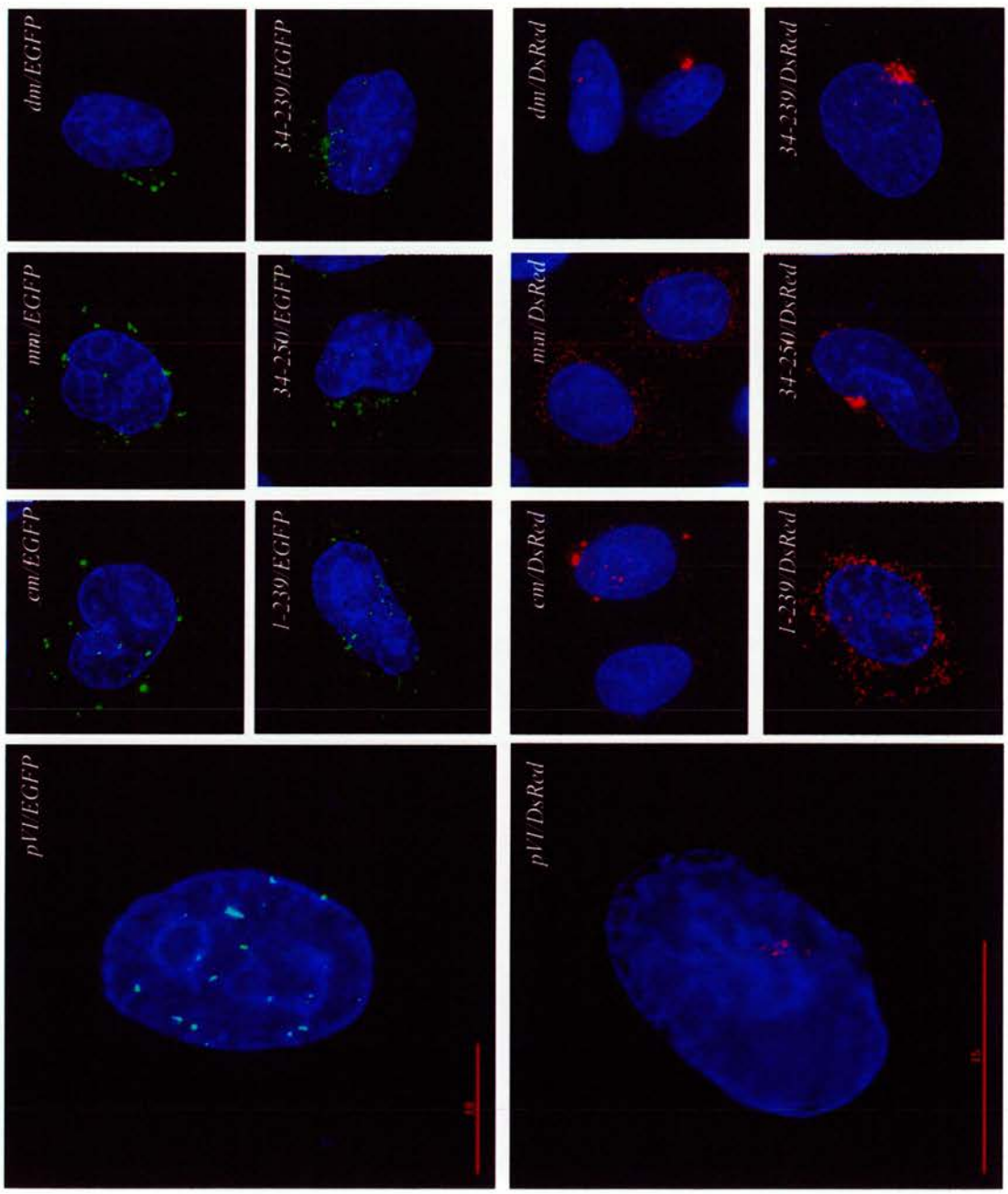
dm/EGFP
34-239/EGFP
dm/DsRed
34-239/DsRed
mm/EGFP
34-250/EGFP
mm/DsRed
34-250/DsRed
cm/EGFP
1-239/EGFP
cm/DsRed
1-239/DsRed
pVI/EGFP
pVI/DsRed

A.

Because of the possible disruption to the protein structure in the case of truncated version 34-250 (or iVI), the localisation pattern seen with mature VI/EGFP could be disputed. However, the fact that the localisation of the iVI was very similar to that of the cm, served as a confirmation that the mature VI (truncated version 34-239) was incapable of complete nuclear accumulation without the second NLS, present on the activating peptide sequence. Overall, the results indicated that the KRPRP and KRRR motifs function to enhance each other in the nuclear accumulation of the pVI protein.

4.5 Discussion

The nuclear localisation experiments presented in this thesis stemmed from the activation and binding studies, according to which KRRR-motif of pVIct could have an additional role. Previous results (Pollard, 2001) showed that this sequence was capable of directing a cytoplasmic protein to the nucleus and that the minimum requirement for nuclear accumulation was the tripeptide KRR.

4.5.1 Nuclear localisation conundrum of the protease molecules

The ability of the activating peptide to associate with the protease and to transport it to the nucleus was assessed using a fluorescent-peptide and by transfecting a fluorescently-tagged protease. Although these experiments did not reveal *in vivo*-association between the components to support the hypothesis, they lead to the development of useful double-fluorescent (pdf) constructs.

While the pdf-fluorescent constructs did not indicate that pVIct nuclear translocates AVP, they were shown to be successful substrates for *in vitro* and *in vivo* protease activity. Also, the pdf-constructs could be further optimised to examine cytoplasmic activity of the protease during adenovirus infection, the exact timing of which is not known. Furthermore, these types of experiments could reveal additional cellular substrates for the protease. This could be achieved by employing another signal on the substrate-construct, in addition to the NLS, which would target the protein-complex immediately after synthesis. The role of a C-terminal hydrophobic domain in Polyoma virus middle T antigen is to bind the protein to the plasma membrane (review: Garcia-Bustos *et al.*, 1991). Previous hybrid experiments have shown that this membrane anchor is capable of overriding a NLS causing cytoplasmic distribution (Roberts *et al.*, 1987). In this study, such a signal could be fused to the N-terminus of the EYFP protein, targeting the expressed protein complex to the appropriate compartment. In this manner, the substrate would be present in the vicinity of the separately expressed protease. Consequently, the maturation of the fluorescent substrate, mediated by the protease, would result in the release of the cleavage product bearing a NLS. The localisation of this cleavage product, and whether in a complex with the expressed fluorescent protease, could be followed.

If not by the action of pVI or pVIct, could any other adenovirus protein nuclear localise the protease? In order to avoid premature cleavage of the viral pre-proteins, it would be non-beneficial for the protease to associate and nuclear accumulate in complex with those viral proteins, which are in fact its substrates. This theory clearly rules out pVI and leaves protein V as the sole candidate transporter with identified nuclear and nucleolar targeting sequences, which is not processed by the protease.

According to previous reports, protease is found in both the cytoplasm and nucleus at 36 and 52 hours post-infection (Webster *et al.*, 1994) and is active in both cellular compartments towards the end of the infection (Chen *et al.*, 1993). Unless this equilibrium changes towards nuclear accumulation at a certain point, approximately half of the protease molecules would remain cytoplasmic. Perhaps therefore, the most plausible scenario is that the protease molecules are not actively transported to the nucleus after their synthesis. Instead, they passively diffuse through the NPC, which allows for this type of signal-independent entry in the case of ions and small molecules or proteins up to 60 kD size (Paine *et al.*, 1975, review: Garcia-Bustos *et al.*, 1991). As the protease molecules do not possess specific nuclear retention signals, they would be equally subject to export from the nucleus. Some of the protease molecules inside the nucleus would become associated at the packaging and assembly events, whereas the ones removed from the nucleus, relocate in the cytoplasm. There, they would associate with actin and aid in the lysis of the host cell.

However, according to this theory the virus, while relying on the cellular transport machinery for the nuclear import of its structural proteins, does not control more specifically the localisation its protease. This would seem risky, especially since the protease is such a pivotal component of an infectious particle, required for the efficacy and success of the infection.

4.5.2 Nuclear localisation of pVI protein

In this study, transfections with pVI revealed a dot-like nuclear distribution for the protein. The gene for the polypeptide pVI encodes two putative NLS. Mutational analysis on these NLS showed that for complete pVI nuclear localisation both, the KRPRP and KRRR motifs, are required. The KRPRP NLS on pVI is identical to that used by the adenoviral E1A protein (Lyons *et al.*, 1987). A similarity search for the

KRRR motif using NPS@ Network Protein Sequence Analysis revealed that proteins, such as the Tupaia adenovirus type 1 E1B protein (residues AKRRRL$^{15-20}$), also contain this motif (Flugel *et al.*, 1985).

The need for multiple NLS on a single protein can be rationalised by weaker NLS acting cooperatively and additively. In the case of yeast MATα2 protein, the dual NLS have been proposed to perform different functions; one is involved in binding at the nuclear pore complex whilst the other mediates translocation (Hall *et al.*, 1990).

In the case of adenoviral DNA-binding protein (DBP), two signal sequences have been identified which seem to complement the effect of one another (Morin *et al.*, 1989). Disruption to either one of the DBP NLS (PPKKR$^{42-46}$or PKKKKK$^{84-89}$) prevents nuclear localisation during transient transfection. During an Ad2 infection, however, other viral factors are capable of rescuing the DBP NLS mutants (Morin *et al.*, 1989). It would be interesting to examine whether this occurs with pVI dm (double-mutant) during Ad infection. Do other viral factors also contribute to the nuclear accumulation of pVI? Or is pVI capable of transporting other adenoviral proteins to the nucleus, in a similar manner to that of the adenoviral pre-terminal protein, pTP and DNA polymerase (Zhao & Padmanabhan, 1988)?

During the preparation of this thesis, Wodrich *et al.* (2003) published data showing that pVI protein, rather like HIV-1 Rev protein (Meyer & Malim, 1994), undergoes bi-directional nucleocytoplasmic shuttling. According to their report, in addition to the two NLS signals, the presence of two nuclear export signals (NES) on the pVI protein causes pVI to 'ferry' between the nucleus and cytoplasm transporting hexon to the nucleus via importin α/β-dependent mechanism in the process.

How do the findings by Wodrich *et al.* compare with results presented here? The two NES studied by the above authors, KLK$^{70-72}$ and LGV$^{239-241}$, were not investigated in this thesis following the consistent nuclear distribution of expressed pVI. Transfected pVI localised identically to that observed with pVI/iVI/VI during infection, in a foci-manner avoiding the nucleolus. Further, with the pdf-substrate constructs 20.1-20.6 used in this study (with the exception of 20.2), a similar distribution to that of pVI/iVI/VI in infection was obtained by transient transfection. In addition, rather than fusing the full-length pVI sequence, utilising a part of the C-terminus of the protein was sufficient to confer this type of localisation within cells. Although the proposed NES on pVI are

leucine-containing sequences, they seem weaker signals than for instance the LERLTL-stretch identified in HIV-1 Rev, which is also a nucleocytoplasmic shuttling protein (Meyer & Malim, 1994).

Some mutual conclusions from these two studies can be drawn. First, both NLS signals are required to confer efficient nuclear accumulation of pVI, as illustrated by the constructed NLS-mutants. The need for both NLS could be rationalised on the basis of the NES sequences, in that if the ratio of NES to NLS is altered from 2:2 to 2:1 (shown by cm and mm/EGFP mutants), the cytoplasmic accumulation of the fusion proteins is promoted. Further, the double fluorescent experiments with pdf-constructs performed in this study, in particular constructs 20.1, 20.3 and 20.4, suggest that in a 1:1 ratio of pVI NLS to NES, the NLS predominates.

Also, on the basis of these two studies, the pVIct and the KRRR-sequence at its carboxy-terminus, is a sufficient NLS. Here, the inability of the deletion mutant 1-239/EGFP (iVI) to accumulate into the nucleus, in a similar manner to that of the pVI/EGFP, confirms that the 11-residue peptide is necessary for pVI/VI nuclear accumulation. These results also affirm the concept that the protease does not cleave off the activating peptide for maximal activation and proteolysis until the maturation stage, taking place in the nucleus during the final steps of the infectious cycle.

Wodrich *et al.* have provided an elegant proposal of how protein VI switches to its assembly role from nuclear cytoplasmic shuttling-and-transport function. Previously, Matthews and Russell (1994) have demonstrated that the processed, mature VI has more hexon-binding affinity than the unprocessed pVI. Moreover, a previously identified temperature-sensitive strain of Ad5, *ts147*, indicated the importance of hexon binding to pVI for nuclear import: infection with *ts147* resulted in the degradation of pVI as well as in the cytoplasmic accumulation of hexon (Kauffman & Ginsberg, 1976). Hence, the proposal is that following the nuclear import of hexon with pVI, the concentration of hexon increases, leading to more pVI molecules associating with hexon. This in turn reduces the amount of pVI shuttling between cytoplasm and nucleus and the increasing intranuclear concentration of pVI would trigger the activation of the protease. The cleavage of the activating peptide, between residues 239 and 240 of pVI, would separate the NLS from the proposed, C-terminal NES on the pVIct. The maturation of pVI to VI

Figure 20. Model diagram for the role of adenovirus pVI protein in the nuclear import of hexon and the relevance of the two NLS signals on the nuclear accumulation of pVI itself. The importance of pVI as a shuttling protein, which transports hexon to the nucleus is based upon the recent observations by Wodrich *et al.* (2003). pVI protein requires both the C-terminal NLS located within the pVIct and the internal NLS motif for complete nuclear accumulation, and associates with import receptors α and β. Wodrich *et al.* have also proposed two NES signals on the pVI protein, which guarantee the recycling of the pVI back to the cytoplasm by associating with export receptors. As the export complex dissociates in the cytoplasm, the released pVI may export more hexon molecules to the nucleus. According to data presented in this thesis, neither pVI nor pVIct import the protease into the nucleus and the component responsible for this, whether cellular or viral, is yet unidentified. The protease cleaves pVI releasing pVIct in the nucleus later during infection, and hence the proposed NLS and NES sequences would be separated. This in turn leads to the mature VI having increased binding affinity for hexon during assembly.

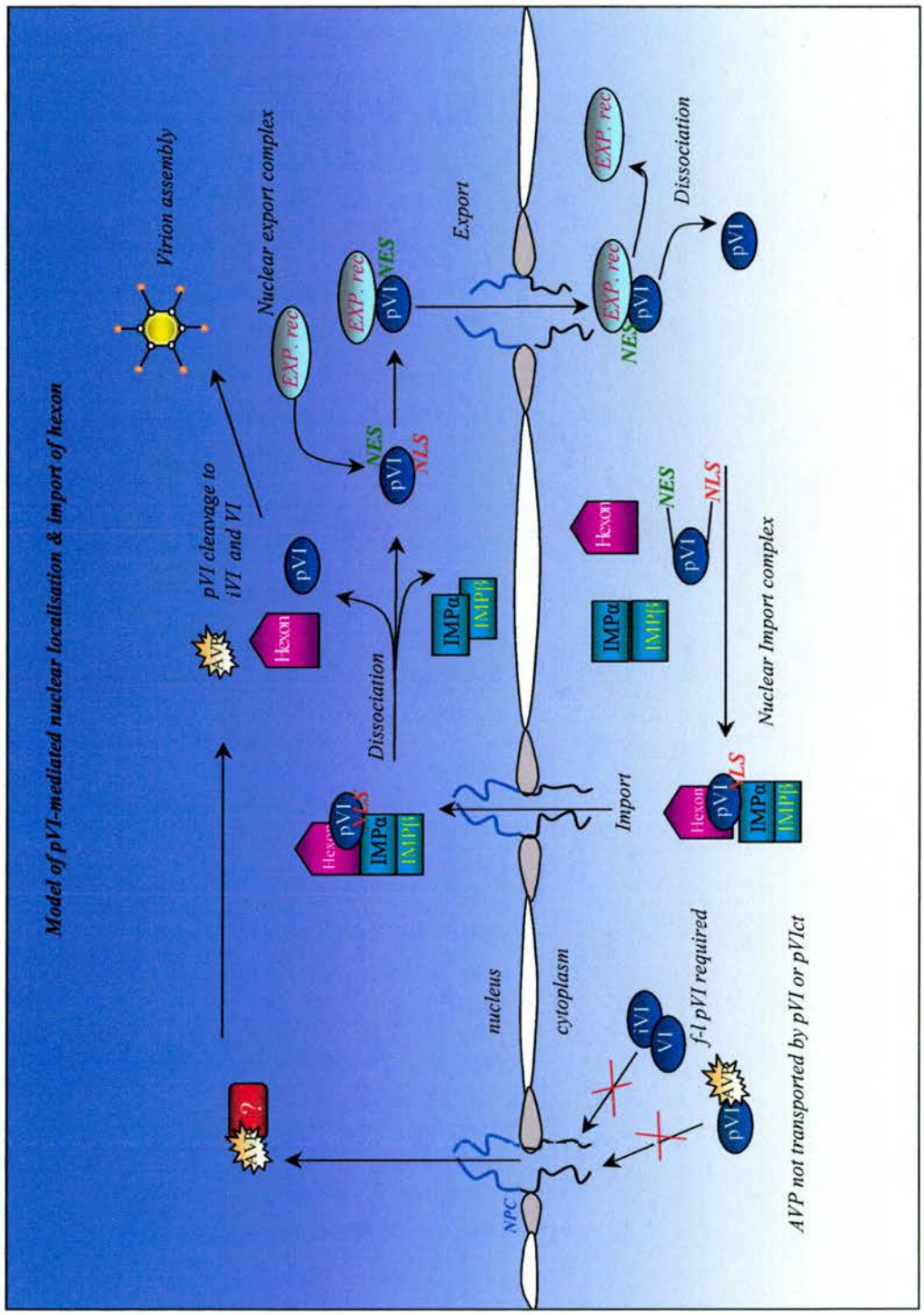
Model of pVI-mediated nuclear localisation & import of hexon
Virion assembly
pVI cleavage to iVI and VI
Nuclear export complex
EXP. rec
NES
NLS
pVI
Hexon
AVP
IMPα
IMPβ
Dissociation
Export
Import
Nuclear Import complex
NPC
nucleus
cytoplasm
iVI
VI
f-l pVI required
AVP not transported by pVI or pVIct

would improve its binding ability to hexon and therefore enhance the assembly of protein VI into the virus. The proposed model by Wodrich *et al.* is depicted in Figure 20, together with observations made in this study.

Another adenoviral late protein pμ was recently shown to affect the accumulation of early E2 proteins as well as to target itself specifically to the nucleolus (Lee *et al.*, 2004), and it will be interesting to find out what type of activities pμ mediates following its specific localization during adenoviral infection. Interestingly, the localisation of pTP at 20 hpi, which was shown in the study by Lee *et al.*, displayed a similar type of nuclear distribution to that seen here with pVI. Hence, the observed speck-like distribution of pVI/iVI/VI in the nucleus could in fact reveal an additional function for the protein. Future studies into the pVI localisation should include a closer look at the distribution of the protein within the nucleus. Is pVI colocalising with promyelocytic leukaemia protein (PML) bodies? PML bodies, a major component of nuclear domain 10 (ND10) structures have been implicated in transcription/replication, antiviral response and apoptosis and already one adenovirus component, Ad4 ORF3, has been proposed to disrupt ND10 and to redistribute PML (Carvalho *et al.*, 1995, Leppard & Everett, 1999).

In conclusion, recent studies combined with earlier observations offer a more complex regulatory role for the activating peptide. The nuclear localisation role of its KRRR-sequence together with the previously discussed role in promoting an association with viral DNA-protease-complex (see section 3.6.3) raises the question whether this short karyophilic sequence might in fact perform multiple tasks during adenovirus infection.

The adenovirus protease/peptide represents an interesting model system for studying important molecular interactions required for successful infection. For efficient catalysis, the 11-mer peptide needs to be cleaved from the precursor protein VI and associate via a disulphide bond with the enzyme. Furthermore, these components need to associate at correct timepoints during the infection in order to serve their purpose for the virus.

What characteristics of the GVQSLKRRRCF-peptide have been identified to date as essential components for the interaction with AVP? And what, if anything, did the assays performed in this study further reveal of this interaction?

First and foremost, previous studies have shown that the Cysteine residue at C-terminus of the peptide performs an essential duty in the binding process by forming a disulphide bond with Cys'104 of the protease and contributes to the activation of the protease (Webster *et al.*, 1993, Jones *et al.*, 1996, Cabrita *et al.*, 1997). Recent mutational studies, however, showed that if the Cysteine was mutated to Alanine, the inclusion of DNA could suppress the effects of the mutation when binding to AVP and to enhance the constants for substrate hydrolysis (McGrath *et al.*, 2001b). Most interesting is the observation by McGrath *et al.* (2001b) that the maximal rate of substrate hydrolysis was reached *in vitro* by 160 sec and prior to disulphide bond formation. These authors suggest that in fact the disulphide bond formation must not therefore be essential for AVP stimulation.

How about the N-terminus of the peptide? The importance of the N-terminal Glycine and Valine in binding to the protease and in stimulation of activity was noted by Cabrita *et al.* (1997), and from the structure of the heterodimer complex (discussed in section 3), it is apparent that the N-terminus of pVIct is surrounded by the protease-formed pocket. Additionally, the distance between the Cysteine and the N-terminus of the peptide was concluded important in that there needs to be nine residues preceding the Cysteine residue as peptides of shorter length were ineffective in binding (Cabrita, 1997).

From this study, the conserved, aromatic residue at the C-terminus of the peptide can be added to the list of pVIct residues playing an important role. The examination of the crystal structure of the complex showed that similarly to the N-terminus, the final C-terminal residue seems to be contained within a protease-formed pocket. The presence of Phe or Tyr residue next to Cys has been previously researched: these residues may stabilise the Cys-Cys disulphide interaction by contacts mediated between the aromatic ring and side chain of Cys (Viguera & Serrano, 1995). This could therefore also explain the prevalence of an aromatic residue at the 11^{th} position in the adenovirus peptide sequences, and especially in those serotypes, which contain Tyrosine residues on both sides of the Cysteine'10, such as EDS and snake (Figure 6: alignment of pVI sequences).

However, the KRRR-motif and its strong conservation throughout human adenovirus serotypes, examined in this study, could not be fully explained on the basis of the activation and binding data. While mutational *in vitro* assays highlighted the significance of the last C-terminal residue for protease activity, a more *in vivo*-type of role for the cationic-stretch during adenovirus infection was explored. It was in fact found that the activating peptide sequence could be employed as a nuclear localisation signal and that this signal was required for the sufficient nuclear accumulation of the pVI protein itself, together with a KRPRP-sequence contained within the pVI sequence. A hypothesis that a protease/peptide interaction *in vivo* could be responsible for nuclear localisation of the protease was also examined, although this was not found to occur. However, if the human adenovirus pVIct sequence is responsible for transporting the pVI protein to the nucleus during Ad infection, where does it leave those distant adenovirus serotypes lacking the KRRR-motif? Serotypes such as EDS and snake adenovirus have in fact a cationic stretch located further upstream of their peptide sequence ($KKRKR^{201\text{-}205}$ in the pVI sequence of EDS), which could potentially substitute for the KRRR-motif. Further *in vivo* studies with the recently identified adenovirus serotypes, their proteases and virion components, would be very interesting in examining potential differences and adaptations following evolution of these viruses.

Oligonucleotides used in this study.

[1] For the generation of the deletion and NLS-mutants in EGFP-C1 and dsRED2-C1 vectors.
oligo (1) with oligo (2) for wt, full-length pVI. (*BamH*I and *Eco*RI sites are underlined)
oligo (1) with oligo (3) for the C-terminal NLS-mutant of pVI. (mutations introduced in bold)
oligo (1) with oligo (4) for the middle NLS mutation. The product of the PCR was used with oligo (2) to generate the full-length mutant.
oligo (5) with oligo (2) for the 34-250 deletion mutant.
oligo (1) with oligo (6) for the 1-239 deletion mutant
oligo (5) and (6) for the generation of the 34-239 mutant

(1) 5'-GCTCAAGCTTCGAATTCCATGGAAGAC-3'
(2) 5'-CGGTGGATCCTTAGAAGCATCGTCG-3'
(3) 5'-CGGTGGATCCTTAGAAGCA**TGCTGCGGCCGC**CAGGGATTGCAC-3'
(4) 5'-CCTGTC**GGCCGCCGCCGCCGC**TTCGCCACGCCC-3'
(5) 5'-GCTTCGAATTCTGCCTTCAGCTGGGGCTCG-3'
(6) 5'-GGAGGATCCTTACAGACCCACGATGCTG-3'

[2] For the generation of constructs pdf20.1-20.6.
oligo (1) with oligo (2) for the constructs 20.1 & 20.2
oligo (1) with oligo (3) for the constructs 20.3 & 20.4
oligo (1) with oligo (4) for the constructs 20.5 & 20. 6
(*Apa*I and *Xba*I sites are underlined, inserted glycine residues in italics and pVI sequences in bold)

(1) 5'-CAAAAGGGCCC*ACCGCC*AGCGGCCGCGAAGCATCGTCGGCGCTTCAGGGA-3'
(2) 5'-GAAAATCTAGA*GGTGGCGGA*GAATTC**GGTCCGCGATCGATGCGGCCCGTAGCC**-3'
(3) 5'-GAAAATCTAGA*GGTGGCGGA*GAATTC**GTGCTGGGCCAGCACACACCTGTAACG**-3'
(4) 5'-GAAAATCTAGA*GGTGGCGGA*GAATTC**ATGGAAGACATCAACTTTGCGTCTCTGG**-3'

[3] For the generation of the pVI gene in pGEX-2T- expression vector.
N-terminal oligo (1) with C-terminal oligo (2).
(*BamH*I and *Eco*RI sites are underlined)

(1) 5'-CTCGGATCCATGGAAGACATCAACTTTGCG-3'
(2) 5'-CGTGAATTCGAAGCATCGTCGGCGCTTCAG-3'

Akusjärvi, G., Aleström, P., Pettersson, M., Lager, M., Jörnvall, H., and Pettersson, U. (1984). The gene for the adenovirus 2 hexon polypeptide. *Journal of Biological Chemistry,* **259**: 13976-13979.

Akusjärvi, G., and Persson, H. (1981). Gene and mRNA for precursor polypeptide VI from adenovirus type 2. *Journal of Virology*, **38**: 469-482.

Aleström, P., Akusjärvi, G., Lager, M., Yeh-Kai, L., and Petterson, U. (1984). Genes encoding the core proteins of adenovirus type 2. *Journal of Biological Chemistry,* **259**: 13980-13985.

Aleström, P., Akusjärvi, G., Perricaudet, M., Mathews, M. B., Klessig, D. F., and Pettersson, U. (1980). The gene for polypeptide IX of adenovirus type 2 and its unspliced messenger RNA. *Cell*, **19**: 671-681.

Anderson, C. W. (1990). The proteinase polypeptide of adenovirus serotype 2 virions. *Virology,* **177**: 259-72.

Anderson, C. W., Baum, P. R., and Gesteland, R. F. (1973). Processing of adenovirus 2-induced proteins. *Journal of Virology,* **12**: 241-252.

Anderson, H. O. (1999). Structure-aided design of antiviral drugs: application of the method on HIV-1 protease and SIV reverse transcriptase. *PhD Thesis, Acta Universitatis Upsaliensis,* Uppsala.

Andrés, G., Alejo, A., Simón-Mateo, C., and Salas, M. L. (2001). African swine fever virus protease, a new viral member of the SUMO-1-specific protease family. *Journal of Biological Chemistry,* **276**: 780-787.

Angeletti, P. C., and Engler, J. A. (1998). Adenovirus preterminal protein binds to the Cad enzyme active sites of viral DNA replication on the nuclear matrix. *Journal of Virology,* **72**: 2896-2904.

Arnberg, N., Edlund, K., Kidd, A. H., and Wadell, G. (2000). Adenovirus type 37 uses sialic acid as a cellular receptor. *Journal of Virology,* **74**: 42-48.

Athappilly, F. K., Murali, R., Rux, J. J., Cai, Z., and Burnett, R. M. (1994). The refined crystal structure of hexon, the major coat protein of adenovirus type 2, at 2.9Å resolution. *J. Mol. Biol.,* **242**: 430-455.

Atherton, E., and Sheppard, R. C. (1989). Solid phase peptide synthesis: a practical approach. In *Practical approach series*. IRL Press, Oxford. pp. 203.

Bai, M., Harfe, B., and Freimuth, P. (1993). Mutations that alter an Arg-Gly-Asp (RGD) sequence in the adenovirus type 2 penton base protein abolish its cell-rounding activity and delay virus reproduction in flat cells. *Journal of Virology,* **67**: 5198-5205.

Balakirev, M. Y., Jaquinod, M., Haas, A. L., and Chroboczek, J. (2002). Deubiquitinating function of adenovirus proteinase. *Journal of Virology,* **76**: 6323-6331.

Baniecki, M. L., McGrath, W. J., McWhirter, S. M., Li, C., Toledo, D. L., Pellicena, P., Barnard, D. L., Thorn, K. S., and Mangel, W. F. (2001). Interaction of the human adenovirus proteinase with its 11-amino acid cofactor pVIc. *Biochemistry*, **40**: 12349-12356.

Barrett, A. J., and Rawlings, N. D. (2001). Evolutionary lines of cysteine peptidases. *Biol. Chem.*, **382**: 727-733.

Bartenschlager, R., Ahlborn-Laake, L., Mous, J., and Jacobsen, H. (1994). Kinetic and structural analyses of hepatitis C virus polyprotein processing. *Journal of Virology,* **68**: 5045-5055.

Baum, E. Z., Siegel, M. M., Bebernitz, G. A., Hulmes, J. D., Sridharan, L., Sun, L., Tabei, K., Johnston, S. H., Wildey, M. J., Nygaard, J., Jones, T. R., and Gluzman, Y.

(1996). Inhibition of human cytomegalovirus UL80 protease by specific intramolecular disulfide bond formation. *Biochemistry,* **35**: 5838-5846.

Benkő, M., Élő, P., Ursu, K., Ahne, W., LaPatra, S. E., Thomson, D., and Harrach, B. (2002). First molecular evidence for the existence of distinct fish and snake adenoviruses. *Journal of Virology*, **76**: 10056-10059.

Bergelson, J. M., Cunnigham, J. A., Droguett, G., Kurt-Jones, E. A., Krithivas, A., Hong, J. S., Horwitz, M. S., Crowell, R. L., and Finberg, R. W. (1997). Isolation of a common receptor for coxsackie B viruses and adenoviruses 2 and 5. *Science*, **275**: 1320-1323.

Bhatti, A. R., and Weber, J. (1979). Protease of adenovirus type 2: partial characterisation. *Virology*, **96**: 478-485.

Birboim, H. C., and Doly, J. (1979). A rapid alkaline extraction procedure for screening recombinant plasmid DNA. *Nucleic Acids Res.,* **7**: 1513-1523.

Boudin, M-L., D'Halluin, J-C., Cousin, C., and Boulanger, P. A. (1980). Human adenovirus type 2 protein IIIa. *Virology,* **101**: 144-156.

Boudin, M-L., Moncany, M., D'Halluin, J-C., and Boulanger, P. A. (1979). Isolation and characterization of adenovirus type 2 vertex capsomer (penton base). *Virology,* **92**: 125-138.

Boyer, T. G., Martin, M. E. D., Lees, E., Ricciardi, R. P., and Berk, A. J. (1999). Mammalian Srb/mediator complex is targeted by adenovirus E1A protein. *Nature,* **399**: 276-279.

Bradford, M. M. (1976). A rapid and sensitive method for the quantitation of microgram quantities of protein utilizing the principle of protein-dye binding. *Anal. Biochem.*, **72**: 248-254.

Brown, D. T., Westphal, M., Burlingham, B. T., Winterhoff, U., and Doerfler, W. (1975). Structure and composition of the adenovirus type 2 core. *Journal of Virology,* **16**: 366-387.

Brown, M. T., and Mangel, W. F. (2004). Interaction of actin and its 11-amino acid C-terminal peptide as cofactors with the adenovirus proteinase. *FEBS letters,* **28240**: 1-6.

Brown, M. T., McBride, K. M., Baniecki., M. L., Reich, N. C., Marriott, G., and Mangel, W. F. (2002). Actin can act as a cofactor for viral proteinase in the cleavage of the cytoskeleton. *Journal of Biological Chemistry*, **277**: 46298-46303.

Cabrita, G. (1997). The mechanism of activation of the adenovirus type 2 protease. *PhD Thesis*, University of St Andrews.

Cabrita, G., Iqbal, M., Reddy, H., and Kemp, G. (1997). Activation of the adenovirus protease requires sequence elements from both ends of the activating peptide. *Journal of Biological Chemistry,* **272**: 5635-39.

Carvalho, T., Seeler, J. S., Ohman, K., Jordan, P., Pettersson, U., Akusjärvi, G., Carmo-Fonseca, M., and Dejean, A. (1995). Targeting of adenovirus E1A and E4-ORF3 proteins to nuclear matrix-associated PML bodies. *Journal of Cell Biology*, **131**: 45-56.

Chakrabarti, S., Mautner, V., Osman, H., Collingham, K. E., Fegan, C. D., Klapper, P. E., Moss, P. A. H., and Milligan, D. W. (2002). Adenovirus infection following allogeneic stem cell transplantation: the incidence and outcome in relation to graft manipulation, immunosuppression and immune recovery. *Blood,* **100**: 1619-1627.

Challberg, M. D., and Kelly, T. J. (1981). Processing of the adenovirus terminal protein. *Journal of Virology*, **38**: 272-277.

Chatterjee, P. K., and Flint, S. J. (1987). Adenovirus type 2 endopeptidase: an unusual phosphoprotein enzyme matured by autocatalysis. *Proc. Natl. Acad. Sci. USA*, **84**: 714-718.

Chatterjee, P. K., Vayda, M. E., and Flint, S. J. (1985). Interactions among the three adenovirus core proteins. *Journal of Virology,* **55**: 379-386.

Chen, M., Mermod, N., and Horwitz, M. S. (1990). Protein-protein interactions between adenovirus DNA polymerase and nuclear factor I mediate formation of the DNA replication preinitiation complex. *Journal of Biological Chemistry*, **265**: 18634-18642.

Chen, P. H., Ornalles, D. A., and Shenk, T. (1993). The adenovirus L3 23-kilodalton proteinase cleaves the amino-terminal head domain from cytokeratin 18 and disrupts the cytokeratin network of HeLa cells. *Journal of Virology*, **67**: 3507-14.

Chen, P., Tsuge, H., Almassy, R. J., Gribskov, C. L., Katoh, S., Vanderpool, D. L., Margosiak, S. A., Pinko, C., Matthews, D. A., and Kan, C.-C. (1996). Structure of the human cytomegalovirus protease catalytic domain reveals a novel serine protease fold and catalytic triad. *Cell*, **86**: 835-843.

Clark, H. F., Michalski, F., Tweedell, K. S., Yohn, D., and Zeigel, R. F. (1973). An adenovirus, FAV-1, isolated from the kidney of a frog (*Rana pipiens*). *Virology*, **51**: 392-400.

Coenjaerts, F. E J., van Oosterhout, J A. W. M., and van der Vliet, P. C. (1994). The Oct-1 POU domain stimulates adenovirus DNA replication by a direct interaction between the viral precursor terminal protein–DNA polymerase complex and the POU homeodomain. *EMBO J.,* **13**: 5401-5409.

Colby, W. W., and Shenk, T. (1981). Adenovirus type 5 virions can be assembled in vivo in the absence of detectable polypeptide IX. *Journal of Virology*, **39**: 977-980.

Cotten, M., and Weber, J. M. (1995). The adenovirus protease is required for virus entry into host cells. *Virology,* **213**: 494-502.

Crossland, L. D., and Raskas, H. J. (1983). Identification of adenovirus genes that require template replication for expression. *Journal of Virology*, **46**: 737-748.

Cuesta, R., Xi, Q., and Schneider, R. J. (2004). Structural basis for competitive inhibition of eIF4G-Mnk1 interaction by the adenovirus 100-kilodalton protein. *Journal of Virology*, **78**: 7707-7716.

Darke, P. L., Cole, J. L., Waxman, L., Hall, D. L., Sardana, M. K., and Kuo, L. C. (1996). Active human cytomegalovirus protease is a dimer. *Journal of Biological Chemistry,* **271**: 7445-7449.

Davis, D. A., Dorsey, K., Wingfield, P. T., Stahl, S. J., Kaufman, J., Fales, H. M., and Levine, R. L. (1996). Regulation of HIV-1 protease activity through cysteine modification. *Biochemistry*, **35**: 2482-2488.

Davison, A. J., Benkő, M., and Harrach, B. (2003). Genetic content and evolution of adenoviruses. *Journal of General Virology,* **84**: 2895-2908.

Davison, A. J., Wright, K. M., and Harrach, B. (2000). DNA sequence of frog adenovirus. *Journal of General Virology*, **81**: 2431-2439.

de Felipe, P., and Ryan, M. D. (2004). Targeting of proteins derived from self-processing polyproteins containing multiple signal sequences. *Traffic*, **5**: 616-626.

De Jong, J. C., Wermenbol, A. G., Verweij-Uijterwaal, M. W., Slaterus, K. W., Wertheim-Van Dillen, P., Van Doornum, G. J. J., Khoo, S. H., and Hierholzer, J. C. (1999). Adenoviruses from human immunodeficiency virus-infected individuals, including two strains that represent new candidate serotypes Ad50 and Ad51 of species B1 and D, respectively. *J. Clin. Microbiol.,* **37**: 3940-3945.

Derossi, D., Calvet, S., Trembleau, A., Brunissen, A., Chassaing, G., and Prochiantz, A. (1996). Cell internalization of the third helix of the Antennapedia homeodomain is receptor-independent. *J. Biol. Chem.* **271**: 18188-18193.

Devaux, C., Caillet-Boudin, M-L., Jacrot, B., and Boulanger, P. (1987). Crystallization, enzymatic cleavage, and the polarity of the adenovirus type 2 fiber. *Virology,* **161**: 121-128.

D'Halluin, J.-C. (1995). Virus assembly. In *The Molecular Repertoire of Adenoviruses I.* Springer-Verlag, Heidelberg. pp. 47-66.

Dimmock, N. J., and Primrose, S. B. (1994). Introduction to modern virology. (4th edition). University Press, Cambridge.

Ding, J., McGrath, W. J., Sweet, R. M., and Mangel, W. F. (1996). Crystal structure of the human adenovirus proteinase with its 11 amino acid cofactor. *EMBO J.*, **15**: 1778-83.

Diouri, M., Geoghegan, K. F., and Weber, J. M. (1995). Functional characterization of the adenovirus proteinase using fluorogenic substrates. *Protein and Peptide Letters,* **2**: 363-370.

Diouri, M., Keyvani-Amineh, H., Geoghegan, K. F., and Weber, J. M. (1996). Cleavage efficiency by adenovirus protease is site-dependent. *Journal of Biological Chemistry* **271**: 32511-32514.

Dolph, P. J., Huang, J., and Schneider, R. J. (1990). Translation by the adenovirus tripartite leader: elements which determine independence from cap-binding protein complex. *Journal of Virology,* **64**: 2669-2677.

Erdman, D. D., Xu, W., Gerber, S. I., Gray, G. C., Schnurr, D., Kajon, A. E., and Anderson, L. J. (2002). Molecular epidemiology of adenovirus type 7 in the United States, 1966-2000. *Emerging Infectious Diseases,* **8**: 269-277.

Everitt, E., Lutter, L., and Philipson, L. (1975). Structural proteins of adenoviruses. *Virology,* **67**: 197-208.

Everitt, E., and Ingelman, M. (1984). Core and chromatin association of the adenovirus type 2 specific endoproteinase. *Microbios. Lett.,* **25**: 75-82.

Fahrenkrog, B., Köser, J., and Aebi, U. (2004). The nuclear pore complex: a jack of all trades? *Trends in Biochemical Sciences,* **29**: 175-182.

Failla, C., Tomei, L., and De Francesco, R. (1994). Both NS3 and NS4A are required for proteolytic processing of hepatitis C virus non-structural proteins. *Journal of Virology,* **68**: 3753-3760.

Farkas, S. L., Benkő, M., Élő, P., Ursu, K., Dán, Á., Ahne, W., and Harrach, B. (2002). Genomic and phylogenetic analyses of an adenovirus isolated from a corn snake (*Elaphe guttata*) imply a common origin with members of the proposed genus *Atadenovirus*. *Journal of General Virology*, **83**: 2403-2410.

Flint, S. J., Berget, S. M., and Sharp, P. A. (1976). Characterization of single-stranded viral DNA sequences present during replication of Adenovirus types 2 and 5. *Cell*, **9**: 559-571.

Flint, S. J., Racaniello, V. R., Enquist, L. W., and Skalka, A. M. (2000). Adenoviruses. In *Principles of Virology: molecular biology, pathogenesis, and control of animal viruses.* ASM Press, Washington, D. C. pp. 804-806.

Flugel, R. M., Bannert, H., Suhai, S., and Darai, G. (1985). The nucleotide sequence of the early region of the Tupaia adenovirus DNA corresponding to the oncogenic region E1b of human adenovirus 7. *Gene*, **34**: 73-80.

Fredman, J. N., and Engler, J. A. (1993). Adenovirus precursor to terminal protein interacts with the nuclear matrix in vivo and in vitro. *Journal of Virology*, **67**: 3384-3395.

Freimuth, P., and Anderson, C. W. (1993). Human adenovirus serotype 12 virion precursors pMu and pVI are cleaved at amino-terminal and carboxy-terminal sites that conform to the adenovirus 2 endoproteinase cleavage consensus sequence. *Virology*, **193**: 348-355.

Gao, M., Matusick-Kumar, L., Hurlburt, W., Feuer DiTusa, S., Newcomb, W. W., Brown, J. C., McCann III, P. J., Deckman, I., and Colonno, R. J. (1994). The protease of herpes simplex virus type 1 is essential for functional capsid formation and viral growth. *Journal of Virology*, **68**: 3702-3712.

Garcia-Bustos, J., Heitman, J., and Hall, M. N. (1991). Nuclear protein localization. *Biochimia and Biophysica Acta,* **1071**: 83-101.

Gavin, P., and Katz, B. (2002). Intravenous ribavirin treatment of severe adenovirus infection in immunocompromised children. *Pediatrics*, **110**: 1-8.

Goldenberg, D. P. (1989). Analysis of protein conformation by gel electrophoresis. In *Protein structure: a practical approach.* Information Press Ltd, Oxford. pp. 225-250.

Goobar-Larsson, L., Luukkonen, M. B. G., Unge, T., Schwartz, S., Utter, G., Strandberg, B., and Öberg, B. (1995). Enhancement of HIV-1 proteinase activity by HIV-1 reverse transcriptase. *Virology,* **206**: 387-394.

Graham, F. L., and van der Eb, A. J. (1973). A new technique for the assay of infectivity of human adenovirus 5 DNA. *Virology*, **52**: 456.

Grakoui, A., McCourt D. W., Wychowski, C., Feinstone, S. M., and Rice, C. M. (1993). Characterization of the hepatitis C virus-encoded serine proteinase: determination of proteinase-dependent polyprotein cleavage sites. *Journal of Virology*, **67**: 2832-2843.

Grand, R. J. A., Parkhill, J., Szestak, T., Rookes, S. M., Roberts, S., and Gallimore, P. H. (1999). Definition of a major p53 binding site on Ad2E1B58K protein and a possible nuclear localization signal on the Ad12E1B54K. *Oncogene,* **18**: 955-965.

Greber, U. F. (1998). Virus assembly and disassembly: the adenovirus cysteine protease as a trigger factor. *Rev. Med. Virol.*, **8**: 213-222.

Greber, U. F., Suomalainen, M., Stidwell, R. P., Boucke, K., Ebersold, M. W., and Helenius, A. (1997). The role of the nuclear pore complex in adenovirus DNA entry. *EMBO J.*, **16**: 5998-6007.

Greber, U. F., Webster, P., Weber, J., and Helenius A. (1996). The role of the adenovirus protease in virus entry into cells. *EMBO J.*, **15**: 1766-77.

Greber, U. F., Willets, M., Webster, P., and Helenius, A. (1993). Stepwise dismantling of adenovirus 2 during entry into cells. *Cell,* **75**: 477-486.

Green, M., and Piña, M. (1963). Biochemical studies on adenovirus multiplication IV. Isolation, purification, and chemical analysis of Adenovirus. *Virology*, **20**: 199-207.

Green, N. M., Wrigley, N. G., Russell, W. C., Martin, S. R., and McLachlan, A. D. (1983). Evidence for repeating cross-β sheet structure in the adenovirus fibre. *EMBO J.*, **2**: 1357-1365.

Grierson, A. W., Nicholson, R., Talbot, P., Webster, A., and Kemp, G. (1994). The protease of adenovirus serotype 2 requires cysteine residues for both activation and catalysis. *Journal of General Virology*, **75**: 2761-2764.

Hahm, B., Han, D. S., Back, S. H., Song, O-K., Cho, M-J., Kim, C-J., Shimotohno, K., and Jang, S. K. (1995). NS3-4A of hepatitis C virus is a chymotrypsin-like protease. *Journal of Virology,* **69**: 2534-2539.

Hall, M. N., Craik, C., and Hiraoka, Y. (1990). Homeodomain of yeast repressor alpha 2 contains a nuclear localization signal. *Proc. Natl. Acad. Sci. USA*, **87**: 6954-6958.

Harrach, B., Meehan, B. M., Benkö, M., Adair, B. M., and Todd, D. (1997). Close phylogenetic relationship between egg drop syndrome virus, bovine adenovirus serotype 7 and ovine adenovirus strain 287. *Virology*, **229**: 302-306.

Hateboer, G., Hijmans, M. E., Nooij, J. B. D., Schlenker, S., Jentsch, S., and Bernards, R. (1996). mUBC9, a novel adenovirus E1A-interacting protein that complements a yeast cell cycle defect. *Journal of Biological Chemistry,* **271**: 25906-25911.

Hay, R. T. (1985). Origin of adenovirus DNA replication: role of the nuclear factor I binding site *in vivo*. *J. Mol. Biol.,* **186**: 129-136.

Hay, R. T. (1996). Adenovirus DNA replication. In *DNA Replication in Eukaryotic Cells*, Cold Spring Harbor Laboratory Press, New York. pp. 699-719.

Hay, R. T., and Russell, W. C. (1989). Recognition mechanisms in the synthesis of animal virus DNA. *Biochem. J.,* **258**: 3-16.

Hay, R. T., Stow, N. D., and McDougall, I. M. (1984). Replication of adenovirus mini-chromosomes. *J. Mol. Biol.*, **175**: 493-510.

Hayashi, S. (2002). Latent adenovirus infection in COPD. *Chest,* **121**: 183-187.

Hayes, B. W., Telling, G. C., Myat, M. M., Williams, J. F., and Flint, S. J. (1990). The adenovirus L4 100-kilodalton protein is necessary for efficient translation of viral late mRNA species. *Journal of Virology,* **64**: 2732-2742.

Hearing, P., Samulski, R. J., Wishart, W. L., and Shenk, T. (1987). Identification of a repeated sequence element required for efficient encapsidation of the adenovirus type 5 chromosome. *Journal of Virology*, **61**: 2555-2558.

Hilleman, M. R., and Werner, J. H. (1954). Recovery of a new agent from patients with acute respiratory illness. *Proc. Soc. Exp. Biol. Med.,* **85**:183-188.

Hogg, J. C. (1999). Childhood viral infection and the pathogenesis of asthma and chronic obstructive lung disease. *American Journal of Respiratory and Critical Care Medicine,* **160**: 26-28.

Holwerda, B. C. (1997). Herpesvirus proteases: targets for novel antiviral drugs. *Antiviral Research,* **35**: 1-21.

Hong, J. S., and Engler, J. A. (1991). The amino terminus of the adenovirus fiber protein encodes the nuclear localization signal. *Virology*, **185**: 758-767.

Hong, S. S., Karayan, L., Tournier, J., Curiel, D. T., and Boulanger, P. A. (1997). Adenovirus type 5 fiber knob binds to MHC class I α2 domain at the surface of human epithelial and B lymphoblastoid cells. *EMBO J.,* **16**: 2294-2306.

Hong, Z., Ferrari, E., Wright-Minogue, J., Chase, R., Risano, C., Seelig, G., Lee, C-G., and Kwong, A. D. (1996). Enzymatic characterization of hepatitis C virus NS3/4A complexes expressed in mammalian cells by using the herpes simplex virus amplicon system. *Journal of Virology,* **70**: 4261-4268.

Honkavuori, K. S, Pollard, B. D., Rodriguez, M. S., Hay, R. T., and Kemp, G. D. (2004). Dual role for the adenovirus pVI C-terminus as a nuclear localization signal and activator of the viral protease. *Journal of General Virology*, **85** (In Press)

Hoogerhout, P., Stittelaar, K. J., Brugghe, H. F., Timmermans, J. A. M., ten Hove, G. J., Jiskoot, W., and Hoekman, J. H. G. (1999). Solid-phase synthesis and application of double-fluorescent-labeled lipopeptides, containing a CTL-epitope from the measles fusion protein. *J. Peptide Res.* **54**: 436-443.

Horne, R. W., Brenner, S., Waterson, A. P., and Wildy, P. (1959). The icosahedral form of an adenovirus. *J. Mol. Biol.,* **1**: 84-86.

Horwitz, M. S., Scharff, M. D. and Maizel, J. V. (1969). Synthesis and assembly of adenovirus type 2. *Virology*, **39**: 682-694.

Hosokawa, K., and Sung, M. T. (1976). Isolation and characterization of an extremely basic protein from adenovirus type 5. *Journal of Virology*, **17**: 924-934.

Houde, A., and Weber, J. M. (1990). Adenovirus proteinase: comparison of amino acid sequences and expression of the cloned cDNA in *Escherichia coli*. *Gene*, **88**: 269-273.

Howe, A. Y. M., Chase, R., Taremi, S. S., Risano, C., Beyer, B., Malcolm, B., and Lau, J. Y. N. (1999). A novel recombinant single-chain hepatitis C virus NS3-NS4A protein with improved helicase activity. *Protein Science*, **8**: 1332-1341.

Huang, J., and Schneider, R. J. (1991). Adenovirus inhibition of cellular protein synthesis involves inactivation of cap-binding protein. *Cell*, **65**: 271-280.

Hughes, L. (2003). Analysis of the Foot-and-Mouth Disease Virus 2A-mediated polyprotein processing event. *PhD Thesis*, University of St Andrews.

Javier, R. T. (1994). Adenovirus type 9 E4 open reading frame 1 encodes a transforming protein required for the production of mammary tumours in rats. *Journal of Virology,* **68**: 3917-3924.

Jones, S. J., Iqbal, M., Grierson, A. W., and Kemp, G. (1996). Activation of the protease from human adenovirus type 2 is accompanied by a conformational change that is dependent on the cysteine-104. *Journal of General Virology*, **77**: 1821-1824.

Kalderon, D., Richardson, W. D., Markham, A. F., and Smith, A. E. (1984). Sequence requirements for nuclear location of simian virus 40 large-T antigen. *Nature*, **311**: 33-38.

Kauffman, R. S., and Ginsberg, H. S. (1976). Characterization of a temperature-sensitive, hexon transport mutant of type 5 adenovirus. *Journal of Virology,* **19**: 643-658.

King, A. J., and van der Vliet, P. C. (1994). A precursor terminal protein-trinucleotide intermediate during initiation of adenovirus DNA replication: regeneration of molecular ends *in vitro* by a jumping back mechanism. *EMBO J.*, **13**: 5786-5792.

Kovács, G. M., LaPatra, S. E., D'Halluin, J.-C., and Benkő, M. (2003). Phylogenetic analysis of the hexon and protease genes of a fish adenovirus isolated from white sturgeon (*Acipenser transmontanus*) supports the proposal of a new adenovirus genus. *Virus Research,* **98**: 27-34.

Kräusslich, H.-G., and Wimmer, E. (1988). Viral proteinases. *Ann. Rev. Biochem.*, **57**: 701-754.

Lee, T. W. R., Blair, E. G., and Matthews, D. A. (2003). Adenovirus core protein VII contains distinct sequences that mediate targeting to the nucleus and nucleolus, and colocalization with human chromosomes. *Journal of General Virology,* **84**: 3423-3428.

Lee, T. W. R., Lawrence, F. J., Dauksaite, V., Akusjärvi, G., Blair, G. E., and Matthew, D. A. (2004). Precursor of human adenovirus core polypeptide Mu targets the nucleolus and modulates the expression of E2 proteins. *Journal of General Virology,* **85**: 185-196.

Leong, L. E., Walker, P. A., and Porter, A. G. (1993). Human rhinovirus-14 protease 3C binds specifically to the 5'-noncoding region of the viral RNA. *J. Biol. Chem.,* **268**: 25735-25739.

Leopold, P. L., Kreitzer, G., Miyazawa, N., Rempel, S., Pfister, K. K., Rodriguez-Boulan, E., and Crystal, R. G. (2000). Dynein-and microtubule-mediated translocation of adenovirus serotype 5 occurs after endosomal lysis. *Human Gene Therapy,* **11**:151-165.

Leppard, K. N. (1997). E4 gene function in adenovirus, adenovirus vector and adeno-associatcd virus infections. *Journal of General Virology,* **78**: 2131-2138.

Leppard, K. N., and Everett, R. D. (1999). The adenovirus type 5 E1b 55K and E4 Orf3 proteins associate in infected cells and affect Nd10 components. *Journal of General Virology,* **80**: 997-1008.

Leytus, S. P., Melhado, L. L., and Mangel, W. F. (1983). Rhodamine-based compounds as fluorogenic substrates for serine proteinases. *Biochem. J.*, **209**: 299-307.

Li, S-J., and Hochstrasser, M. (1999). A new protease required for cell-cycle progression in yeast. *Nature,* **398**: 246-251.

Liu, G.-Q., Babiss, L. E., Volkert, F. C., Young, C. S. H., and Ginsberg, H. S. (1985). A thermolabile mutant of adenovirus 5 resulting from substitution mutation in the protein VIII gene. *Journal of Virology,* **53**: 920-925.

Look, D. C., Roswit, W. T., Frick, A. G., Gris-Alevy, Y., Dickhaus, D. M., Walter, M. J., and Holtzman, M. J. (1998). Direct suppression of Stat1 function during adenoviral infection. *Immunity,* **9**: 871-880.

López-Otín, C., Simón-Mateo, C., Martínez, L., and Viñuela, E. (1989). Gly-Gly-X, a novel consensus sequence for the proteolytic processing of viral and cellular proteins. *Journal of Biological Chemistry,* **264**: 9107-9110.

Louis, N., Fender, P., Barge, A., Kitts, P., and Chroboczek, J. (1994). Cell-binding domain of adenovirus serotype 2 fiber. *Journal of Virology*, **68**: 4104-4106.

Lucher, L. A. (1995). Abortive adenovirus infection and host range determinants. In *The Molecular Repertoire of Adenoviruses I.* Springer-Verlag, Heidelberg, pp. 119-152.

Lutz, P., and Kedinger, C. (1996). Properties of the adenovirus IVa2 gene product, an effector of late-phase-dependent activation of the major late promoter. *Journal of Virology,* **70**: 1396-1405.

Lutz, P., Rosa-Calatrava, M., and Kedinger, C. (1997). The product of the adenovirus intermediate gene IX is a transcriptional activator. *Journal of Virology,* **71**: 5102-5109.

Lyons, R. H., Ferguson, B. Q., and Rosenberg, M. (1987). Pentapeptide nuclear localization signal in adenovirus E1a. *Molecular and Cellular Biology,* **7**: 2451-2456.

Maizel, J. V., White, D. O., and Scharff, M. D. (1968). The polypeptides of Adenovirus I. Evidence for multiple protein components in the virion and a comparison of types 2, 7A, and 12. *Virology*, **36**: 115-125.

Mangel, W. F., McGrath, W. J., Toledo, D., and Anderson, C. W. (1993). Viral DNA and a viral peptide are cofactors of adenovirus virion proteinase activity. *Nature,* **361**: 274-275.

Mangel, W. F., Toledo, D. L., Ding, J., Sweet, R. M., and McGrath, W. J. (1997). Temporal and spatial control of the adenovirus proteinase by both a peptide and the viral DNA. *TIBS,* **22**: 393-398.

Matayoshi, E. D., Wang, G. T., Krafft, G. A., and Erickson, J. (1990). Novel fluorogenic substrates for assaying retroviral proteases by resonance energy transfer. *Science*, **247**: 954-958.

Mathews, M. B., and Shenk, T. (1991). Adenovirus virus-associated RNA and translation control. *Journal of Virology,* **65**: 5657-5662.

Matthews, D. A. (2001). Adenovirus protein V induces redistribution of nucleolin and B23 from nucleolus to cytoplasm. *Journal of Virology,* **75**: 1031-1038.

Matthews, D. A., and Russell, W. C. (1994). Adenovirus protein-protein interactions: hexon and protein VI. *Journal of General Virology,* **75**: 3365-3374.

Matthews, D. A., and Russell, W. C. (1995). Adenovirus protein-protein interactions: molecular parameters governing the binding of protein VI to hexon and the activation of the adenovirus 23K protease. *Journal of General Virology,* **76**: 1959-1969.

Matthews, D. A., and Russell, W. C. (1998). Adenovirus core protein V interacts with p32- a protein which is associated with both the mitochondria and the nucleus. *Journal of General Virology*, **79**: 1677-1685.

McDonald, D., Stockwin, L., Matzow, T., Blair Zajdel, M. E., and Blair, G. E. (1999). Coxsackie and adenovirus receptor (CAR)-dependent and major histocompatibility complex (MHC) class I-independent uptake of recombinant adenoviruses into human tumour cells. *Gene Therapy*, **6**: 1497-1498.

McGrath, W. J., Baniecki, M. L., Li, C., McWhirter, S. M., Brown, M. T., Toledo, D. L., and Mangel, W. F. (2001a). Human adenovirus proteinase: DNA binding and stimulation of proteinase activity by DNA. *Biochemistry*, **40**:13237-13245.

McGrath, W. J., Baniecki M. L., Peters E., Green D. T., and Mangel, W. F. (2001b). Roles of two conserved cysteine residues in the activation of human adenovirus proteinase. *Biochemistry,* **40**: 14468-14474.

Meyer, B. E., and Malim, M. H. (1994). The HIV-1 rev transactivator shuttles between the nucleus and the cytoplasm. *Genes & Development*, **8**: 1538-1547.

Moore, M., Schaack, J., Baim, S. B., Morimoto, R. I., and Shenk, T. (1987). Induced heat-shock mRNAs escape the nucleocytoplasmic transport block in adenovirus-infected HeLa cells. *Molecular and Cellular Biology,* **7**: 4505-4512.

Morin, N., Delsert, C., and Klessig, D. F. (1989). Nuclear localization of the adenovirus DNA-binding protein: requirement for two signals and complementation during viral infection. *Molecular and Cellular Biology,* **9**: 4372-4380.

Mossessova, E., and Lima, C. D. (2000). Ulp1-SUMO crystal structure and genetic analysis reveal conserved interactions and a regulatory element essential for cell growth in yeast. *Molecular Cell*, **5**: 865-876.

Nagata, K., Guggenheimer, R. A., Enomoto, T., Lichy, J. H., and Hurwitz, J. (1982). Adenovirus DNA replication in vitro: identification of a host factor that stimulates synthesis of the preterminal protein-dCMP complex. *Proc. Natl. Acad. Sci. USA,* **79**: 6438-6442.

Neumann, E., Schaefer-Ridder, M., Wang, Y., and Hofschneider, P. H. (1982). Gene transfer into mouse lyoma cells by electroporation in high electric fields. *EMBO J.*, **1**: 841.

Oosterom-Dragon, E. A., and Ginsberg, H. S. (1981). Characterization of two temperature-sensitive mutants of type 5 adenovirus with mutations in the 100,000-dalton protein gene. *Journal of Virology*, **40**: 491-500.

Orr, D. C., Long, A. C., Kay, J., Dunn, B. M., and Cameron, J. M. (1989). Hydrolysis of a series of synthetic peptide substrates by the human rhinovirus 14 3C proteinase, cloned and expressed in *Escherichia coli*. *Journal of General Virology*, **70**: 2931-2942.

Paine, P. L., Moore, L. C., and Horowitz, S. B. (1975). Nuclear envelope permeability. *Nature*, **254**: 109-114.

Panté, N., and Kann, M. (2002). Nuclear pore complex is able to transport macromolecules with diameters of ~ 39 nm. *Molecular Biology of the Cell,* **13**: 425-434.
Parks, R. J. (2005). Adenovirus protein IX: a new look at an old protein. *Molecular Therapy*, **11**: 19-25.

Peters, S. A., Voorhorst, W. G., Wery, J., Wellink, J., and van Kammen, A. (1992). A regulatory role for the 32K protein in proteolytic processing of cowpea mosaic virus polyproteins. *Virology*, **191**: 81-89.

Philipson, L. (1995). Adenovirus-an eternal archetype. In *The Molecular Repertoire of Adenoviruses I*, Springer-Verlag, Heidelberg. pp. 2-24.

Ploegh, H. L. (1998). Viral strategies of immune evasion. *Science,* **280**: 248-253.

Pollard, B. D. (2001). The activation of adenovirus type 2 protease and the function of the activating peptide. *PhD Thesis*, University of St Andrews.

Preuss M., Tecle, M., Shah, I., Matthews D. A., and Miller, A. D. (2003). Comparison between the interactions of adenovirus-derived peptides with plasmid DNA and their

role in gene delivery mediated by liposome-peptide-DNA virus-like nanoparticles. *Org. Biomol. Chem.*, **1**: 2430-2438.

Puvion-Dutilleul, F., Roussev, R., and Puvion, E. (1992). Distribution of viral RNA molecules during the adenovirus type 5 infectious cycle in HeLa cells. *Journal of Structural Biology*, **108**: 209-220.

Querido, E., Marcellus, R. C., Lai, A., Charbonneau, R., Teodoro, J. G., Ketner, G., and Branton, P. E. (1997). Regulation of p53 levels by the E1B 55-kilodalton protein and E4orf6 in adenovirus-infected cells. *Journal of Virology,* **71**: 3788-3798.

Rawlings, N. D., and Barrett, A. J. (1994). Families of cysteine peptidases. *Methods in Enzymology,* **244**: 461-486.

Rawlings, N. D., and Barrett, A. J. (2000). MEROPS- the protease database. Release 5.3. http://www.bi.bbsrc.ac.uk/Merops/Merops.htm.

Rice, A. P., and Roberts, B. E. (1983). Vaccinia virus induces cellular mRNA degradation. *Journal of Virology,* **47**: 529-539.

Richard, J. P., Melikov, K., Vives, E., Ramos, C., Verbeure, B., Gait, M. J., Chernomordik, L. V., and Lebleu, B. (2003). Cell-penetrating peptides; a reevaluation of the mechanism of cellular uptake. *Journal of Biological Chemistry*, **278**: 585-590.

Roberts, B. L., Richardson, W. D., and Smith, A. E. (1987). The effect of protein context on the nuclear location signal function. *Cell,* **50**: 465-475.

Roberts, M. M., White, J. L., Grütter, M. G., and Burnett, R. M. (1986). Three-dimensional structure of the adenovirus major coat protein hexon. *Science,* **232**: 1148-1151.

Rodriguez, M. S., Desterro, J. M. P., Lain, S., Midgley, C. A., Lane, D. P., and Hay, R. T. (1999). SUMO-1 modification activates the transcriptional response of p53. *EMBO J.,* **18**: 6455-6461.

Rowe, W. P., Huebner, R. J., Gilmore, L. K., Parrott, R. H., and Ward, T. G. (1953). Isolation of a cytopathogenic agent from human adenoids undergoing spontaneous degeneration in tissue culture. *Proceedings of the Society for Experimental Biology and Medicine,* **84**: 570-573.

Russell, W. C. (2000). Update on adenovirus and its vectors. *Journal of General Virology*, **81**: 2573-2604.

Russell, W. C., and Blair, G. E. (1977). Polypeptide phosphorylation in adenovirus-infected cells. *Journal of General Virology,* **34**: 19-35.

Russell, W. C., Patel, G., Precious, B., Sharp, I., and Gardner, P. S. (1981). Monoclonal antibodies against adenovirus type 5: preparation and preliminary characterization. *Journal of General Virology,* **56**: 393-408.

Russell, W. C., and Precious, B. (1982). Nucleic acid-binding properties of adenovirus structural polypeptides. *Journal of General Virology,* **63**: 69-79.

Russell, W. C., and Kemp, G. D. (1995). The role of adenovirus structural proteins in the regulation of adenovirus infection. In *The Molecular Repertoire of Adenoviruses I.* Springer-Verlag, Heidelberg. pp. 81-98.

Rux, J. J., and Burnett, R. M. (2000). Type-specific epitope locations revealed by X-ray crystallographic study of adenovirus type 5 hexon. *Molecular Therapy*, **1**: 18-30.

Ruzindana-Umunyana, A., Imbeault, L., and Weber, J. M. (2002). Substrate specificity of adenovirus protease. *Virus Research,* **89**: 41-52.

Ruzindana-Umunyana, A., Sircar, S., and Weber, J. M. (2000). The effect of mutant peptide cofactors on adenovirus protease activity and virus infection. *Virology,* **270**: 173-179.

Ryan, M. D., and Flint, M. (1997). Virus-encoded proteinases of the picornavirus super-group. *Journal of General Virology,* **78**: 699-723.

Ryan, M. A., Gray, G. C., Smith, B., McKeehan, J. A., Hawksworth, A. W., and Malasig, M. D. (2002). Large epidemic of respiratory adenovirus types 7 and 3 in healthy adults. *Clin. Infect. Dis.,* **34**: 577-582.

Sambrook, J., Fritsch, E. F., and Maniatis, T. (1989). Molecular cloning: a laboratory manual (2nd edition). Cold Spring Harbor Laboratory Press, New York.

Saphire, A. C. S., Guan, T., Schirmer, E. C., Nemerow, G. R., and Gerace, L. (2000). Nuclear import of adenovirus DNA *in vitro* involves the nuclear protein import pathway and hsc70. *Journal of Biological Chemistry,* **275**: 4298-4304.

Segerman, A., Atkinson, J. P., Marttila, M., Dennerquist, V., Wadell, G., and Arnberg, N. (2003). Adenovirus type 11 uses CD46 as a cellular receptor. *Journal of Virology,* **77**: 9183-9191.

Shenk, T. (1996). *Adenoviridae*: the viruses and their replication. In *Fundamental Virology.* Lippincott- Raven Publishers, Philadelphia. pp. 2111-2148.

Söling, A., Simm, A., and Rainov, N. G. (2002). Intracellular localization of Herpes simplex virus type 1 thymidine kinase fused to different fluorescent proteins depends on choice of fluorescent tag. *FEBS Letters,* **527**:153-158.

Stewart, P. L., Burnett, R. M., Cyrklaff, M., and Fuller, S. D. (1991). Image reconstruction reveals the complex molecular organization of adenovirus. *Cell,* **67**: 145-154.

Stuiver, M. H., and van der Vliet, P. C. (1990). Adenovirus DNA-binding protein forms a multimeric protein complex with double-stranded DNA and enhances binding of nuclear factor I. *Journal of Virology,* **65**: 379-386.

ten Dam, E., Flint, M., and Ryan, M. D. (1999). Virus-encoded proteinases of the *Togaviridae*. *Journal of General Virology,* **80**: 1879-1888.

Thomas, P. G., and Mathews, M. B. (1980). DNA replication and the early to late transition in adenovirus infection. *Cell,* **22**: 523-533.

Tihanyi, K., Bourbonnière, M., Houde, A., Rancourt, C., and Weber, J. M. (1993). Isolation and properties of adenovirus type 2 proteinase. *Journal of Biological Chemistry,* **268**: 1780-1785.

Tollefson, A. E., Ryerse, J. S., Scaria, A., Hermiston, T. W., and Wold, W. S. M. (1996). The E3-11.6-kDa adenovirus death protein (ADP) is required for efficient cell death: characterization of cells infected with *adp* mutants. *Virology,* **220**: 152-162.

Tomko, R. P., Johansson, C. B., Totrov, M., Abagyan, R., Frisén, J., and Philipson, L. (2000). Expression of the adenovirus receptor and its interaction with the fiber knob. *Experimental Cell Research,* **255**: 47-55.

Tomko R. P., Xu, R., and Philipson, L. (1997). HCAR and MCAR: The human and mouse cellular receptors for subgroup C adenoviruses and group B coxsackieviruses *Proc. Natl. Acad. Sci. USA,* **94**: 3352-3356.

Toogood, C. I. A., Crompton, J., and Hay, R. T. (1992). Antipeptide antisera define neutralizing epitopes on the adenovirus hexon. *Journal of General Virology,* **73**: 1429-1435.

Toogood, C. I. A., Murali, R., Burnett, R. M., and Hay, R. T. (1989). The adenovirus type 40 hexon: sequence, predicted structure and relationship to other adenovirus hexons. *Journal of General Virology,* **70**: 3203-3214.

Tremblay, M. L., Dery, C. V., Talbot, B. G., and Weber, J. (1983). *In vitro* cleavage specificity of the adenovirus type 2 proteinase. *Biochimica et Biophysica Acta*, **743**: 239-245.

Trentin, J. J., Yabe, Y., and Taylor, G. (1962). The quest for human cancer viruses. *Science*, **137**: 835-849.

Trotman, L. C., Mosberger, N., Fornerod, M., Stidwill, R. P., and Greber, U. F. (2001). Import of adenovirus DNA involves the nuclear pore complex receptor CAN/Nup214 and histone H1. *Nature Cell Biology*, **3**: 1092-1100.

Tsuzuki, J., and Luftig, R. B. (1983). The adenovirus type 5capsid protein IIIa is phosphorylated during an early stage of infection of HeLa cells. *Virology*, **129**: 529-533.

van Oostrum, J., and Burnett, R. M. (1985). Molecular composition of the adenovirus type 2 virion. *Journal of Virology*, **56**: 439-448.

Vaughan, O. A. (1997). The adenovirus type 2 protease: The generation and characterisation of monoclonal antibodies and their use in determining the subcellular distribution of the protease within lytically infected cells. *PhD Thesis*, University of St. Andrews.

Velicer, L. F., and Ginsberg, H. S. (1970). Synthesis, transport and morphogenesis of type 5 adenovirus capsid proteins. *Journal of Virology,* **5**: 338-352.

Viguera, A. R., and Serrano, L. (1995). Side-chain interactions between sulfur-containing amino acids and phenylalanine in alpha-helices. *Biochemistry,* **34**: 8771-8779.

Vives, E., Brodin, P., and Lebleu, B. (1997). A truncated HIV-1 Tat protein basic domain rapidly translocates through the plasma membrane and accumulates in the cell nucleus. *J. Biol. Chem.*, **272**: 16010-16017.

Vos, P., Verver, J., Jaegle, M., Wellink, J., van Kammen, A., and Goldbach, R. (1988). Two viral proteins involved in the proteolytic processing of the cowpea mosaic virus polyproteins. *Nucleic Acids Research*, **16**: 1967-1985.

Walls, T., Shankar, A. G., and Shingadia, D. (2003). Adenovirus: an increasingly important pathogen in paediatric bone marrow transplant patients. *The Lancet Infectious Diseases,* **3**: 79-86.

Wang, K., Huang, S., Kapoor-Munshi, A., and Nemerow, G. (1998). Adenovirus internalisation and infection require dynamin. *Journal of Virology,* **72**: 3455-3458.

Wang, M. Q., and Johnson, R. B. (2001). Activation of human rhinovirus-14 3C protease. *Virology*, **280**: 80-86.

Weber, J. (1976). Genetic analysis of adenovirus type 2 III temperature sensitive processing of viral proteins. *Journal of Virology,* **17**: 462-471.

Weber, J. M. (1995). Adenovirus endopeptidase and its role in virus infection. In *The Molecular Repertoire of Adenoviruses I.* Springer-Verlag, Heidelberg. pp. 227-235.

Weber, J. M., Khittoo, G., and Bhatti, R. A. (1983). Adenovirus core proteins. *Canadian Journal of Microbiology,* **29**: 235-241.

Webster, A., Hay, R. T., and Kemp, G. (1993). The adenovirus protease is activated by a virus-coded disulphide-linked peptide. *Cell*, **72**: 97-104.

Webster, A., and Kemp, G. (1993). The active adenovirus protease is the intact L3 23K protein. *Journal of General Virology*, **74**: 1415-1420.

Webster, A., Leith, I. R., and Hay, R. T. (1994). Activation of adenovirus-coded protease and processing of preterminal protein. *Journal of Virology,* **68**: 7292-7300.

Webster, A., Russell, S., Talbot, P., Russell, W. C., and Kemp, G. D. (1989a). Characterization of the adenovirus proteinase: substrate specificity. *Journal of General Virology*, **70:** 3225-3234.

Webster, A., Russell, W. C., and Kemp, G. D. (1989b). Characterization of the adenovirus proteinase: development and use of a specific peptide assay. *J. Gen. Virol.*, **70**: 3215-3223.

Welker, R., Janetzko, A., and Kräusslich, H.-G. (1997). Plasma membrane targeting of chimeric intracisternal A-type particle polyproteins leads to particle release and specific activation of the viral proteinase. *Journal of Virology,* **71**: 5209-5217.

White, E. (2001). Regulation of the cell cycle and apoptosis by the oncogenes of adenovirus. *Oncogene,* **20**: 7836-7846.

Whittaker, G., Bui, M., and Helenius, A. (1996). The role of nuclear import and export in influenza virus infection. *Trends in Cell Biology*, **6**: 67-71.

Wickham, T. J., Mathias, P., Cheresh, D. A., and Nemerow, G. R. (1993). Integrins $\alpha_v\beta_3$ and $\alpha_v\beta_5$ promote internalization but not virus attachment. *Cell,* **73**: 309-319.

Winter, N., and D'Halluin, J-C. (1991). Regulation of the biosynthesis of subgroup C adenovirus protein IVa2. *Journal of Virology*, **65**: 5250-5259.

Wodrich, H. Guan, T., Cingolani, G., Von Seggern, D., Nemerow, G., and Gerace, L. (2003). Switch from capsid protein import to adenovirus assembly by cleavage of nuclear transport signals. *EMBO J.,* **22**: 6245-6255.

Yao, N., Hesson, T., Cable, M., Hong, Z., Kwong, A. D., Le, H. V., and Weber, P. C. (1997). Structure of the hepatitis C virus RNA helicase domain. *Nature Structural Biology,* **4**: 463-467

Yao, N., Reichert, P., Taremi, S. S., Prosise, W. W., and Weber, P. C. (1999). Molecular views of viral polyprotein processing revealed by the crystal structure of the hepatitis C virus bifunctional protease-helicase. *Structure,* **7**: 1353-1363.

Yeh-Kai, L., Akusjärvi, G., Aleström, P., Pettersson, U., Tremblay, M., and Weber, J. (1983). *J. Mol. Biol.,* **167**: 217-222.

Yuan, W., and Krug, R. M. (2001). Influenza B virus NS1 protein inhibits conjugation of the interferon (IFN)-induced ubiquitin-like ISG15 protein. *EMBO J.,* **20**: 362-371.

Zhao, L-J., and Padmanabhan, R. (1988). Nuclear transport of adenovirus DNA polymerase is facilitated by interaction with preterminal protein. *Cell,* **55**: 1005-1015.